

AD-A236 836



2

# NAVAL POSTGRADUATE SCHOOL Monterey, California



DTIC  
ELECTE  
JUN 12 1991  
S B D

## THESIS

### A COMPUTATIONAL AND EXPERIMENTAL STUDY OF FLUSH HEAT SOURCES IN LIQUIDS

by

Larry O. Haukenes

June 1990

Thesis Advisor:  
Co-Advisor:

Yogendra Joshi  
Sanjeev Sathe

Approved for public release; distribution is unlimited.

91-01889



91 6 11 167

**Unclassified**

SECURITY CLASSIFICATION OF THIS PAGE

REPORT DOCUMENTATION PAGE				Form Approved OMB No. 0704-0188	
1a. REPORT SECURITY CLASSIFICATION <b>Unclassified</b>		1b. RESTRICTIVE MARKINGS			
2a. SECURITY CLASSIFICATION AUTHORITY		3. DISTRIBUTION AVAILABILITY OF REPORT			
2b. DECLASSIFICATION/DOWNGRADING SCHEDULE		Approved for public release; distribution unlimited.			
4. PERFORMING ORGANIZATION REPORT NUMBER(s)		5. MONITORING ORGANIZATION REPORT NUMBER(s)			
6a. NAME OF PERFORMING ORGANIZATION <b>Naval Postgraduate School</b>		6b. OFFICE SYMBOL (If applicable) <b>ME</b>		7a. NAME OF MONITORING ORGANIZATION <b>Naval Postgraduate School</b>	
6c. ADDRESS (City, State, and ZIP Code) <b>Monterey, CA 93943-5000</b>		7b. ADDRESS (City, State, and ZIP Code) <b>Monterey, CA 93943-5000</b>			
8a. NAME OF FUNDING/SPONSORING ORGANIZATION		8b. OFFICE SYMBOL (If applicable)		9. PROCUREMENT INSTRUMENT IDENTIFICATION NUMBER	
8c. ADDRESS (City, State, and ZIP Code)		10. SOURCE OF FUNDING NUMBERS			
		PROGRAM ELEMENT No.		PROJECT No.	TASK No.
				WORK UNIT	ACCESSION No.
11. TITLE (Include Security Classification) <b>A Computational and Experimental Study of Flush Heat Sources in Liquids</b>					
12. PERSONAL AUTHOR(S) <b>HAUKENES, LARRY O.</b>					
13a. TYPE OF REPORT <b>Thesis for Master of Science and Mechanical Engineer Degrees</b>		13b. TIME COVERED <b>From: June 1989 To: June 1990</b>		14. DATE OF REPORT (Year, Month, Day) <b>1990 June 21</b>	
				15. PAGE COUNT <b>145</b>	
16. SUPPLEMENTARY NOTATION The views expressed in this thesis are those of the author and do not reflect the official policy or position of the Department of Defense or the U. S. Government.					
17. COSATI CODES		18. SUBJECT TERMS (Continue on reverse if necessary and identify by block number)			
FIELD	GROUP	SUB-GROUP			
		Electronic cooling, liquid immersion, natural convection, numerical heat transfer			
19. ABSTRACT (Continue on reverse if necessary and identify by block number)					
<p>A numerical investigation of two-dimensional natural convection flow and heat transfer from a substrate-mounted flush heat source immersed in a liquid-filled square enclosure was conducted. The study is relevant to direct liquid-immersion cooling of electronic components. A control volume based finite-difference model that accounts for conduction heat transfer within the substrate and heat source and the coupled natural convection in the fluid was utilized. Numerical predictions were obtained for a wide range of Rayleigh and Prandtl numbers, substrate to fluid and heat source to fluid thermal conductivity ratios and other geometrical parameters that may be encountered in practice. An increase in Rayleigh number lead to more vigorous flow and promoted cooling. No noticeable effect on the nondimensional temperature was observed when changing the Prandtl number from 7 to 100. Little reduction in maximum temperatures was observed when substrate and component to fluid thermal conductivity ratios were increased beyond 10 and 25, respectively. Component to substrate width ratio change from .25 to .999 resulted in approximately linear decrease in the maximum temperature. A companion experimental study of three-dimensional natural convection transport from a flush mounted array of heat sources in water was also conducted. Computed temperatures compared favorably to appropriate experimental data.</p>					
20. DISTRIBUTION/AVAILABILITY OF ABSTRACT <input checked="" type="checkbox"/> UNCLASSIFIED/UNLIMITED <input type="checkbox"/> SAME AS RPT. <input type="checkbox"/> DTIC USERS				21. ABSTRACT SECURITY CLASSIFICATION <b>Unclassified</b>	
22a. NAME OF RESPONSIBLE INDIVIDUAL <b>Professor Joshi</b>				22b. TELEPHONE (Include Area code) <b>(408) 646-3400</b>	
				22c. OFFICE SYMBOL <b>ME/Ji</b>	

DD Form 1473, JUN 86

Previous editions are obsolete.

SECURITY CLASSIFICATION OF THIS PAGE

**Unclassified**

Approved for public release; distribution is unlimited

**A Computational and Experimental  
Study of Flush Heat Sources in Liquids**

by

**Larry Olaf Haukenes**  
Lieutenant, United States Navy  
B.S., University of Wisconsin-Eau Claire, 1980

Submitted in partial fulfillment of the  
requirements for the degree of

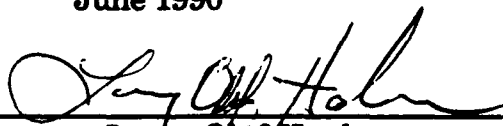
**MASTER OF SCIENCE IN MECHANICAL ENGINEERING  
and  
MECHANICAL ENGINEER**

from the

**NAVAL POSTGRADUATE SCHOOL**

June 1990

Author:

  
Larry Olaf Haukenes

Approved by:



Sanjeev Sathe, Thesis Co-Advisor



Yogendra Joshi, Thesis Advisor

  
Anthony J. Healey, Chairman,  
Department of Mechanical Engineering

  
Dean of Faculty and Graduate Studies

## **ABSTRACT**

A numerical investigation of two-dimensional natural convection flow and heat transfer from a substrate-mounted flush heat source immersed in a liquid-filled square enclosure was conducted. The study is relevant to direct liquid-immersion cooling of electronic components. A control volume based finite-difference model that accounts for conduction heat transfer within the substrate and heat source and the coupled natural convection in the fluid was utilized. Numerical predictions were obtained for a wide range of Rayleigh and Prandtl numbers, substrate to fluid and heat source to fluid thermal conductivity ratios and other geometrical parameters that may be encountered in practice. An increase in Rayleigh number lead to more vigorous flow and promoted cooling. No noticeable effect on the nondimensional temperatures was observed when changing the Prandtl number from 7 to 100. Little reduction in maximum temperatures was observed when substrate and component to fluid thermal conductivity ratios were increased beyond 10 and 25, respectively. Component to substrate width ratio change from .25 to .999 resulted in approximately linear decrease in the maximum temperature. A companion experimental study of three-dimensional natural convection transport from a flush mounted array of heat sources in water was also conducted. Computed temperatures compared favorably to appropriate experimental data.

## TABLE OF CONTENTS

I.	INTRODUCTION.....	1
A.	STATEMENT OF PROBLEM.....	1
B.	OBJECTIVES.....	4
II.	NUMERICAL MODEL.....	7
A.	MATHEMATICAL FORMULATION.....	7
B.	METHOD OF SOLUTION.....	9
III.	PARAMETRIC STUDY.....	12
A.	EFFECT OF $R_a$ .....	12
B.	EFFECT OF $Pr$ .....	24
C.	EFFECT OF SUBSTRATE CONDUCTIVITY RATIO $R_s$ .....	24
D.	EFFECT OF COMPONENT CONDUCTIVITY RATIO $R_c$ .....	41
E.	EFFECT OF COMPONENT TO SUBSTRATE WIDTH RATIO $w/d_t$ .....	51
IV.	EXPERIMENT.....	61
A.	EXPERIMENTAL APPARATUS.....	61
1.	Additions.....	61
2.	Changes.....	62
B.	LIQUID CRYSTAL.....	63
V.	NUMERICAL COMPARISON WITH EXPERIMENT.....	73
A.	WHAT TO COMPARE ?.....	73
B.	0.2 WATT NUMERICAL COMPARISON.....	73
C.	HIGHER POWER NUMERICAL COMPARISON.....	80

D. UPPER/LOWER HEATER NUMERICAL EVALUATION.....	82
VI. CONCLUSIONS.....	91
VII. RECOMMENDATIONS.....	93
APPENDIX A USER PORTION OF FINITE DIFFERENCE PROGRAMS...	94
APPENDIX B CONTOUR PROGRAM.....	106
APPENDIX C TRAVERSE PROGRAM.....	116
APPENDIX D TEMPERATURE ACQUISITION PROGRAM.....	117
APPENDIX E UNIFORM POWER PROGRAM.....	119
APPENDIX F UNIFORM DATA REDUCTION PROGRAM.....	122
APPENDIX G NONUNIFORM POWER PROGRAM.....	125
APPENDIX H NONUNIFORM DATA REDUCTION PROGRAM.....	128
LIST OF REFERENCES.....	132
INITIAL DISTRIBUTION LIST.....	134



<b>Accession For</b>	
NTIS GRA&I	<input checked="" type="checkbox"/>
DTIC TAB	<input type="checkbox"/>
Unannounced	<input type="checkbox"/>
Justification	
By	
Distribution/	
Availability Codes	
Dist	Avail and/or Special
A-1	

## NOMENCLATURE

$c_p$	specific heat at constant pressure [J/kg-K]
$d$	dimension in Fig. 1 [m]
$d_t$	substrate thickness [m]
$g$	gravitational acceleration [m/s <sup>2</sup> ]
$h$	component height [m]
$H$	enclosure height [m]
$k$	thermal conductivity [W/m-K]
$L_t$	dimension in Fig. 1 [m]
$p$	pressure [N/m <sup>2</sup> ]
$P$	non-dimensional pressure, $p/\rho U_o^2$
$Pr$	Prandtl number, $\mu c_p/k_f$
$q$	non-dimensional heat flux [eq.7]
$Q$	Heat generation rate per unit length [W/m]
$P$	Power to the heater
$R_c$	protrusion to fluid thermal conductivity ratio, $k_c/k_f$
$R_s$	substrate to fluid thermal conductivity ratio, $k_s/k_f$
$Ra$	Rayleigh number, $g\beta Qh^3/\alpha k_f \nu$
$S1$	non-dimensional counter clockwise contour distance along the component-fluid/component-substrate interface in Table 2
$S2$	non-dimensional counter clockwise contour distance along the solid-fluid interface in Table 1

$S_b, S_t$	dimensions in Fig. 1 [m]
$R_L$	Lead resistance [ $\Omega$ ]
$R_P$	Precision resistor resistance [ $\Omega$ ]
$t_c$	enclosure wall temperature [K]
$T$	non-dimensional temperature, $(t-t_c)/(Q/k_f)$
$u$	vertical velocity component [m/s]
$U$	non-dimensional vertical velocity component, $u/U_o$
$U_o$	reference velocity, $(g\beta Qh/k_f)^{1/2}$ [m/s]
$v$	horizontal velocity component [m/s]
$V$	non-dimensional horizontal velocity component, $v/U_o$
$V_L$	Voltage measured over the leads and heater [Volts]
$V_T$	Voltage over the precision resistor, leads and heater [Volts]
$w$	component width [m]
$x$	vertical coordinate [m]
$X$	non-dimensional vertical coordinate, $x/h$
$y$	horizontal coordinate [m]
$Y$	non-dimensional horizontal coordinate, $y/h$

### ***Greek Symbols***

$\alpha$	fluid thermal diffusivity [ $m^2/s$ ]
$\beta$	coefficient of thermal expansion [ $1/K$ ]
$\delta X$	non-dimensional vertical distance between grid point and the control volume face
$\delta Y$	non-dimensional horizontal distance between grid point and the control volume face



$\rho$	fluid density [kg/m <sup>3</sup> ]
$\mu$	dynamic viscosity [kg/m-s]
$\nu$	kinematic viscosity [m <sup>2</sup> /s]
$\kappa$	nondimensional conductivity [ $R/(RaPr)^{1/2}$ ]

### ***Subscripts***

$c$	component (chip)
$f$	fluid/liquid
$max$	maximum
$s$	substrate
$sur$	substrate or component surface

## **ACKNOWLEDGMENT**

I would like to express my thanks to Professor Joshi for his guidance and technical assistance in putting together this research project. I also wish to thank Professor Sathe for his instruction in the use of the finite difference computer program.

# **I. INTRODUCTION**

## **A. STATEMENT OF PROBLEM**

Heat removal from electronic equipment is an area of extensive research and will be more important in the future due to the ever increasing component volumetric heat generation rates. The advantages of liquid cooling have been demonstrated in the thermal control of macroelectronic components such as power transistors and power supplies for almost 40 years. However liquid cooling of microelectronic equipment has only recently gained wide attention due to the need for increased power dissipation, the availability of inert dielectric liquids, and the introduction of immersion cooled supercomputers. Bergles and Bar-Cohen [Ref. 1] and Nakayama [Ref. 2] have described various cooling techniques currently under investigation to meet modern component cooling requirements. Incropera [Ref. 3] discusses convective cooling.

In natural convection the flow is induced by buoyancy forces. The buoyancy force is generated when a body force acts on a fluid in which a density gradient is present. Natural convection cooling has the advantages of simplicity of design, low operating cost due to no outside power requirements and minimum maintenance, absence of noise and high reliability. Also, in the event of a mechanical failure, natural convection may be the only method of cooling available [Ref. 4-5]. Natural convection in liquids results in much higher cooling rates compared to those of air and hence numerous studies have recently been performed on natural

convection from discrete heat sources inside liquid filled enclosures [Ref. 6-10].

Gaiser [Ref. 6] experimentally investigated natural convection liquid cooling of a three column array of uniformly heat generating simulated electronic components on a flat plate and in a vertical channel by using foil heaters. The channel was made by placing a smooth movable shroud parallel to the high density heater surface. Temperature measurements and flow visualizations at various power levels and channel spacings were made. Experimental correlations relating local heat transfer with shroud wall spacing and foil heater power levels were developed. Flow was laminar for all power levels studied. For the unshrouded case, the flow of coolant over the center column resulted in a weak fluid entrainment from the side columns and in turn enhanced the cooling of the side columns. For the shrouded case, the fluid entrainment by the center column was much greater and had a greater cooling effect on the side columns. For a channel of 3 mm or less, the increased frictional resistance caused a significant increase in the component temperature and the correlations were no longer followed.

Joshi, Willson and Hazard [Ref. 7] conducted an experimental investigation of steady state and transient natural convection from a column of rectangular heated protrusions in a vertical channel in water. Flow visualizations and component surface temperature measurements were carried out for several power dissipation levels and channel spacings. For the smallest channel spacing, the component surface temperatures increased significantly due to a reduction in fluid velocity.

During transient periods, an initial diffusive transport was observed followed by the evolution of convective effects. No overshoots in component temperatures were observed. Steady transport responses over several component power levels were also examined.

Park and Bergles [Ref. 8] simulated microelectronic circuits with flush mounted and protruding thin foil heaters. Heat transfer coefficients were obtained for various heater heights and widths in water and R-113. The heat transfer coefficient was found to increase with decreasing width, which was attributed to three dimensional boundary layer effects. Protruding heaters were found to have a coefficient about 15 percent above flush mounted heaters. Coefficients for upper flush heaters were found to be less than lower heaters. For protruding heaters, the upper heaters had higher coefficients than the lower heaters.

Bar-Cohen and Schweitzer [Ref. 9] provided an analytical basis for the design and optimization of convective immersion cooling systems. Analytical development and experimental verification of the relations for the natural convection heat transfer coefficients prevailing along the surfaces of immersed, uniformly heated plates in both symmetric and asymmetric configurations were conducted. Milanez and Bergles [Ref. 10] experimentally studied the wake temperature distribution produced by a horizontal line source on a vertical adiabatic surface and compared it to the similarity solution. They also examined the interaction of two heaters. Velocities induced by the lower heater enhanced the heat transfer coefficient at the upper heater, however this effect was offset by the preheating of the fluid by the lower heater. Jaluria [Ref. 11] conducted a

numerical study of heat sources mounted on an adiabatic wall under the influence of natural convection. Sathe and Joshi [Ref. 5] conducted a numerical investigation of natural convection flow and heat transfer arising from a substrate mounted protruding heat source. Their study accounts for conduction heat transfer within the protrusion and substrate and the coupled natural convection in the fluid.

Areas of current concern with the new packaging techniques are stress on the electronic components due to thermal expansion coefficient mismatch. Temperatures throughout the package are needed so thermal stress analysis can be conducted and high stress areas can be located. The complex geometries of the boards and the coupled conduction/convection heat transfer problem lead to intricate heat transfer paths. The difficulty is magnified when the circuit board spacing is small and the flow pattern is populated by numerous non-uniform heat sources. An examination of the heat transfer and fluid flow characteristics of such a system would aid designers in the development of better cooling schemes.

## **B. OBJECTIVES**

This study was performed to determine the effects of changing the various parameters involved in the construction of electronic packages on the heat transfer and to observe the effects of a nonuniform high density grouping of discrete heat sources in a vertical channel for direct liquid natural convection cooling. Gaiser [Ref. 6] describes the high density grouping of heat sources.

The study consisted of two parts. First a computer model was utilized to conduct a two dimensional study to find the effects of various governing parameters on the natural convective heat transfer and fluid flow behaviors for a substrate mounted flush component immersed in a liquid. Then the three dimensional flow over a simulated printed wire circuit board consisting of multiple arrays of flush-mounted heaters was observed experimentally. Results of the computer model were compared to results from past and current experimental studies.

Specific objectives of the numerical parametric study were:

- To determine temperatures and flows throughout and around a simulated direct liquid natural convection cooled flush mounted electronic component.
- To study the effect of various combinations of parameters for an electronic component flush mounted on a substrate.
- To investigate the effect of two component interaction on the heat transfer and flow.

The experimental study had the following objectives:

- To determine the effect of channel spacing on fluid flow and heat transfer.

- To observe the effect of nonuniform powering on heat transfer and fluid flow.
- To observe the surface temperature patterns during uniform and nonuniform heating using liquid crystal.



## II. NUMERICAL MODEL

### A. MATHEMATICAL FORMULATION

The schematic diagram of the configuration examined is shown in Fig. 1. A flush heat source mounted in a vertical substrate is immersed in a two-dimensional fluid-filled square enclosure of height  $H$ . The dark shaded region represents the heat source and the light shaded area the substrate. Uniform volumetric heat generation takes place in the flush mounted heater. The enclosure boundaries are maintained at a constant temperature,  $t_c$ . The heater, the substrate and the fluid have constant but different thermophysical properties. Assuming a steady-state, laminar flow with no viscous dissipation and the Boussinesq approximation to be true, the dimensionless governing equations can be written as:

#### *Fluid Region*

$$\frac{\partial U}{\partial X} + \frac{\partial V}{\partial Y} = 0 \quad (1)$$

$$\frac{\partial(U^2)}{\partial X} + \frac{\partial(UV)}{\partial Y} = (Pr/Ra)^{1/2} \left( \frac{\partial^2 U}{\partial X^2} + \frac{\partial^2 U}{\partial Y^2} \right) + T \cdot \frac{\partial P}{\partial X} \quad (2)$$

$$\frac{\partial(UV)}{\partial X} + \frac{\partial(V^2)}{\partial Y} = (Pr/Ra)^{1/2} \left( \frac{\partial^2 V}{\partial X^2} + \frac{\partial^2 V}{\partial Y^2} \right) - \frac{\partial P}{\partial Y} \quad (3)$$

$$\frac{\partial(UT)}{\partial X} + \frac{\partial(VT)}{\partial Y} = (1/RaPr)^{1/2} \left( \frac{\partial^2 T}{\partial X^2} + \frac{\partial^2 T}{\partial Y^2} \right) \quad (4)$$

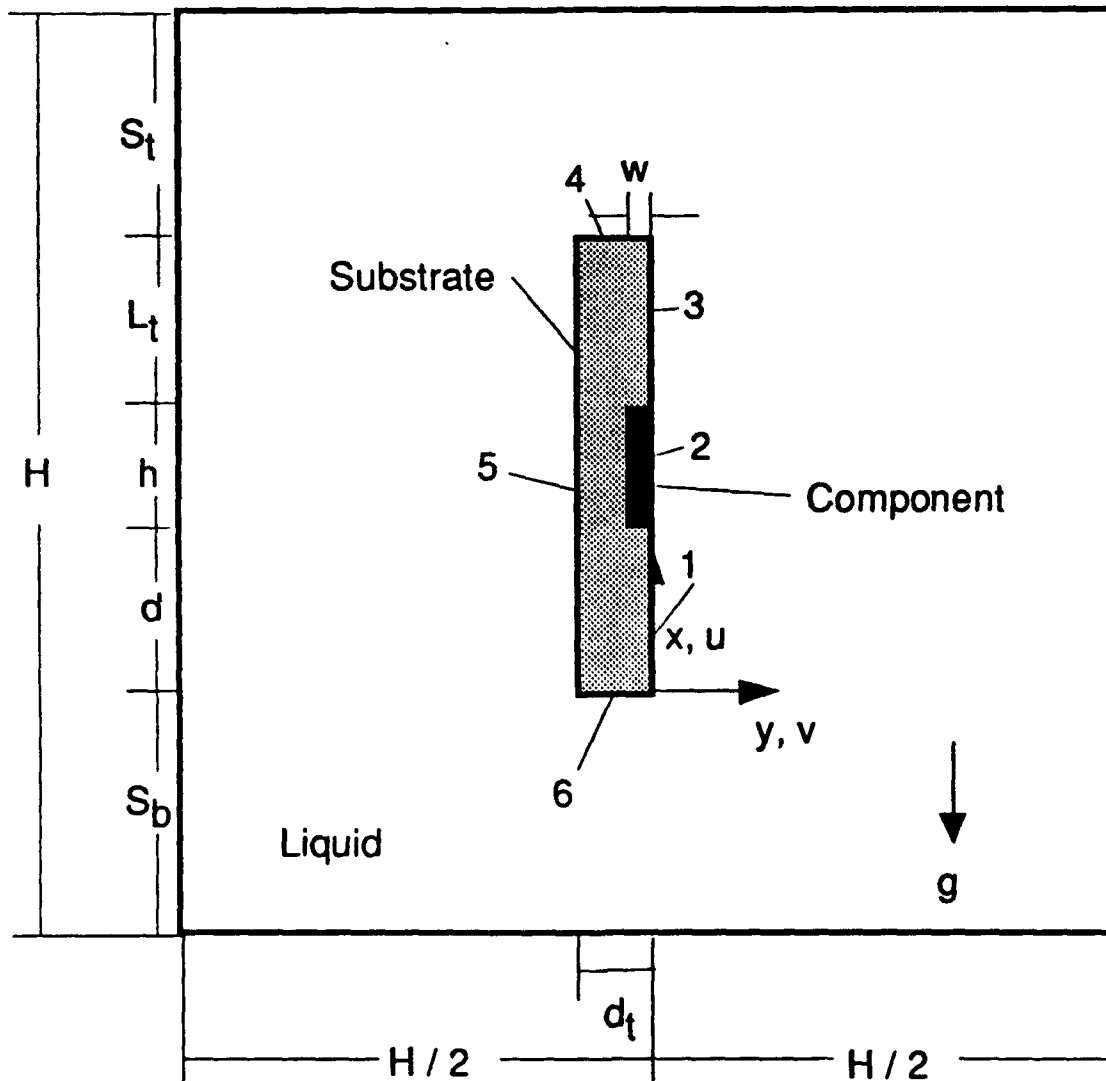


Figure 1. Schematic diagram of configuration for numerical study

***Solid Region (heater)***

$$\frac{\partial^2 T}{\partial X^2} + \frac{\partial^2 T}{\partial Y^2} = \frac{h}{wR_c} \quad (5)$$

***Solid Region (substrate)***

$$\frac{\partial^2 T}{\partial X^2} + \frac{\partial^2 T}{\partial Y^2} = 0 \quad (6)$$

where  $X=x/h$ ,  $Y=y/h$ ,  $U=u/U_o$ ,  $V=v/U_o$ ,  $T=(t-t_c)/(Q/k_f)$ ,  $P=p/\rho U_o^2$ ;  $U_o=(g\beta Qh/k_f)^{1/2}$ ,  $Pr=\mu c_p/k_f$ ,  $Ra=g\beta Qh^3/\alpha k_f \nu$ ,  $R_c=k_c/k_f$  and  $R_s=k_s/k_f$ .

The boundary conditions constitute isothermal enclosure walls at temperature  $t_c$  and the no-slip and impermeable wall conditions for the velocity components; i.e  $U=V=T=0$  at the enclosure walls. Heat fluxes are appropriately matched at the interfaces of dissimilar materials. The following governing parameters emerge as a result of the non-dimensionalized governing equations, boundary and matching conditions:  $Ra$ ,  $Pr$ ,  $R_c$ ,  $R_s$ ,  $S_b/h$ ,  $d/h$ ,  $L_f/h$ ,  $S_f/h$  and  $w/d_t$ . The definitions of the symbols can be found in the Nomenclature.

**B. METHOD OF SOLUTION**

The governing equations are discretized using a finite difference scheme wherein the control volumes for the temperature and pressure are staggered from those for the velocities. Power law profiles are used for the spatial variation of the dependent variables to ensure realistic results for a

wide range of the grid Peclet numbers. Interface diffusivities are calculated using a harmonic-mean formulation in order to handle abrupt changes in the material properties. The details of the discretization process can be found in Patankar [Ref. 12].

The discretized equations were solved iteratively using the line-by-line TDMA (Tri-Diagonal Matrix Algorithm) and the SIMPLER procedure as outlined in Ref. 12. It is noted that even though separate equations are written for the fluid and solid regions, the solid region is numerically simulated by letting its viscosity become very large. Thus the same momentum equation is solved throughout the computational domain. Similarly, for the energy equation, heat sources and property values are used implicitly in the control volume formulation wherein mass, momentum and energy balances are incorporated for individual control volumes [Ref. 12].

Test computations were performed on a series of grids ranging from 30x30 to 73x73 control volumes to determine the grid size effects. The values and locations for the maximum temperature and peak velocities did not change appreciably when the grid was refined beyond 40x40 control volumes. Most calculations were performed on a grid size of 50x50. However for  $Ra > 10^6$  the solution would not converge on a 50x50 grid and it was found that by increasing the control volumes in the area of the suspected high thermal gradient, convergence could be achieved. Therefore for  $Ra = 10^6$  the number of control volumes was increased to 70x70. Convergence was based on a balance of the rate of energy generated

in the component and the rate of energy leaving the enclosure walls. Convergence was based on the energy balance being better than 1 percent.

The program was run on the Mechanical Engineering VAX station 2000 Cluster and the IBM-370/3033 computer. The greater the number of control volumes the the greater the time to run on each system. Also if  $Ra$  was of the order of  $10^6$ , it took up to 120,000 iterations for convergence to take place. The relaxation factor for the velocities, temperatures, pressure and buoyant force were adjusted until a proper combination was found that would make the solution converge. After coming up with a proper set of relaxation factors, they could be used for other high  $Ra$  solutions and the number of iterations required was reduced. The run times could also be reduced when previously computed solutions were used as an initial guess. The VAX system took approximately 10 times longer to run a program with the same number of iterations and control volumes than the IBM system. However, more VAX stations could be used on a continuous basis which made using the VAX system slightly preferable.

### III. PARAMETRIC STUDY

Numerical computations were conducted for various  $Ra$ ,  $Pr$ ,  $R_s$ , and  $R_c$  values that would be found in actual cooling applications [Ref. 5].  $Ra$  numbers from  $10^3$  to  $10^6$  were investigated with the limit of  $10^6$  due to the very slow convergence of the computations for  $Ra$  greater than  $10^6$ . The values of  $Pr$ ,  $R_s$  and  $R_c$  were varied from 7 to 100, 0.1 to 100 and 1 to 100 respectively. The geometric parameters used in the computations were  $S_b/h=2$ ,  $d/h=2$ ,  $L_t/h=2$ ,  $S_t/h=3$ , and  $w/d_t$  varied from 0.25 to 1. A baseline case with  $Ra=10^5$ ,  $Pr=25$ ,  $R_s=10$ ,  $R_c=25$  and  $w/d_t=0.5$  was conducted and when a particular parameter was being studied all other parameters were kept the same as in the baseline case. Table 1 shows the breakdown of the cases studied. Appendix A shows the user portion of the finite difference program used to obtain the numerical data. Appendix B contains the contour program used in making the following figures.

#### A. EFFECT OF $Ra$

The temperature contours for  $Ra=10^3$  to  $10^6$  are shown in Figs. 2(a)-(d). These are nearly symmetric with respect to the enclosure vertical centerline for all  $Ra$ . The high  $R_s$  (10) value tends to spread the heat out to each side even though the heater is placed on the right side of the substrate. As  $Ra$  increases, the extent of thermal stratification increases in the lower portion of the enclosure. All boundary layers get thinner and a larger

**Table 1. Baseline parameters (all parameters except the one being studied revert to these) and the range of parameters**

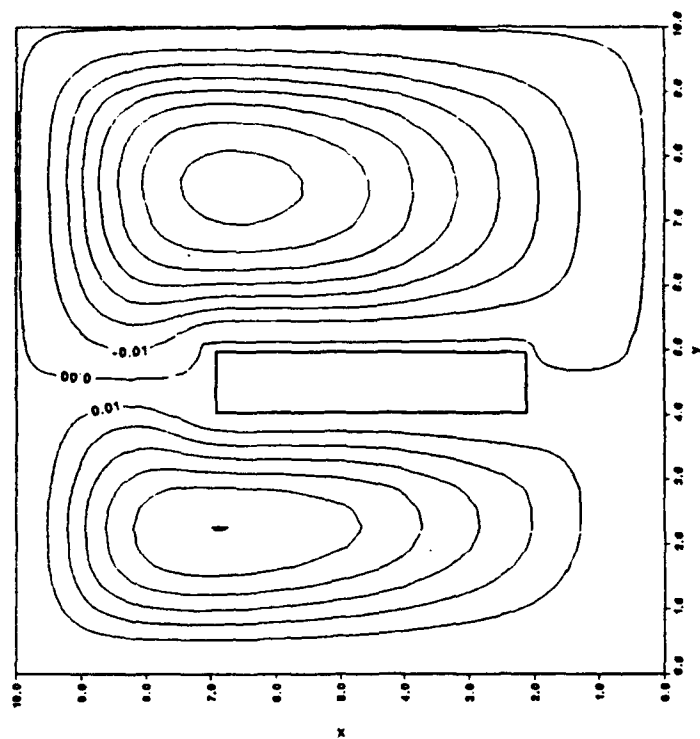
Parameter	Baseline value	Range studied
Ra	$10^5$	$10^3, 10^4, 10^5, 10^6$
Pr	25	7, 25, 100
$R_s$	10	.1, 1, 10, 50, 100
$R_c$	25	1, 25, 50, 100
$w/d_t$	.5	.25, .5, .75, .999

thermal gradient occurs in the fluid next to the substrate and the enclosure top and sides.

Figures 2(a)-(d) also show changes in the streamline patterns with more vigorous flow with an increase of Ra. The flow travels up on both sides of the package. The flow forms two cells with the right cell being somewhat larger and stronger, due to the direct heater-fluid interaction. Flows are nearly symmetric on the right and left and as Ra is increased the eddy centers move up and toward one another. Also as Ra is increased, the fluid in the lower right portion of the enclosure becomes increasingly stagnant.

The heat loss through each face of the component is shown in Fig. 3. As Ra is increased the percentage of the heat lost directly to the fluid i.e. from the front face, is increased due to the increased convection. As Ra increases the percentage of heat lost from the top and bottom of the enclosure decreases as shown in Fig. 4, and the heat lost to the sides of the enclosure increases. The heat loss through the enclosure bottom is below 5

Streamlines



Temperature Contours

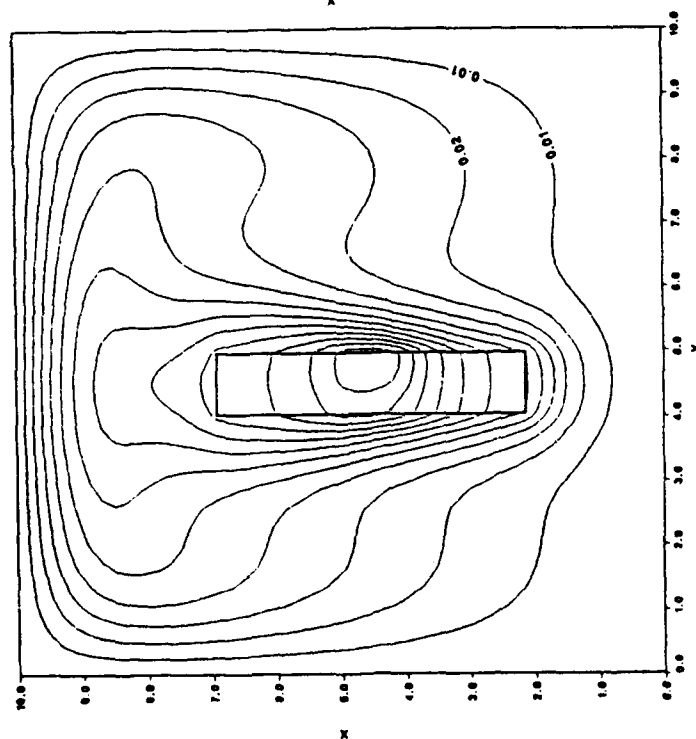
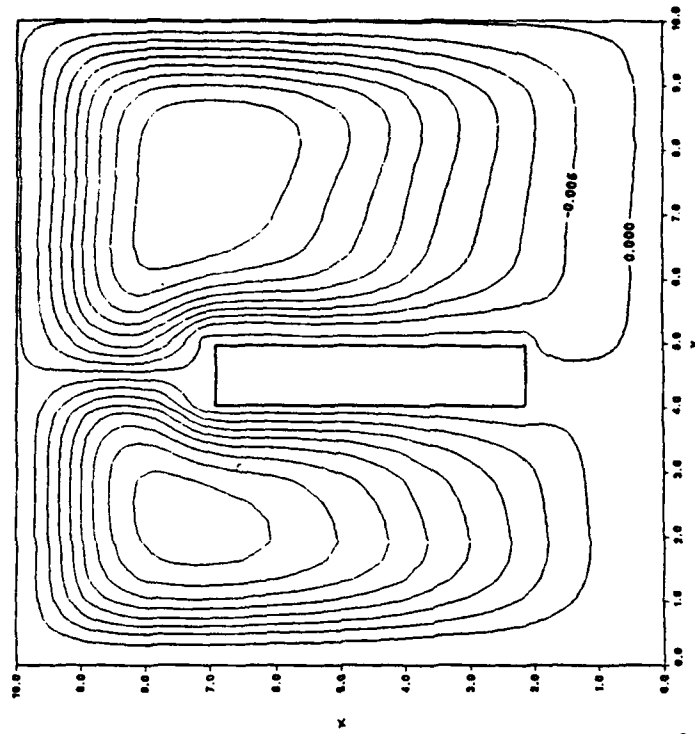


Figure 2(a). Temperature contours and streamlines for  $Ra=10^3$



Streamlines



Temperature Contours

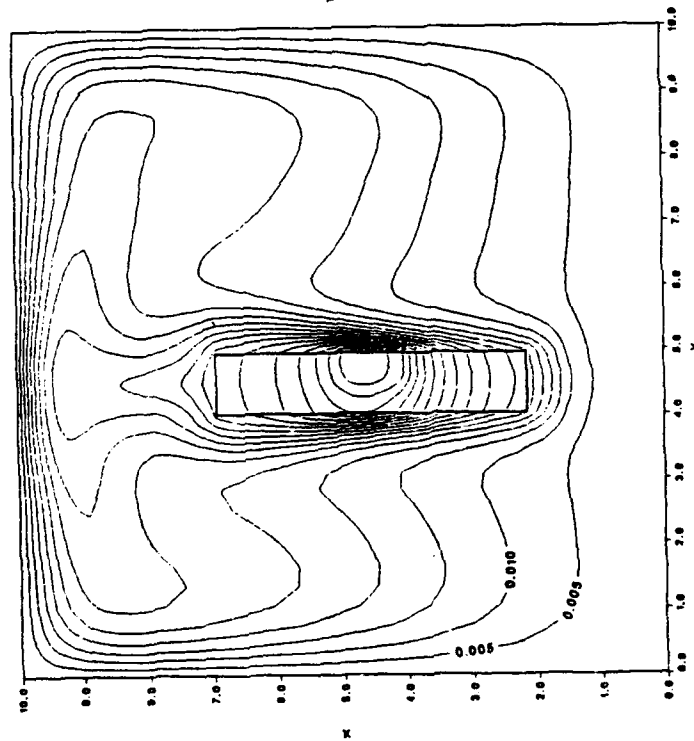
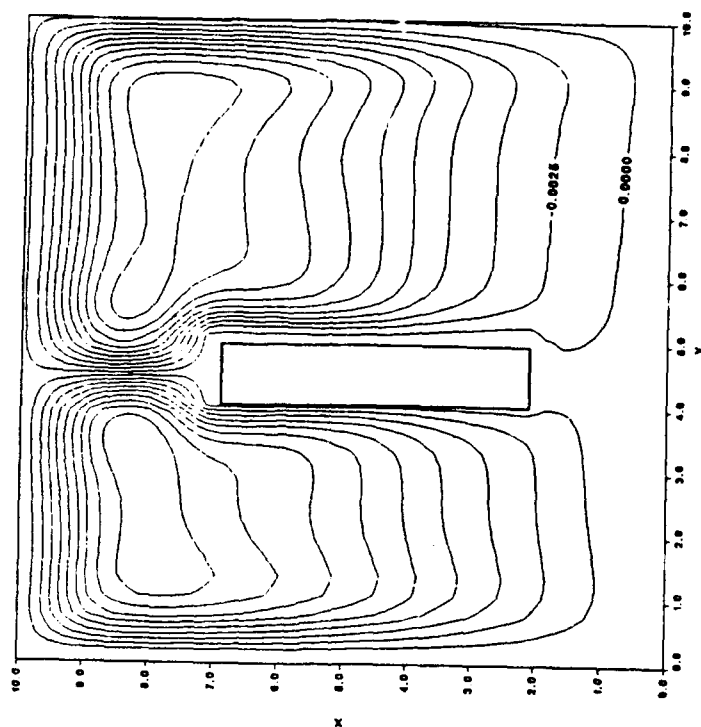


Figure 2(b). Temperature contours and streamlines for  $Ra=10^4$

Streamlines



Temperature Contours

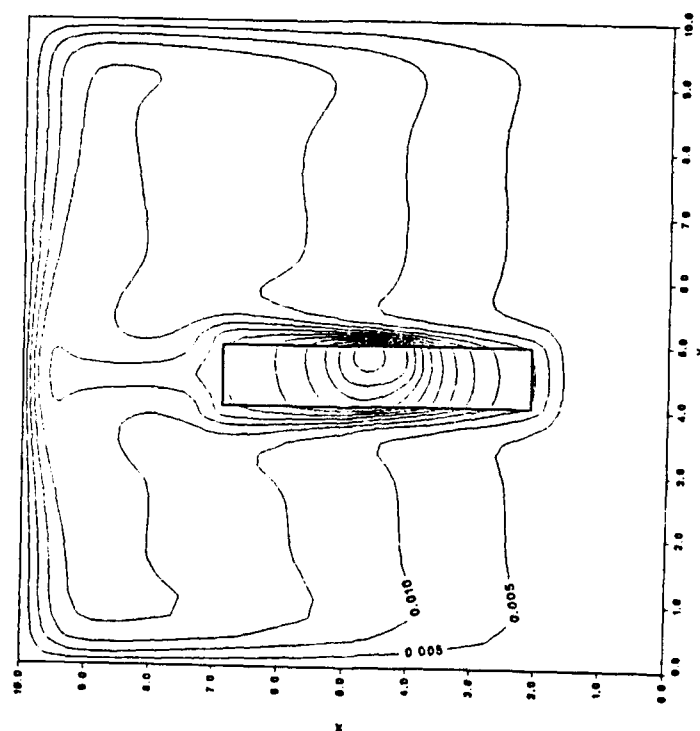
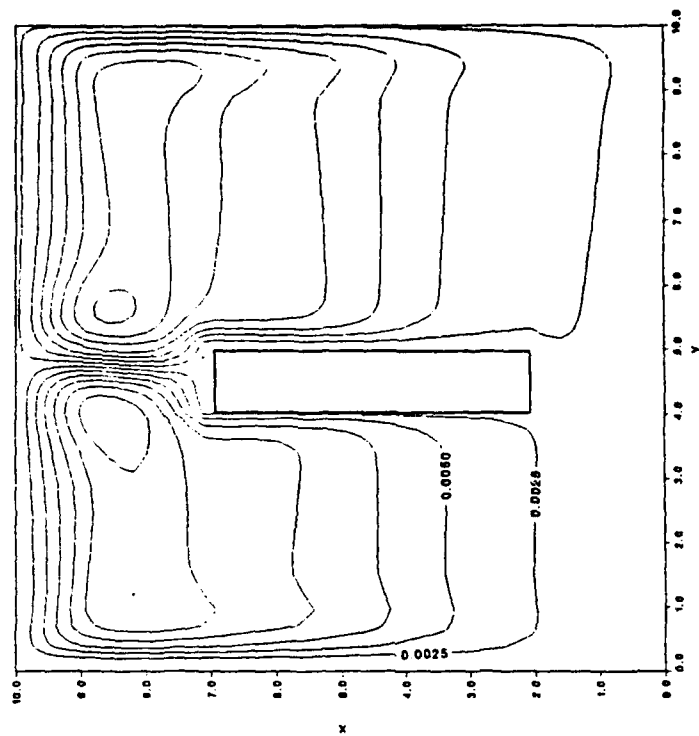


Figure 2(c). Temperature contours and streamlines for  $Ra=10^5$

Streamlines



Temperature Contours

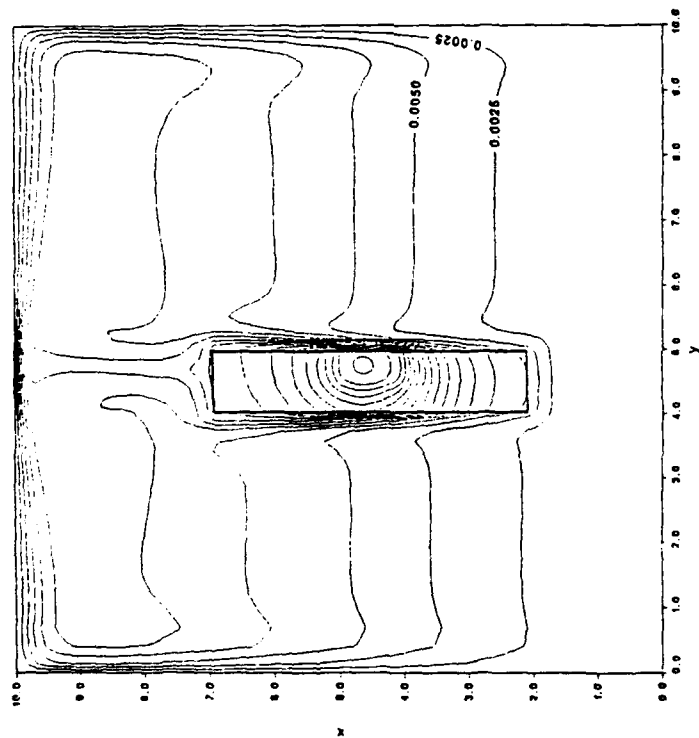


Figure 2(d). Temperature contours and streamlines for  $Ra=10^6$

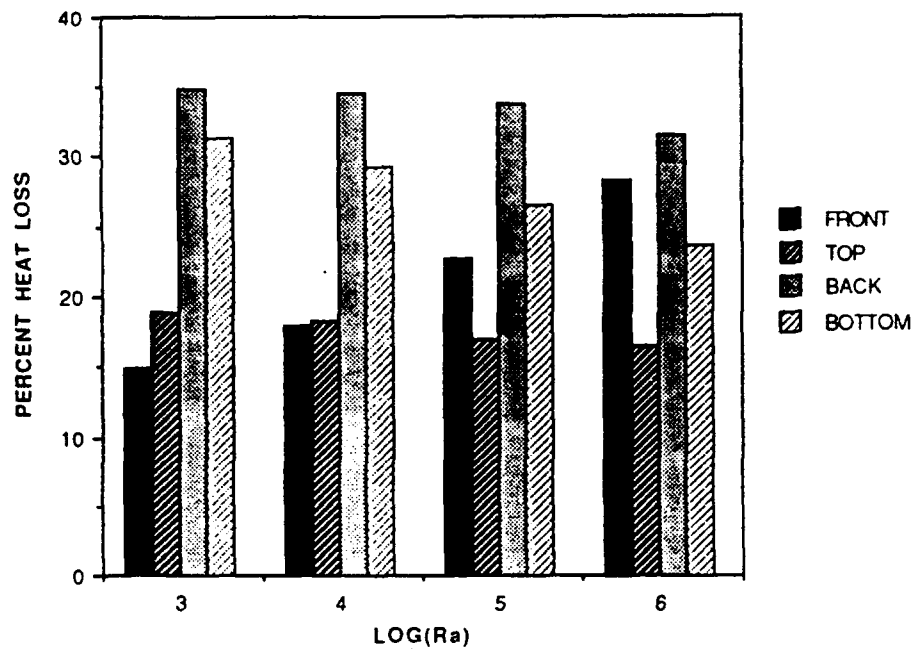


Figure 3. Heat loss through component faces for various  $Ra$

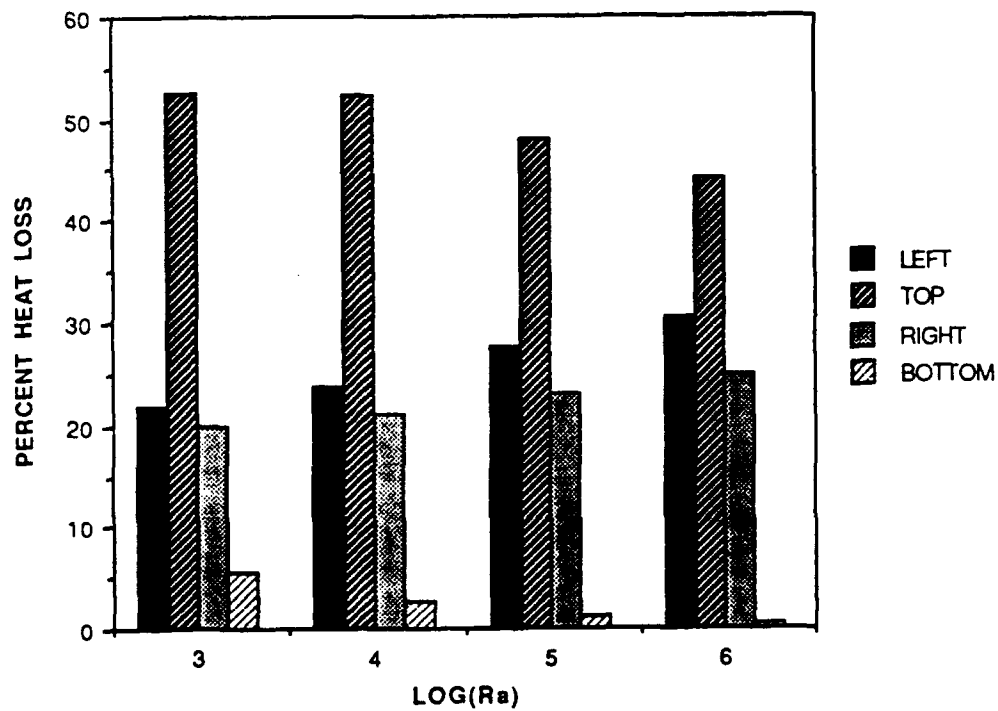


Figure 4. Heat loss through enclosure walls for various  $Ra$

percent for all Ra shown but it decreases with an increase in Ra due to increased thermal stratification near the bottom. There is a greater percentage of heat loss through the left wall than the right even though the right wall faces the component and the flow is greater on the right. This is because the left wall is closer to the substrate and heater than the right wall. It is interesting to note that the top wall dissipates almost half the heat generated by the component.

Figure 5 shows the substrate nondimensional surface heat flux ( $q$ ) which is defined as:

$$q = \frac{(T_s - T_f)}{\left( \frac{\delta x_s}{\kappa_s} + \frac{\delta x_f}{\kappa_f} \right)} \quad (7)$$

Table 2 describes the values of S2 corresponding to its location on the substrate. Heat fluxes are not defined at the corners.  $S2=0$  at the lower right corner of the substrate and goes counter-clockwise around the solid-fluid boundary including the component-fluid boundary. The same general trend for the variation of heat flux with S2 is seen for all Ra. The heat flux goes through a minimum at  $S2 \approx 0.5$  after which it rapidly reaches its maximum value at  $S2=2$ , at the base of the component. The heat flux then decreases going up the component and when the substrate above the component is reached at  $S2=3$  it decreases even more steeply, going through a minimum at  $S2 \approx 4.5$  prior to reaching the top right corner. At the top right corner the heat flux decreases sharply again going over the top substrate face and comes to the minimum heat flux on the substrate at the

**Table 2. Ranges of S2 corresponding to different solid-fluid interfaces**

Surface no. in Fig. 1	X	Y	S2
1	0 to 2	0	0 to 2
2	2 to 3	0	2 to 3
3	3 to 5	0	3 to 5
4	5	0 to -1	5 to 6
5	5 to 0	-1	6 to 11
6	0	-1 to 0	11 to 12

midpoint of the top face at  $S2=5.5$ . Reviewing the temperature contours in Figs. 2(a)-(d), this is where the fluid temperature is the hottest next to the substrate. The heat flux on the top face is nearly symmetric. Proceeding down the substrate left face the heat flux goes through a small dip but quickly increases as one approaches the back of the component. It reaches a local maximum heat flux at the back of the base of the component at  $S2 \approx 9$  and then decreases to a local minimum at  $S2=10.25$ . It then increases and comes to a local maximum at the bottom left corner at  $S2=11$ . The heat flux on the bottom face shows the same symmetry as the top, however it is much higher due to colder fluid in the vicinity of the bottom face.

Nondimensional substrate surface temperatures ( $T_{sur}$ ) for various  $Ra$  are shown in Fig. 6. The substrate surface temperature is computed using the harmonic mean formulation as:

$$T_{sur} = \frac{\left( \left( \frac{\delta X_s}{\kappa_s} \right) T_s + \left( \frac{\delta X_f}{\kappa_f} \right) T_f \right)}{\left( \frac{\delta X_s}{\kappa_s} + \frac{\delta X_f}{\kappa_f} \right)} \quad (8)$$

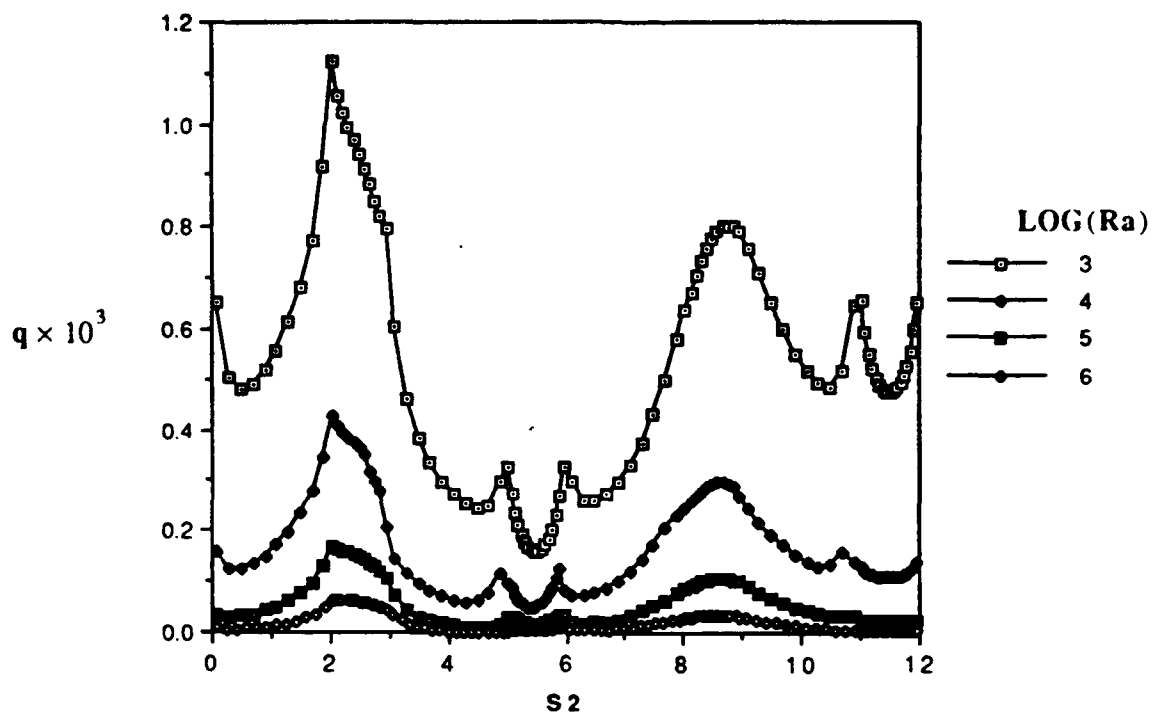


Figure 5. Substrate surface heat flux for various Ra

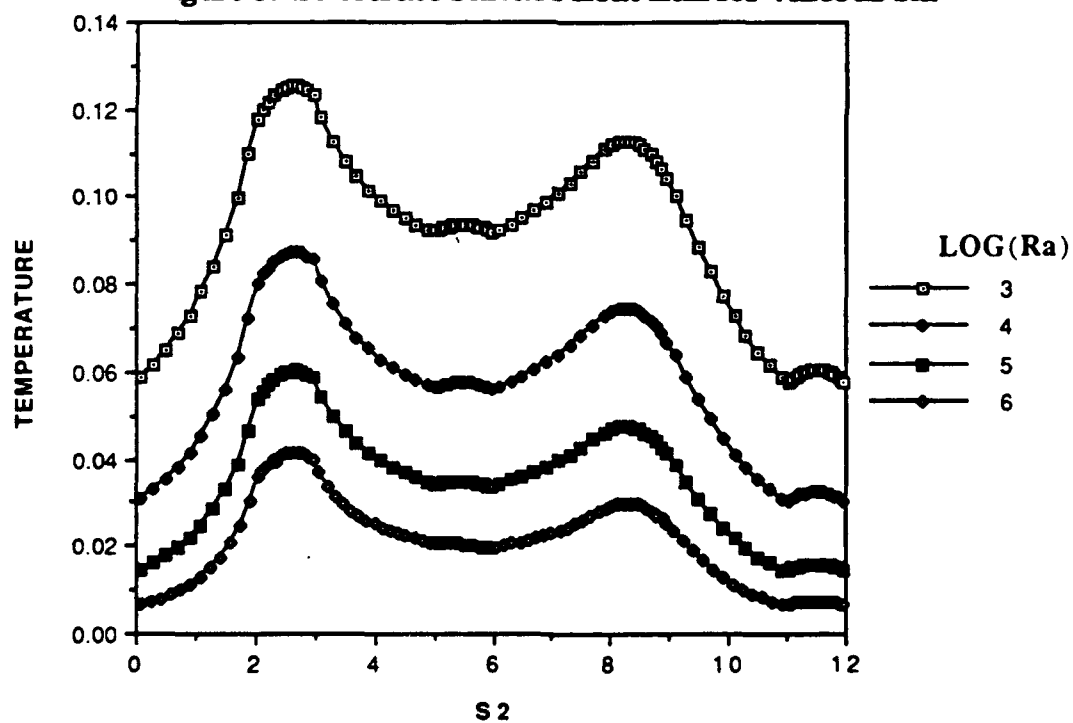


Figure 6. Substrate surface temperature for various Ra

The lowest temperatures are at the bottom of the substrate and the highest are at the top of the component. Local maxima are evident at the back of the substrate due to direct conduction from the heater. The nondimensional temperatures are higher for the lower  $Ra$ . The higher the  $Ra$ , the greater the buoyancy induced flow and hence higher heat transfer from the component, leading to lower non-dimensional temperatures. Note that if  $Q$  and  $k_f$  are held fixed, a higher  $T$  implies a higher actual (dimensional) temperature. In such a case, higher  $Ra$  can be obtained by using a liquid with higher  $\rho$ , leading to higher buoyant forces, enhanced convection and reduced actual temperatures. Thus the dimensional results are consistent with the non-dimensional trends.

Figure 7 shows the nondimensional component surface heat flux for various  $Ra$  versus  $S1$ . Table 3 shows the corresponding position of the component to  $S1$  with  $S1=0$  at the lower right corner of the component and increasing going counter-clockwise around the component. Fluxes for all  $Ra$  show similar trends. The component front face, in direct contact with the fluid, has the lowest heat flux. The top face has the second highest heat flux and the back face has a slightly lower heat flux. The bottom of the component has generally the greatest heat flux. The largest heat flux is near the bottom right corner.

The trends of Fig. 8 show the component nondimensional surface temperatures to be similar for all  $Ra$ . Surface temperatures are fairly uniform around the component with the highest temperature near the top on the front face. The high  $R_h$  and  $R_c$  values allow the heat to be uniformly spread so that the component temperature remains fairly uniform.



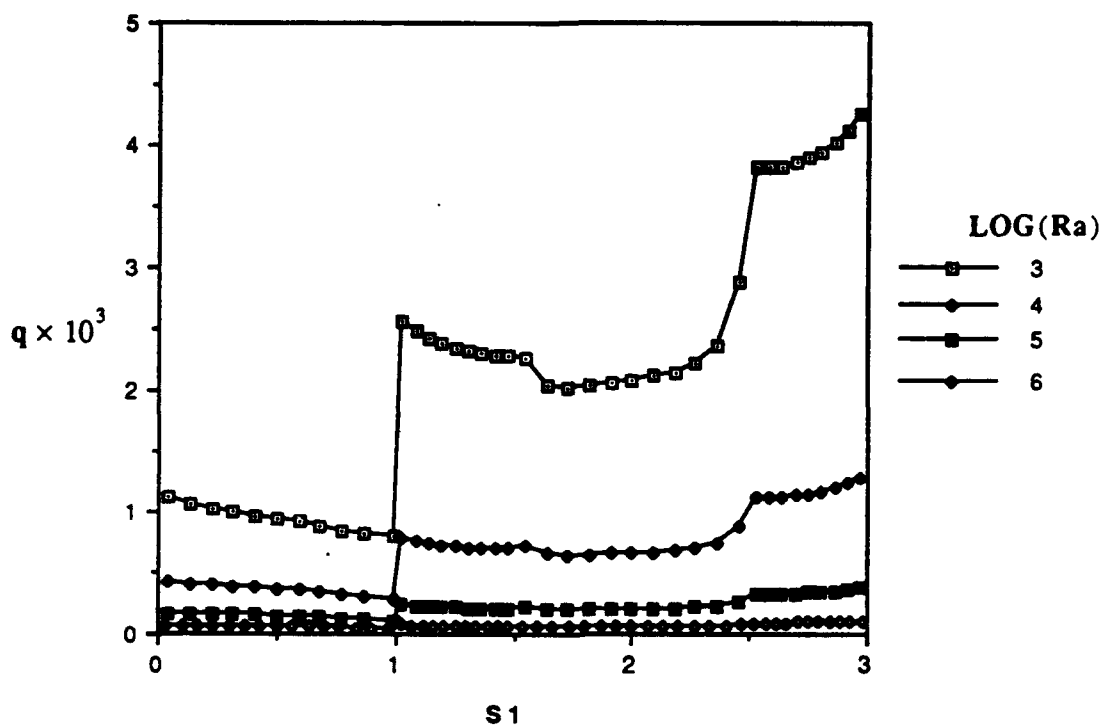


Figure 7. Component surface heat flux for various Ra

Table 3. Ranges of S1 corresponding to different component faces

Component Face	X	Y	S1	Interface*
Front	2 to 3	0	0 to 1	c-f
Top	3	0 to -.5	1 to 1.5	c-s
Back	3 to 2	-.5	1.5 to 2.5	c-s
Bottom	2	-.5 to 0	2.5 to 3	c-s

\* c-f indicates component-fluid interface and c-s indicates component-substrate interface

Maximum temperature versus  $Ra$  is shown in Fig. 9(a). A decrease in the maximum temperature from 0.122 to 0.042 is observed for an increase in  $Ra$  from  $10^3$ - $10^6$ . Fig. 9(b) shows that the change in maximum temperature versus  $Ra$  is similar for all  $w/d_t$ . Although nondimensional temperature decreases, the dimensional temperature may go up because the nondimensional temperature is inversely proportional to the heat transfer coefficient. An increase in  $Q$  would bring about an increase in the dimensional temperature but a decrease in the nondimensional temperature. As  $Q$  increases, the natural convection flow velocities increase and this would increase the heat transfer coefficient.

## **B. EFFECT OF $Pr$**

Fluorinert dielectric liquids used in immersion cooling have  $Pr$  values much greater than 1. Computations for  $Pr=7$ ,  $Pr=25$  and  $Pr=100$  were therefore conducted. These revealed that with other parameters remaining constant,  $Pr$  had a negligible effect on temperature contours, streamlines, heat flux or temperatures as is seen in Figs. 10-17. This would indicate that the results of experimental studies in water with  $Pr=7$  would apply to the dielectric liquids as well for the same value of  $Ra$  and other parameters.

## **C. EFFECT OF SUBSTRATE CONDUCTIVITY RATIO $R_s$**

The streamlines and temperature contours for various  $R_s$  values when  $Ra=10^5$  are shown in Figs. 18(a)-(e). For  $.1 \leq R_s \leq 1$  all the main flow is generated by the heater side with a very weak cell on the left side of the enclosure. When  $R_s$  reaches 10 both cells are of about the same strength and the streamlines form two cells that start on opposite sides of the

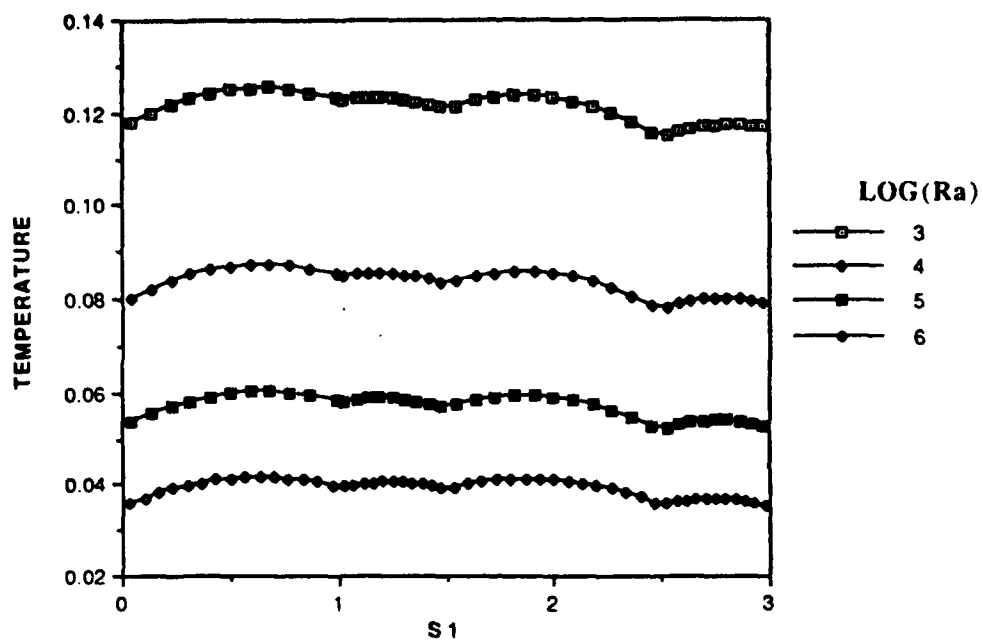


Figure 8. Component surface temperature for various  $Ra$

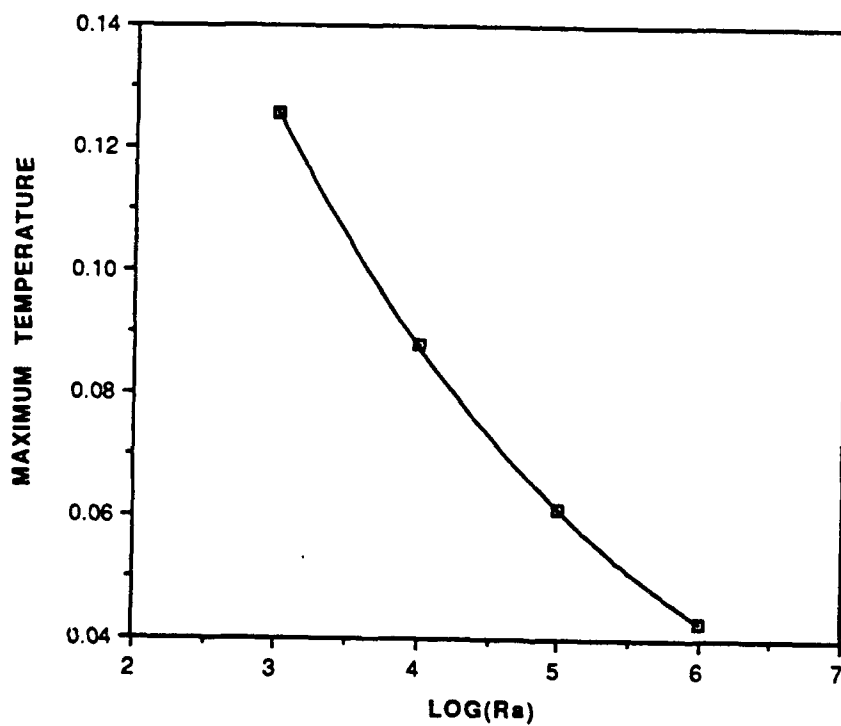


Figure 9(a). Maximum temperature versus  $\text{Log}(Ra)$ ,  $w/d_1=5$

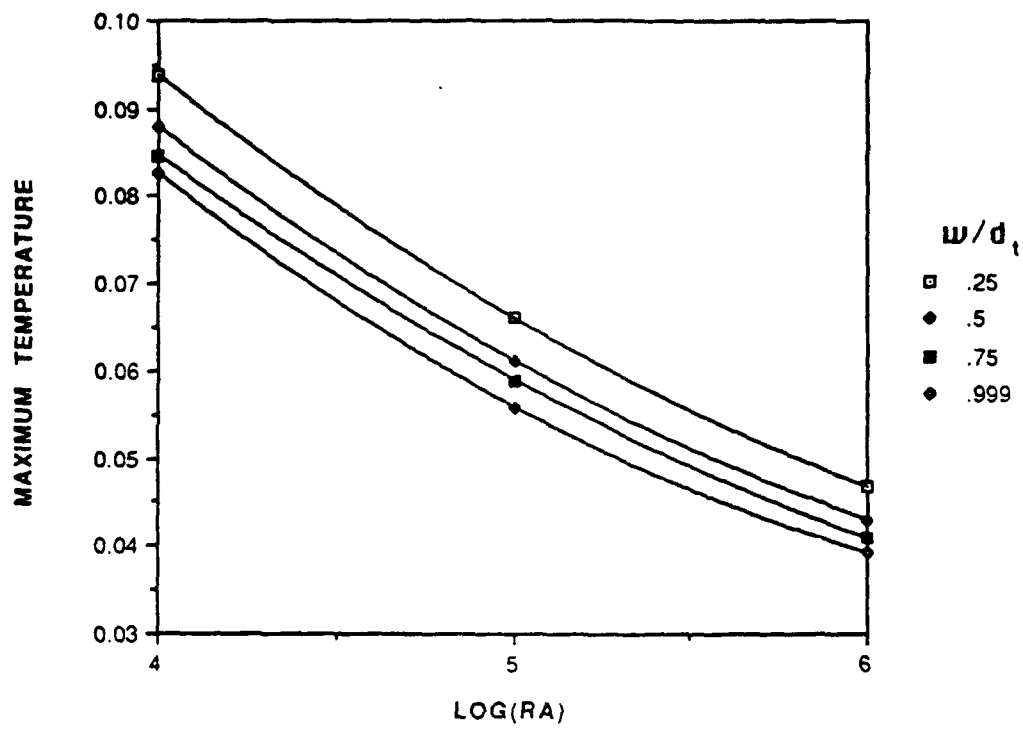
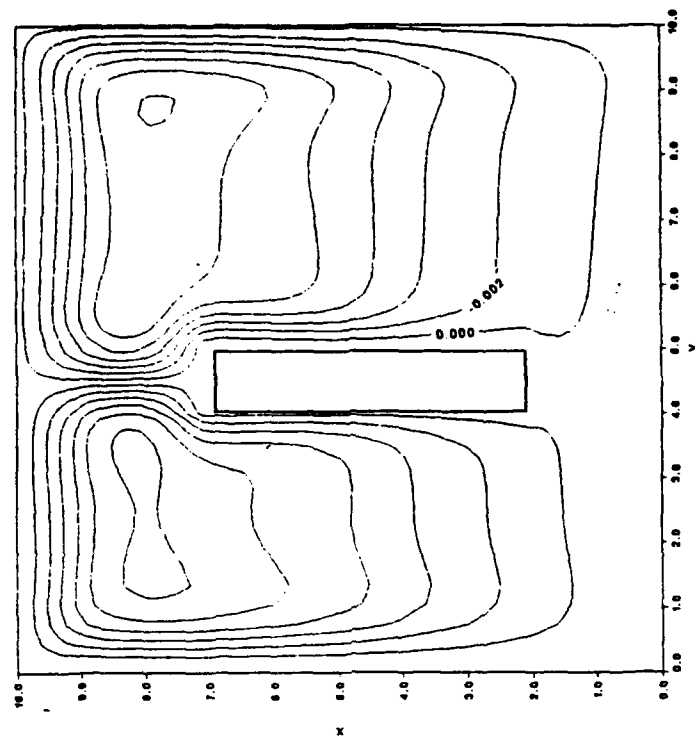


Figure 9(b). Maximum temperature versus Log(Ra) for various  $w/d_t$

Streamlines



Temperature Contours

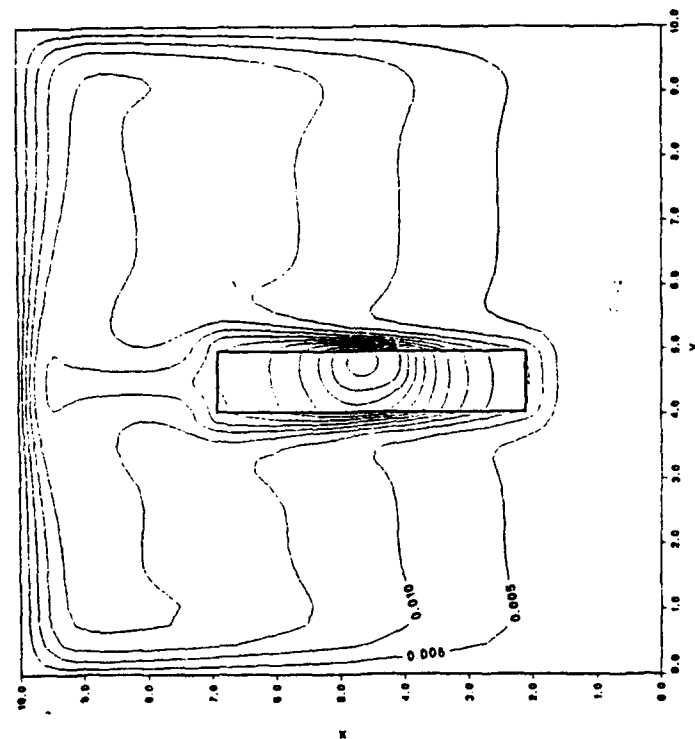
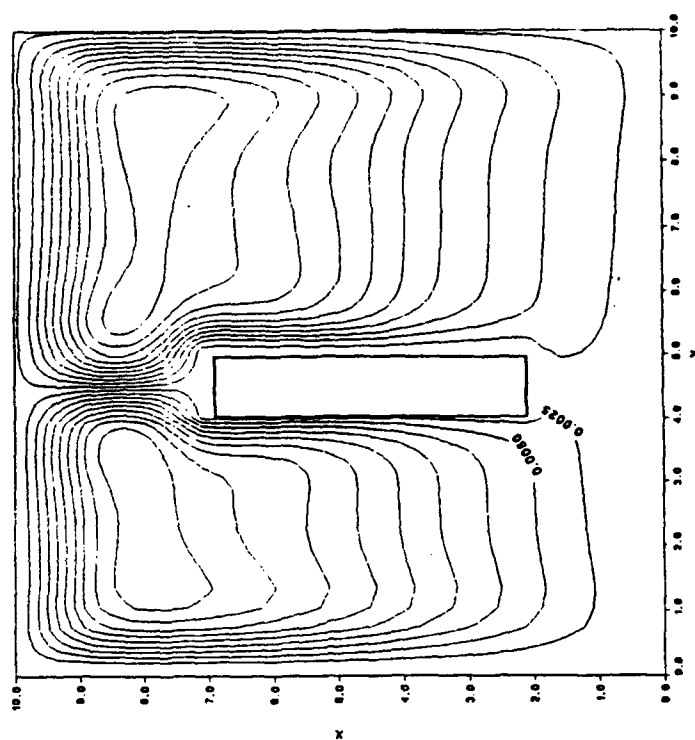


Figure 10(a). Temperature contours and streamlines for  $Pr=7$

Streamlines



Temperature Contours

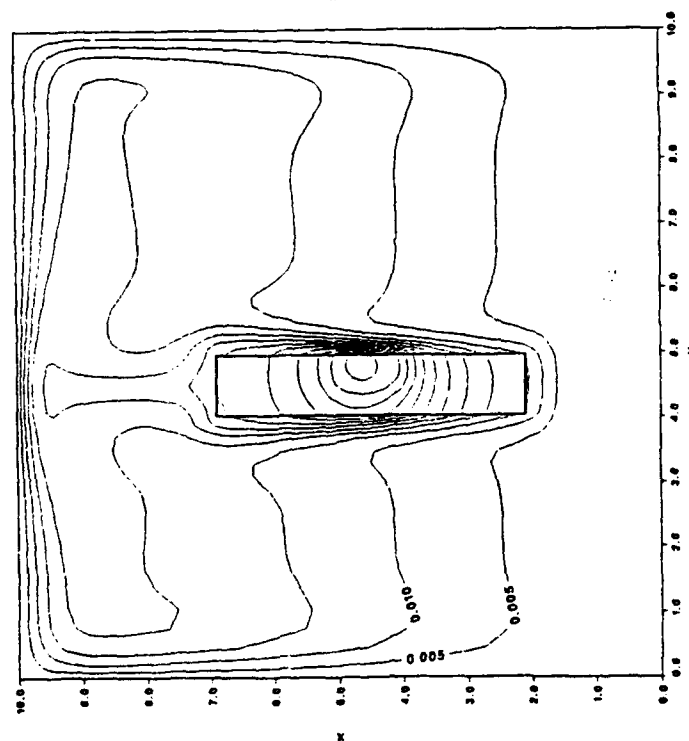
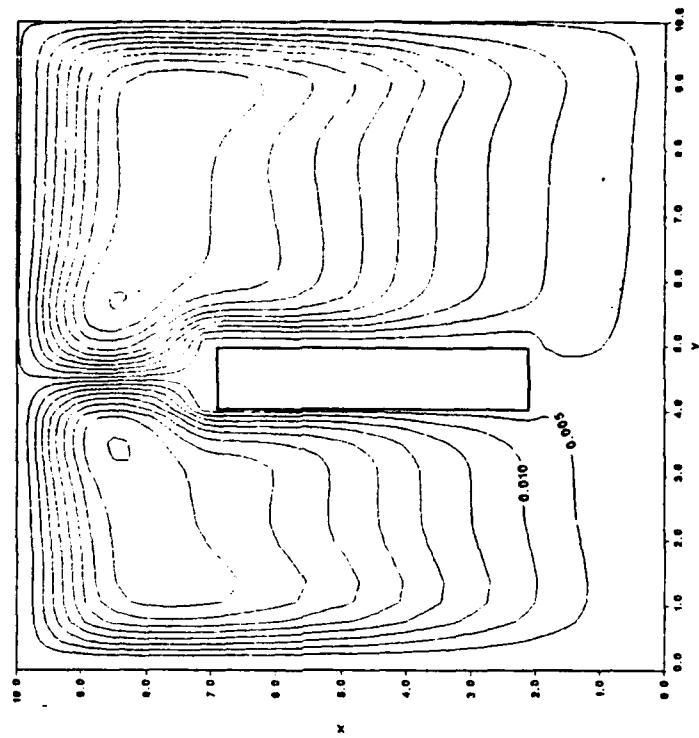


Figure 10(b). Temperature contours and streamlines for  $Pr=25$

Streamlines



Temperature Contours

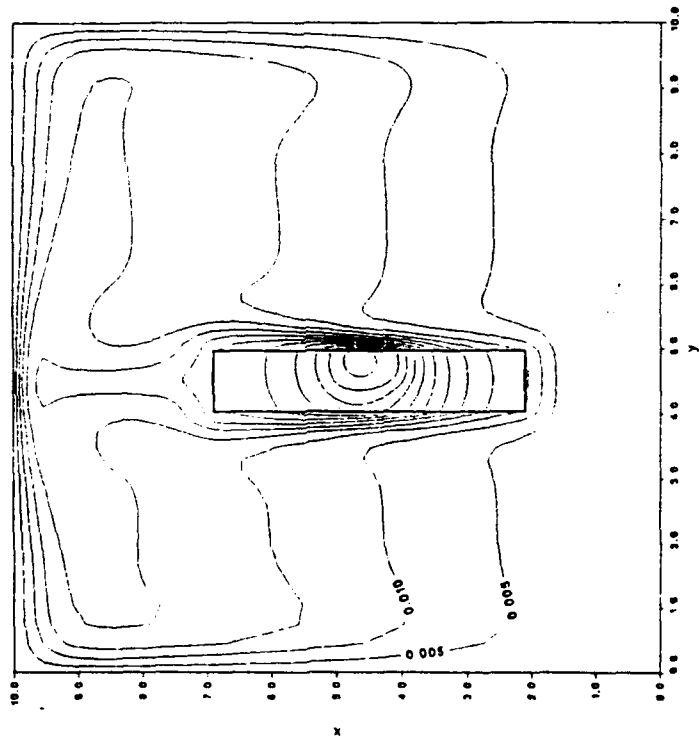


Figure 10(c). Temperature contours and streamlines for  $Pr=100$

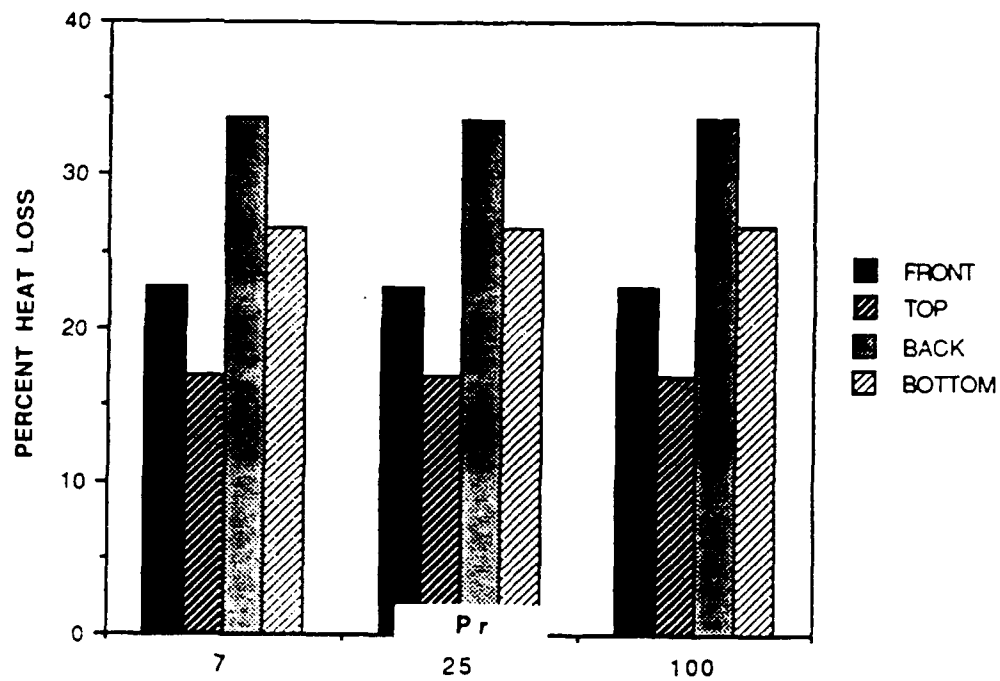


Figure 11. Heat loss through component faces for various Pr

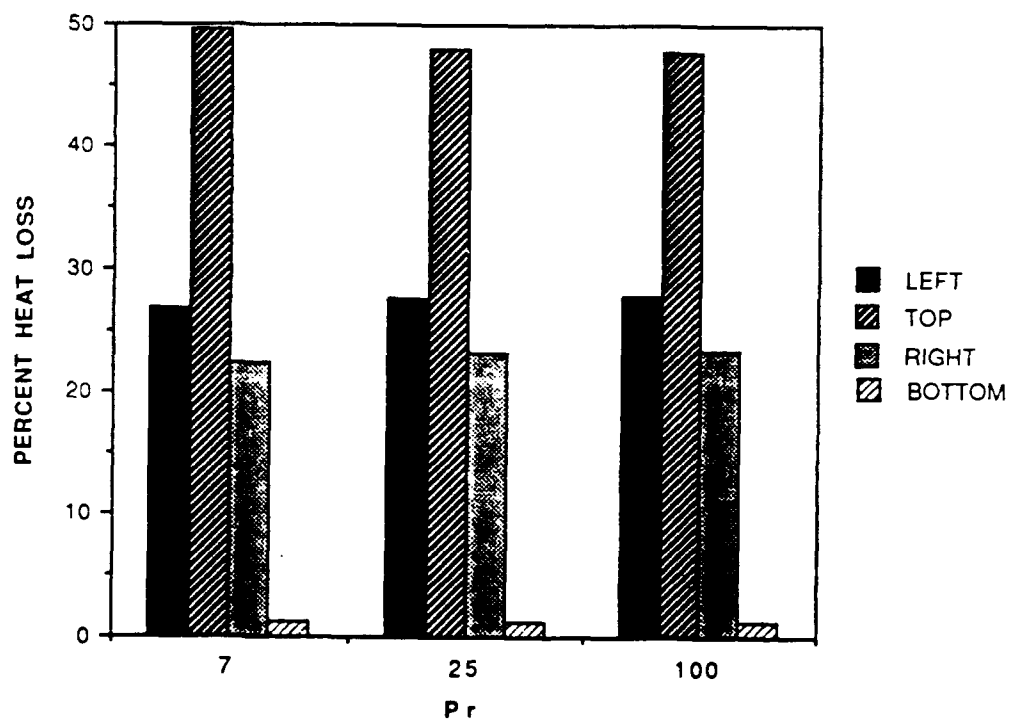


Figure 12. Heat loss through enclosure walls for various Pr



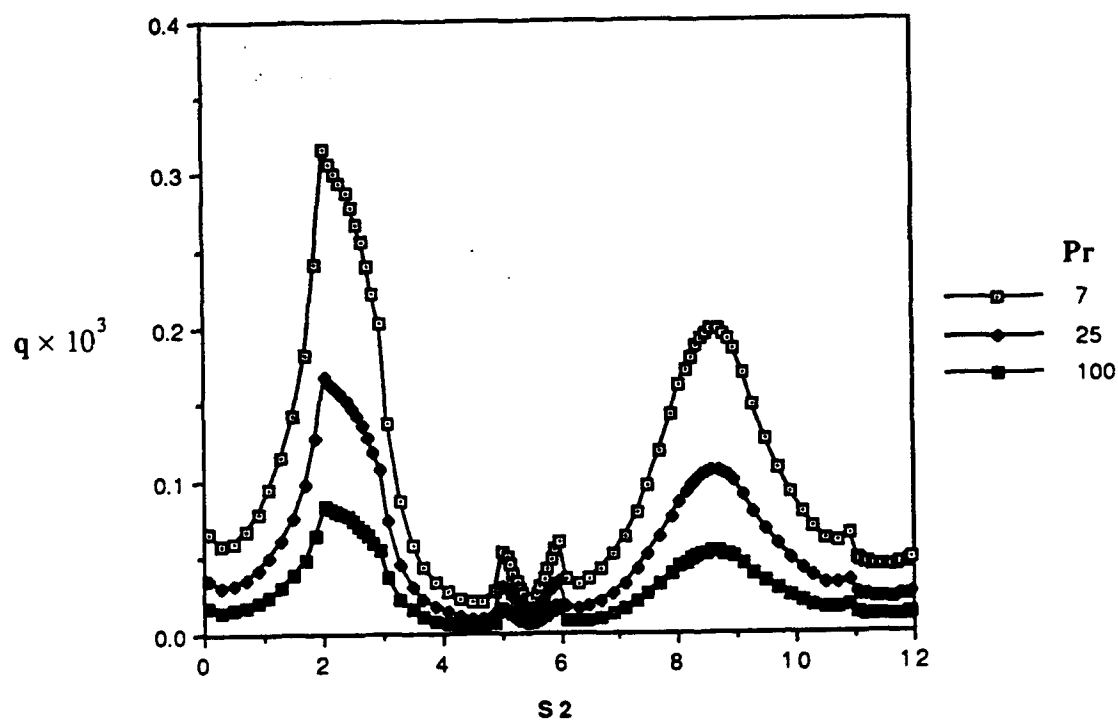


Figure 13. Substrate surface heat flux for various Pr

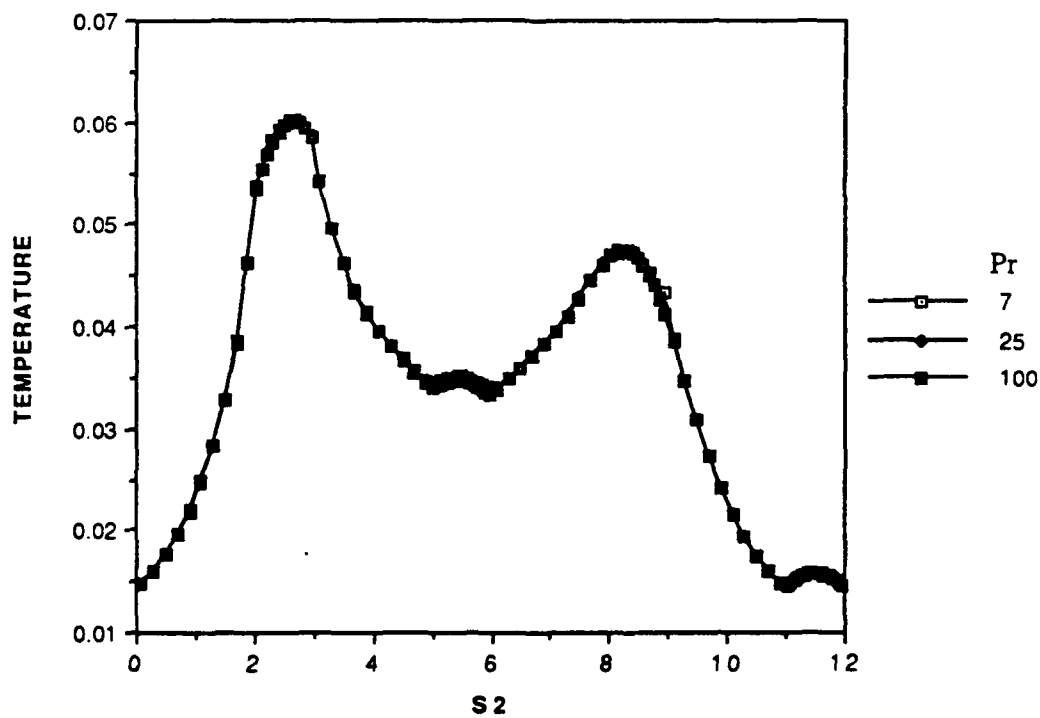


Figure 14. Substrate surface temperature for various Pr

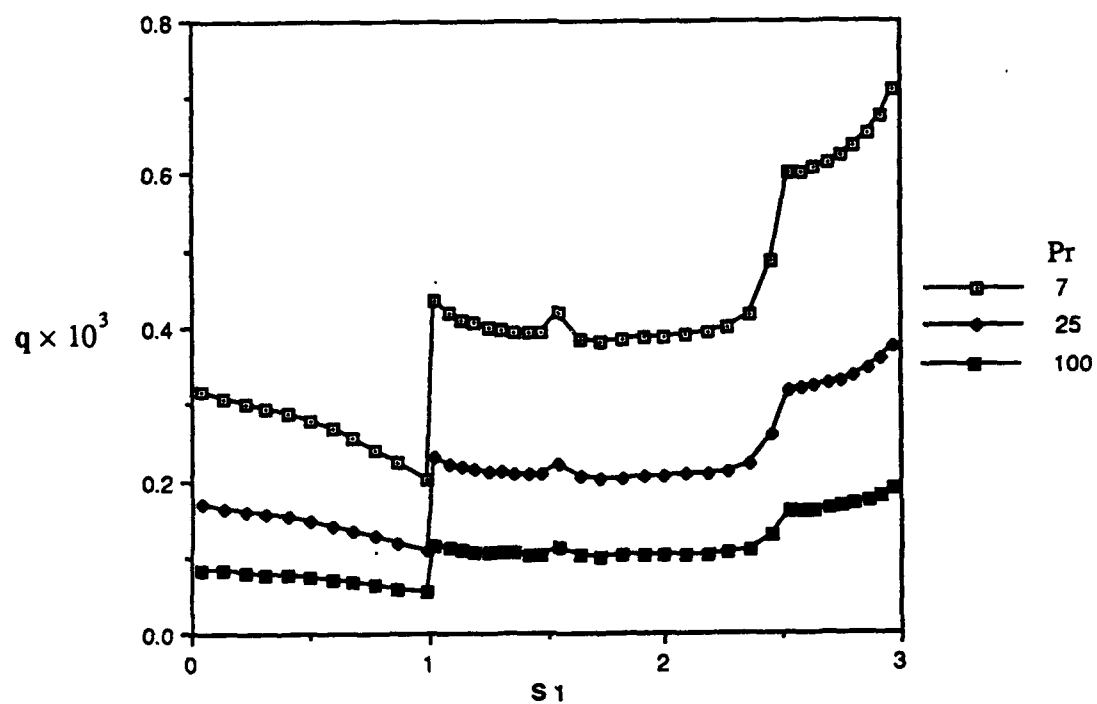


Figure 15. Component surface heat flux for various Pr

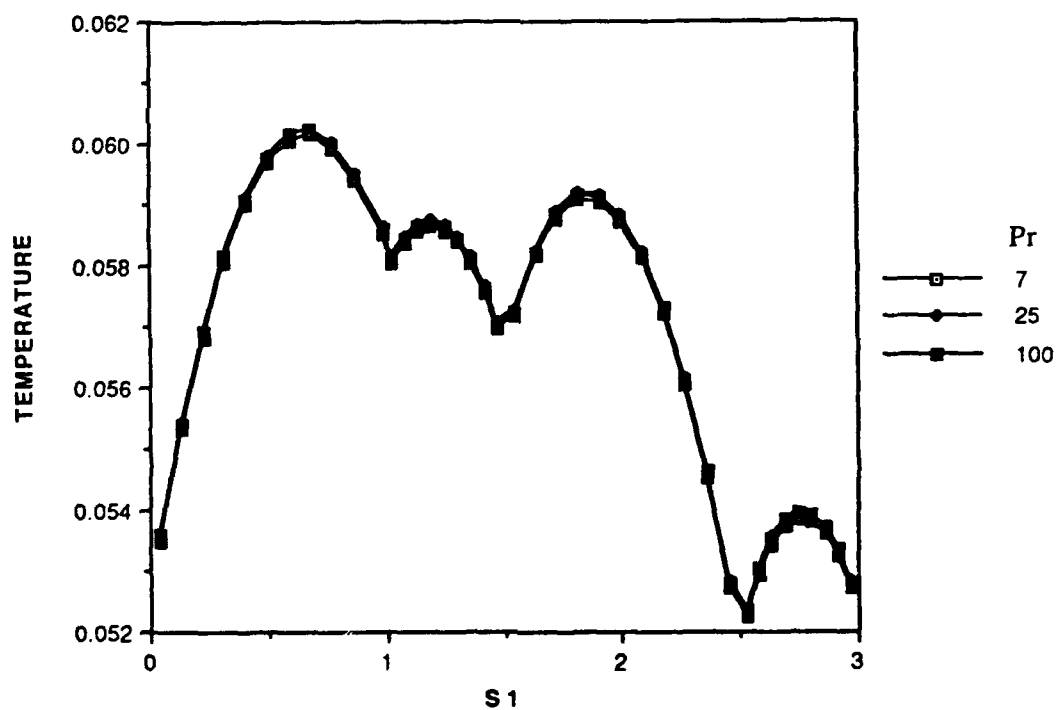


Figure 16. Component surface temperature for various Pr

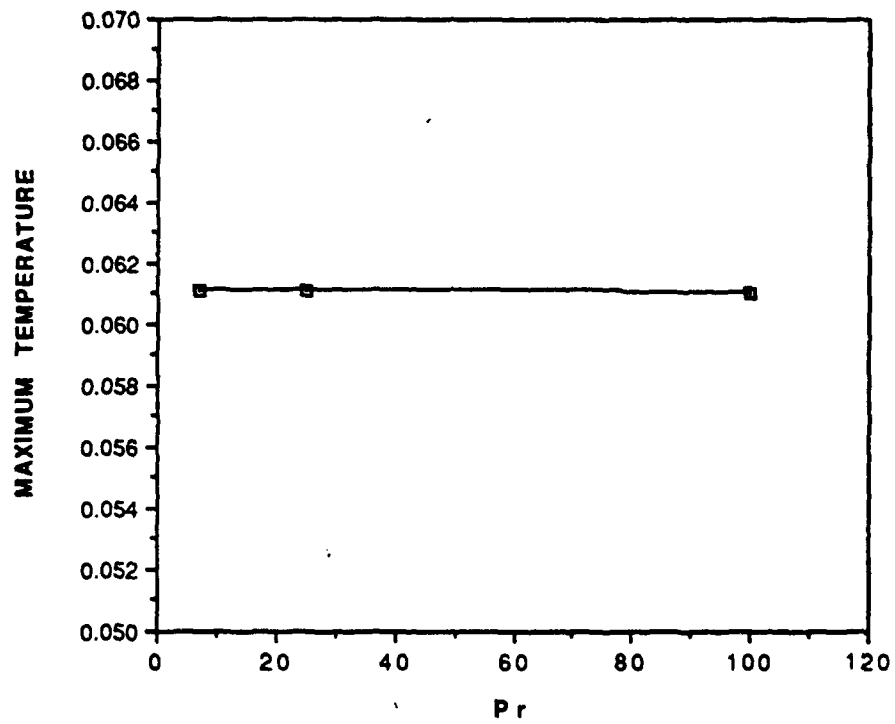
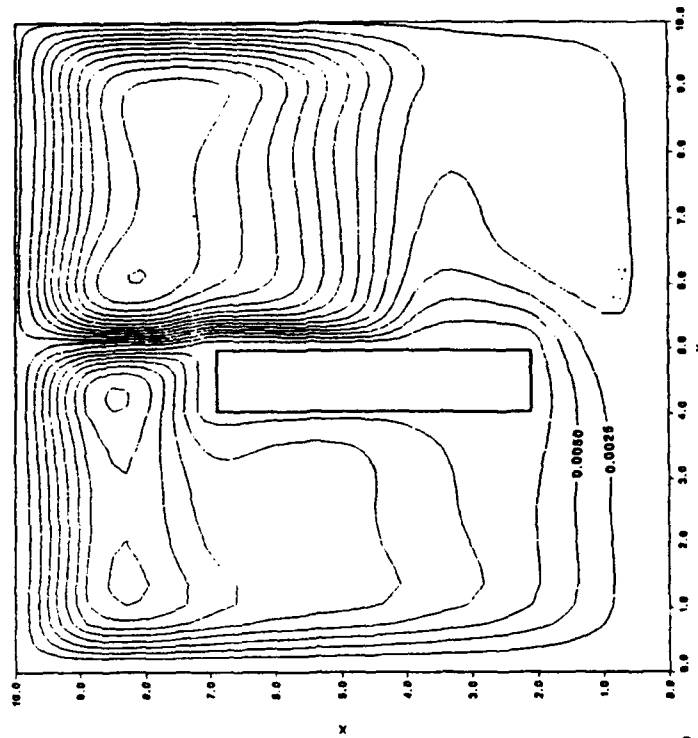


Figure 17. Maximum temperature versus Pr,  $Ra=10^5$

Streamlines



Temperature Contours

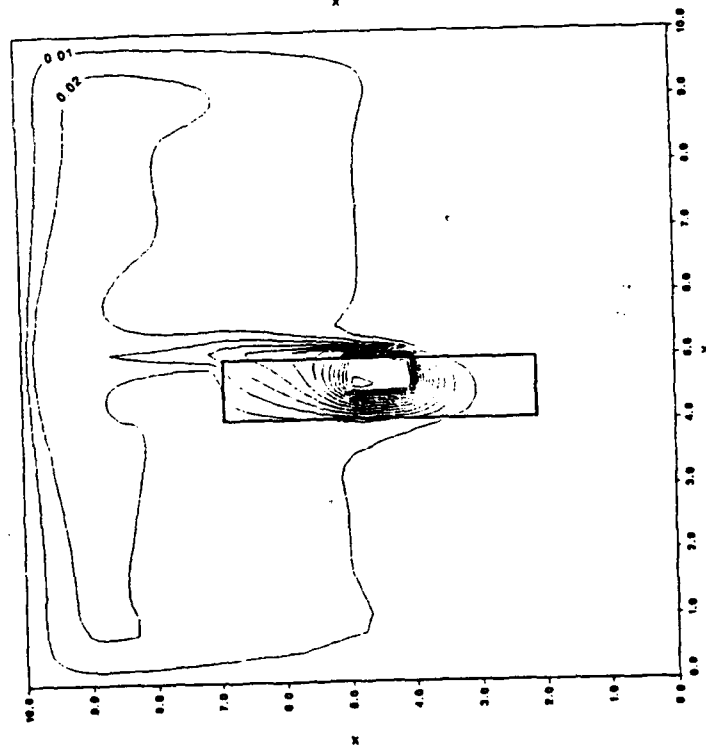
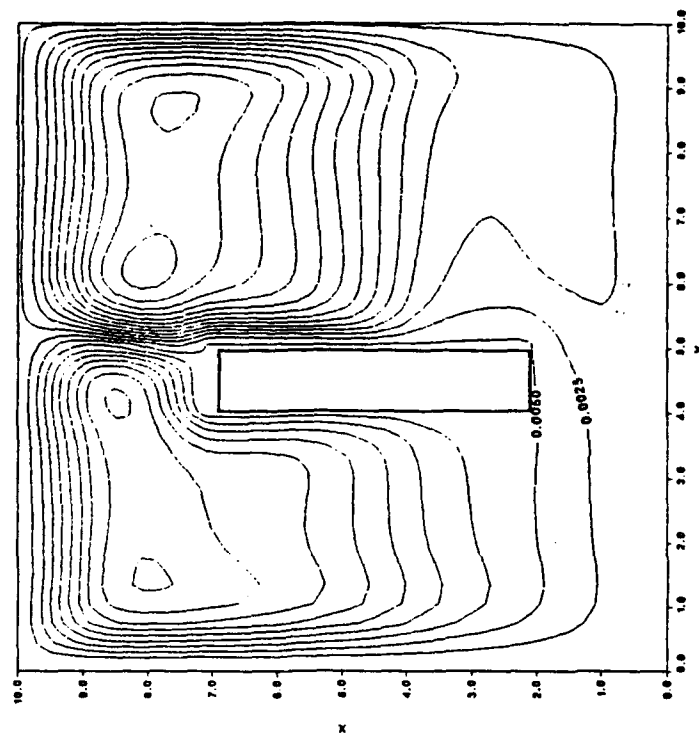


Figure 18(a). Temperature contours and streamlines for  $R_\nu=0.1$

Streamlines



Temperature Contours

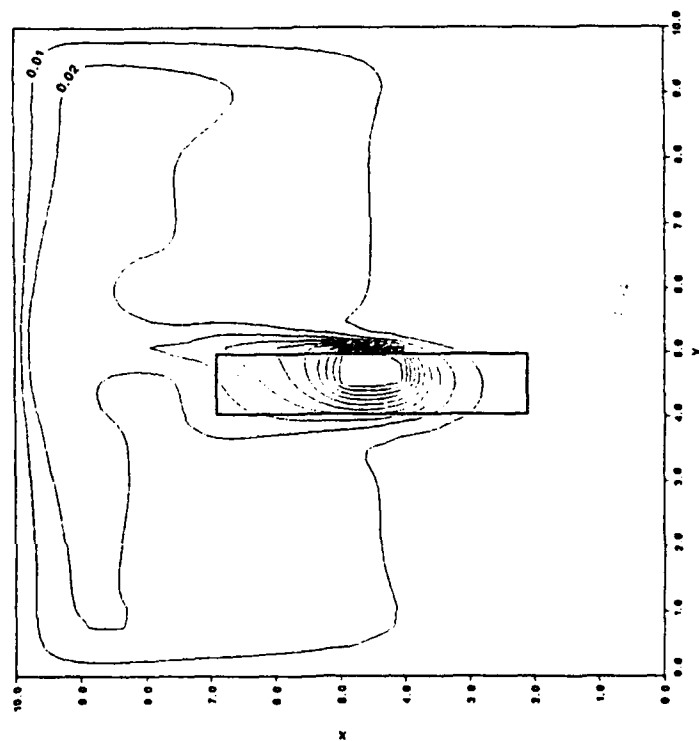
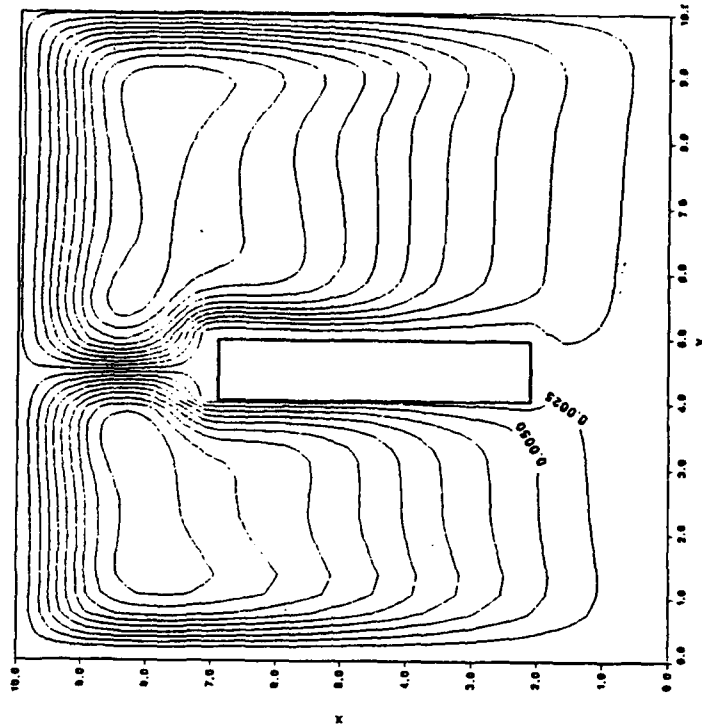


Figure 18(b). Temperature contours and streamlines for  $R_\nu=1$

Streamlines



Temperature Contours

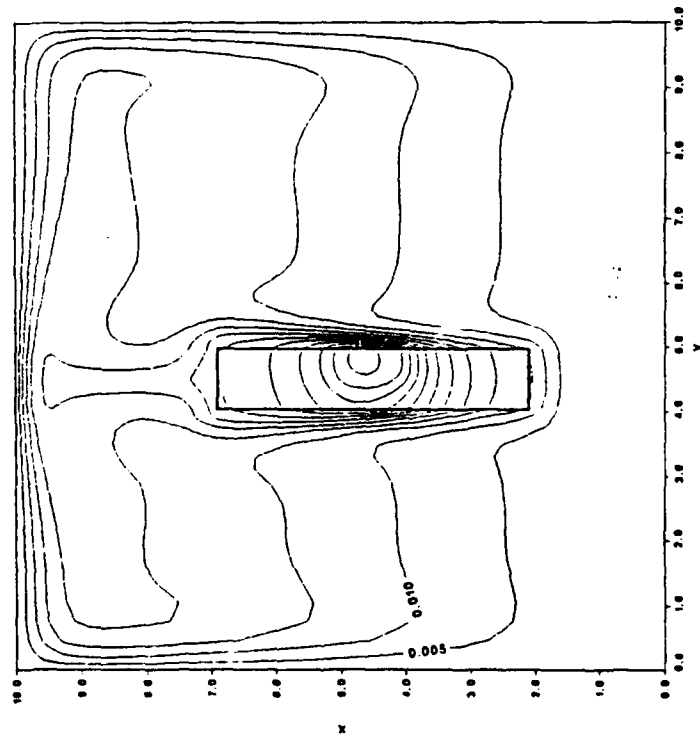
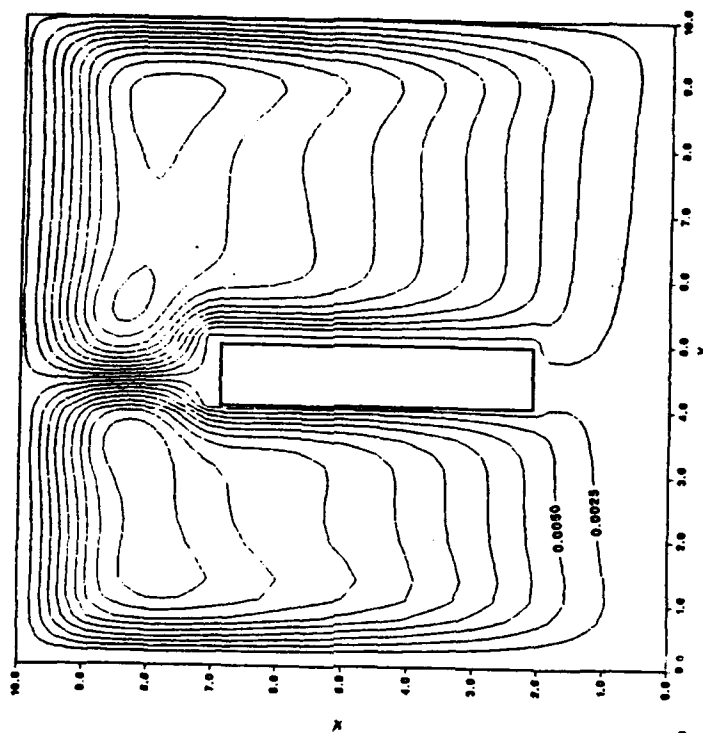


Figure 18(c). Temperature contours and streamlines for  $R_L=10$

Streamlines



Temperature Contours

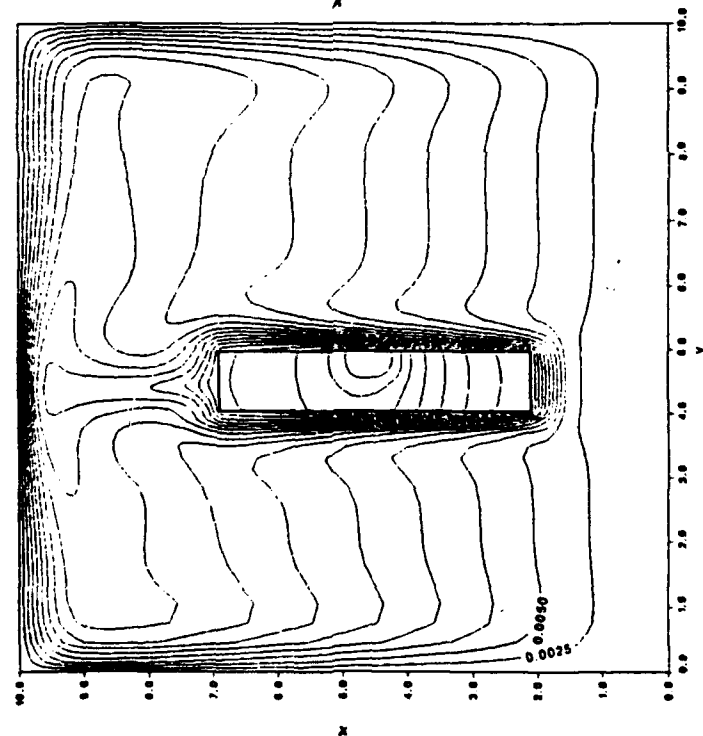
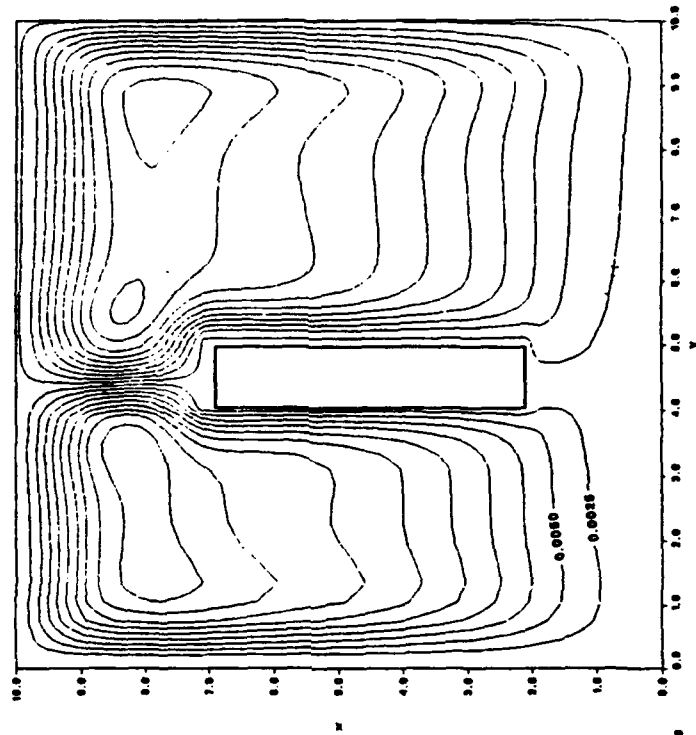


Figure 18(d). Temperature contours and streamlines for  $R_\mu=50$

Streamlines



Temperature Contours

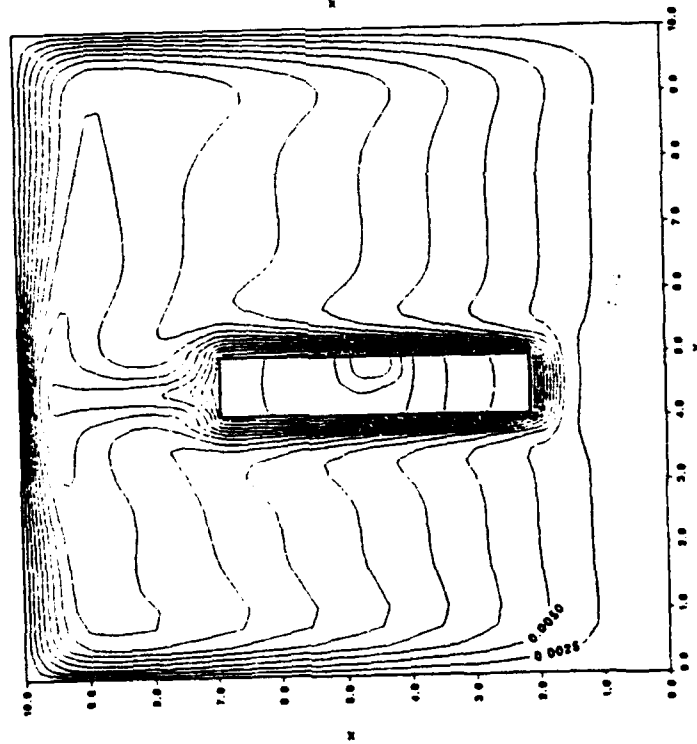


Figure 18(e). Temperature contours and streamlines for  $R_h=100$



substrate. Temperature contours and streamlines for  $10 \leq R_s \leq 100$  essentially look the same and it appears that there is little change in the induced flow beyond  $R_s=10$ . Temperature contours show a very high gradient just outside the component for  $R_s=0.1$  and the hot spot of the component is in the top left corner. For  $R_s=1$  the hot spot moves towards the center of the component and as  $R_s$  increases the component hot spot moves towards the fluid.

Figure 19 shows the percent heat loss through the component faces for various  $R_s$  with  $Ra=10^5$ . There is a tremendous decrease in the percent heat loss to the fluid from the front face when  $R_s$  is increased from 1 to 10 after which it shows only a slight decrease. As the conductivity of the substrate increases it is easier for the heat to flow through faces other than the front. The substrate acts like a fin, increasing the surface area where heat loss can occur. The back face percent heat loss increases throughout the range of  $R_s$  increase. The bottom and top face percent heat loss increase when  $R_s$  is increased from 0.1 to 10 and then remain fairly constant.

The percent heat loss through the enclosure walls for various  $R_s$  is shown in Fig. 20. The bottom wall initially shows a slight decrease when  $R_s$  increases from 0.1 to 1 due the left cell of the flow in the fluid bringing higher temperatures closer to the bottom wall and then a slight increase over the remaining range of  $R_s$  due to the increased heat conduction through the bottom portion of the substrate into the vicinity of the bottom wall. The other percent heat loss changes are a combination of the increased thermal conductivity and flow changes.

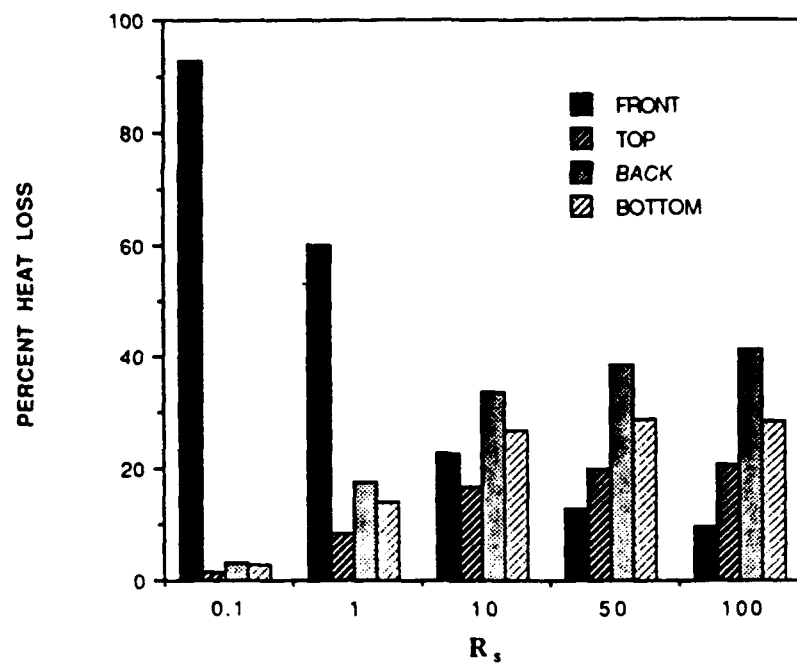


Figure 19. Heat loss through component faces for various  $R_s$ ,  $Ra=10^5$

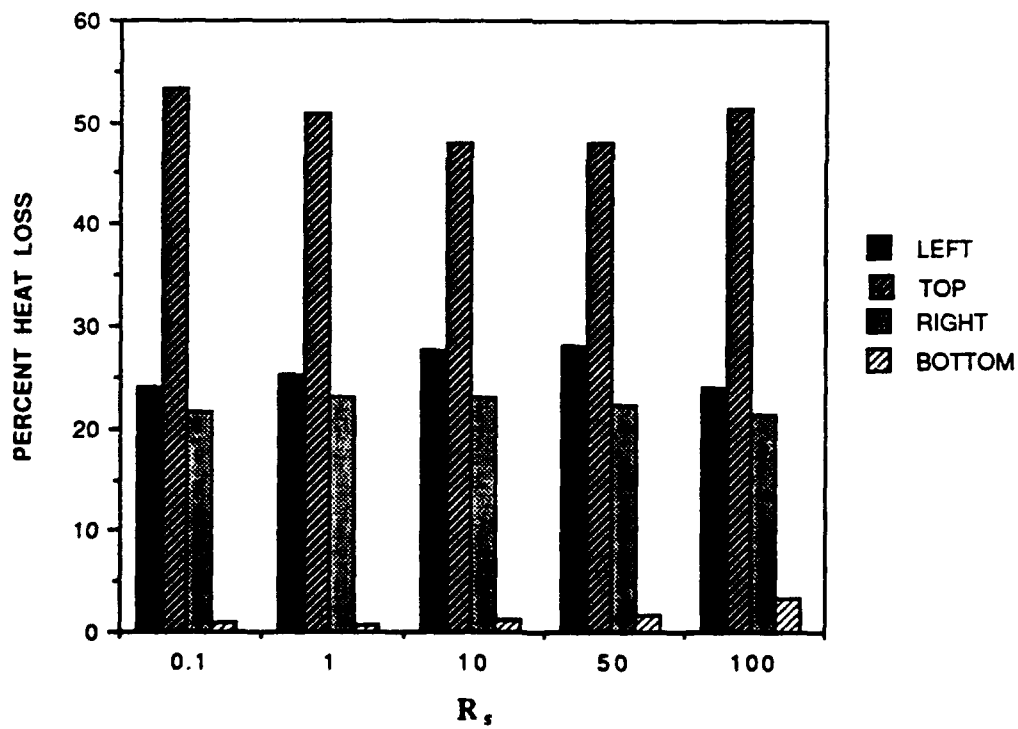


Figure 20. Heat loss through enclosure walls for various  $R_s$ ,  $Ra=10^5$

Figure 21 shows the substrate surface heat flux for various  $R_s$ . For  $R_s \geq 10$  the heat flux for the substrate is fairly uniform. For  $R_s < 10$  most of the heat flux comes from the front face of the component for  $S_2$  ranging from 2-3. The greatest heat flux is at the base of the component at  $S_2=2$ . The same pattern follows for the substrate surface temperatures in Fig. 22 with the temperatures being uniform for  $R_s \geq 10$  and for  $R_s < 10$  the temperatures being higher over the component surface,  $S_2=2-3$ , with the highest temperature at the top of the component, at  $S_2=3$ .

Component surface heat flux is shown in Fig. 23. For  $R_s < 10$  the heat flux through the component-fluid interface is greatest, for  $S_1=0$  to 1. For  $R_s \geq 10$  the component-substrate interface shows the higher heat flux with the bottom face having the maximum. Very little difference occurs when  $R_s$  is increased beyond 50. The component surface temperature is fairly uniform for all  $R_s$  due to the high conductivity of the component as shown in Fig. 24. The surface temperature decreases greatly for  $R_s=0.1$  to 10 and then decreases slightly over the remaining range with very little change between  $R_s=50$  to 100. As the substrate conductivity increases there is less resistance to the flow of heat and hence the surface temperatures decrease.

Maximum temperature versus  $R_s$  is shown in Fig. 25 and shows there is little benefit to increasing  $R_s$  beyond 10.

#### **D. EFFECT OF COMPONENT CONDUCTIVITY RATIO $R_c$**

The effects of  $R_c$  on the temperature contours and streamlines are shown in Fig. 26 (a)-(d). For  $R_c=1$  there is a steep thermal gradient in the component with the maximum temperature near the center of the

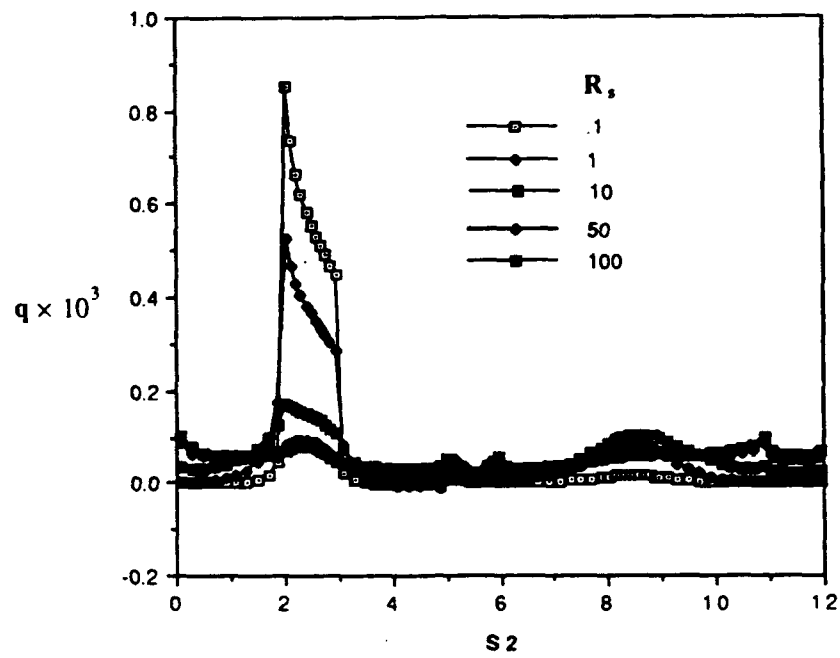


Figure 21. Substrate surface heat flux for various  $R_s$ ,  $Ra=10^5$

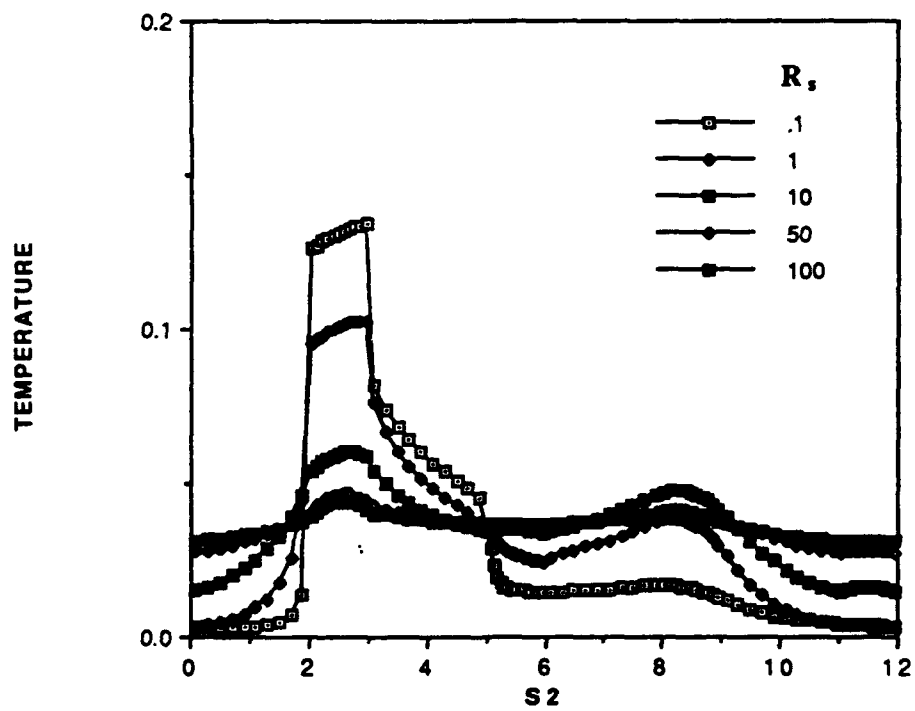


Figure 22. Substrate surface temperature for various  $R_s$ ,  $Ra=10^5$

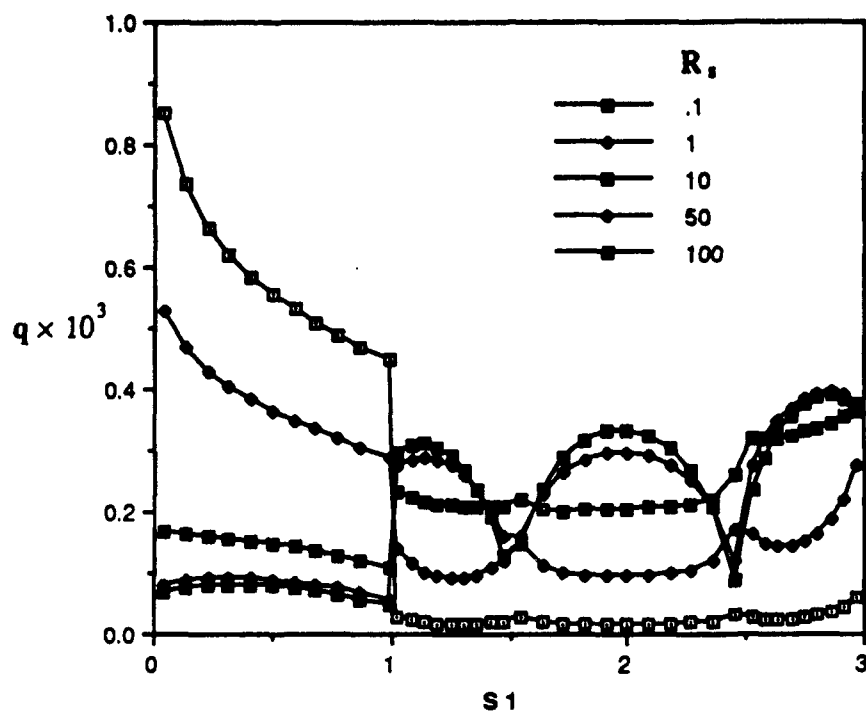


Figure 23. Component surface heat flux for various  $R_s$ ,  $Ra=10^5$

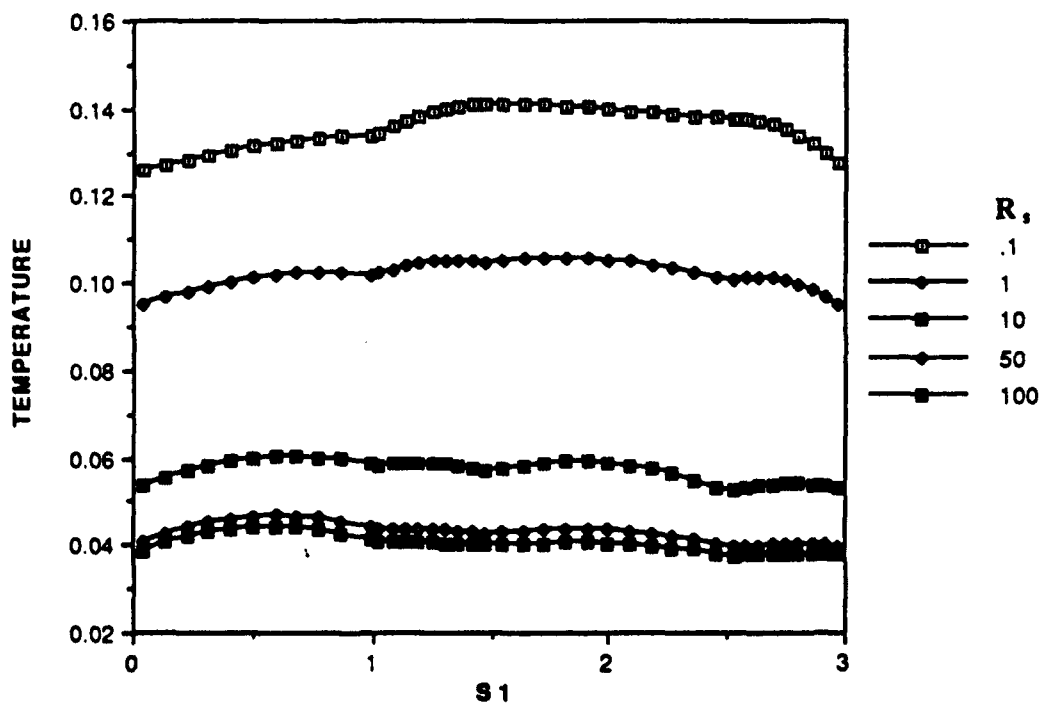


Figure 24. Component surface temperature for various  $R_s$ ,  $Ra=10^5$

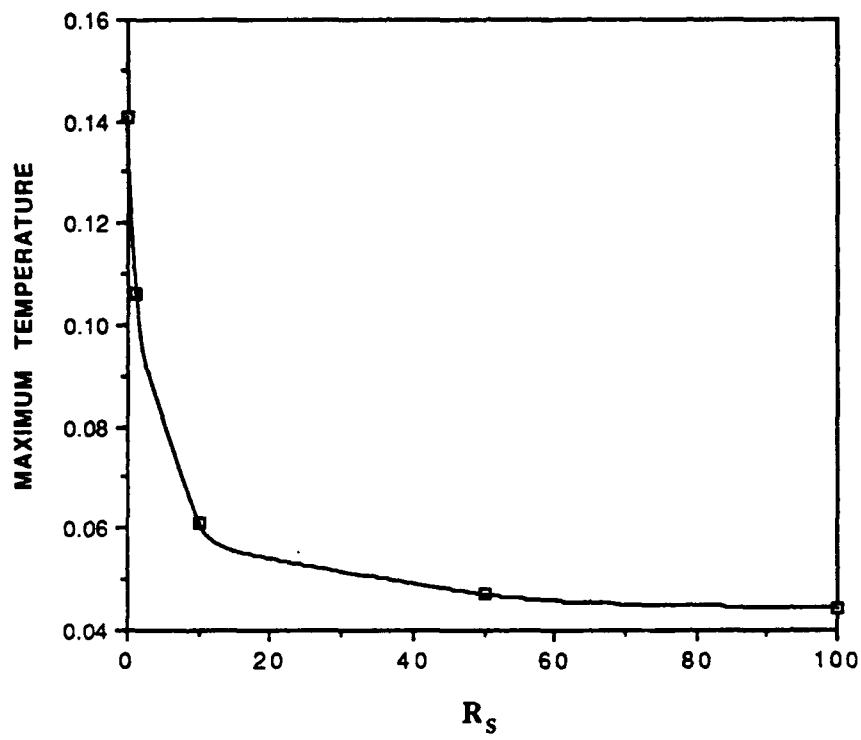
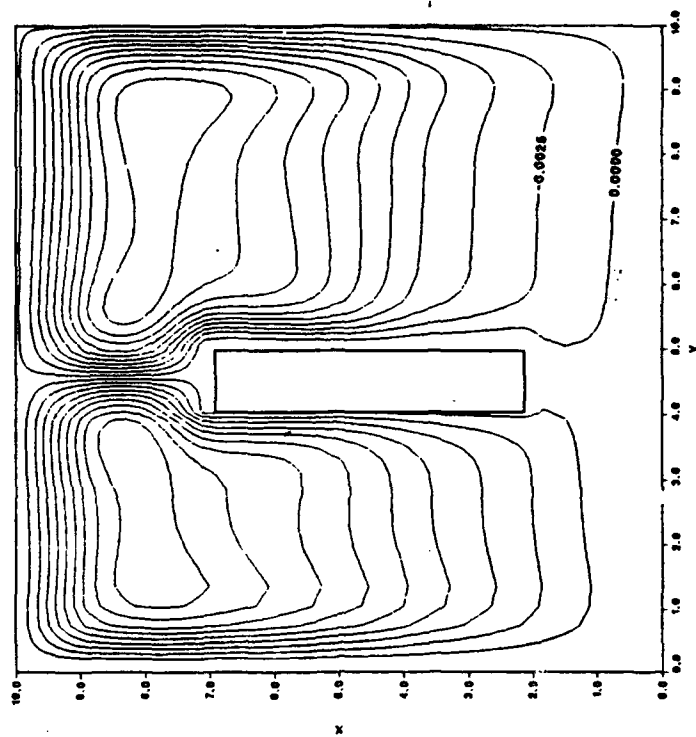


Figure 25. Maximum temperature versus  $R_s$ ,  $Ra=10^5$

Streamlines



Temperature Contours

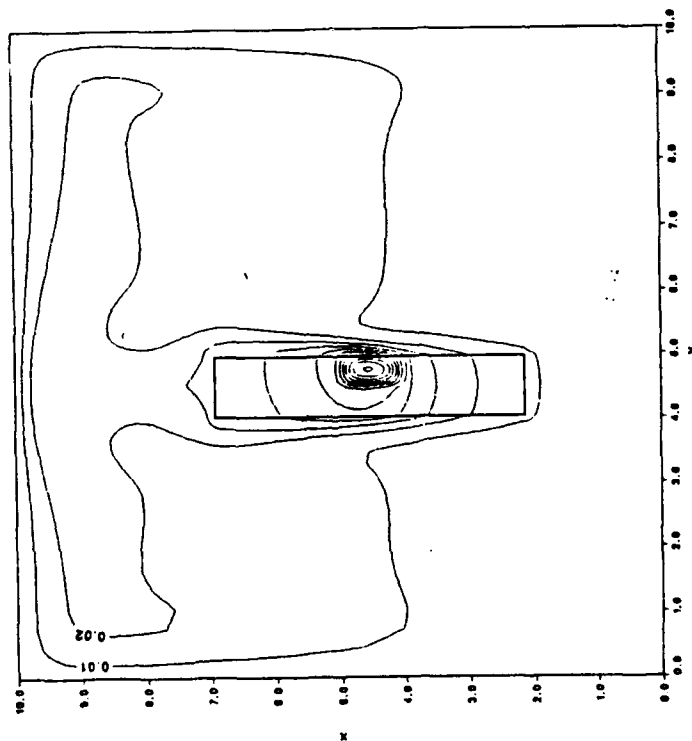
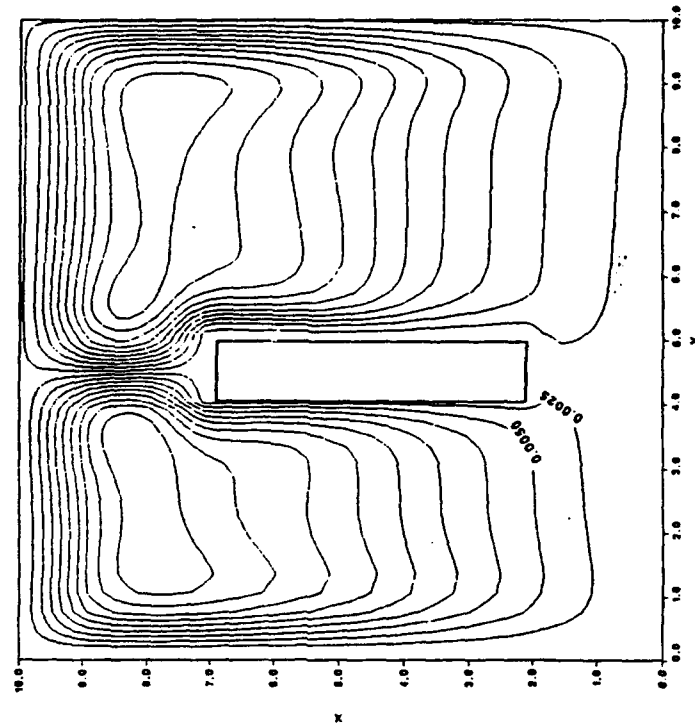


Figure 26(a). Temperature contours and streamlines for  $R_c=1$

Streamlines



Temperature Contours

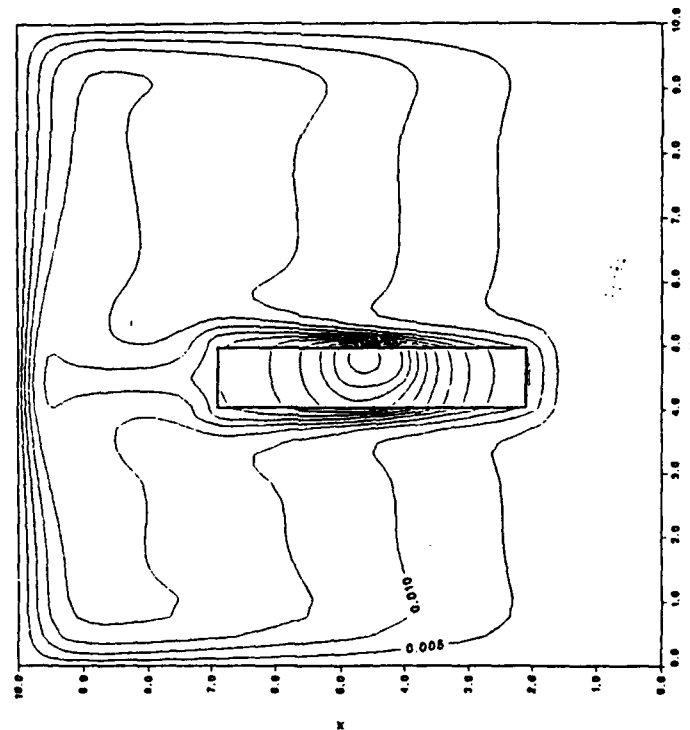
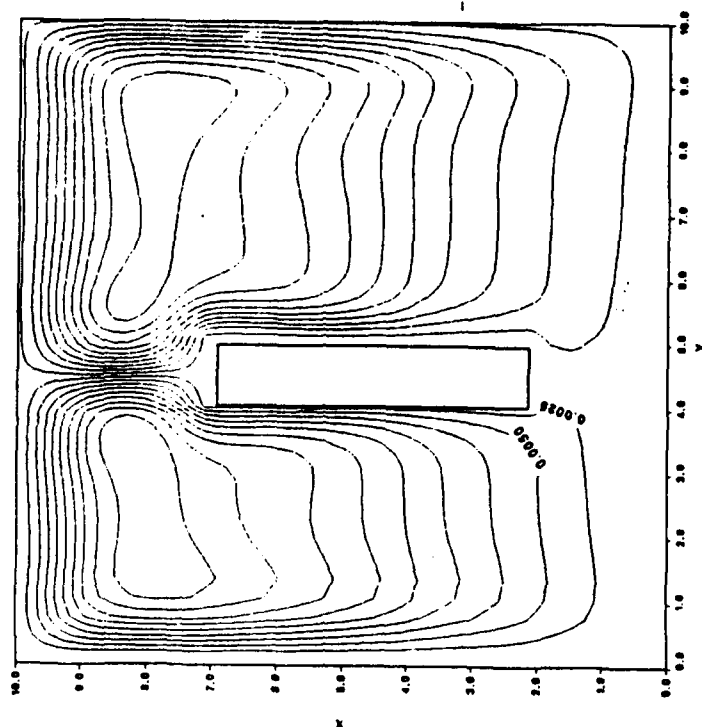


Figure 26(b). Temperature contours and streamlines for  $R_c=25$



Streamlines



Temperature Contours

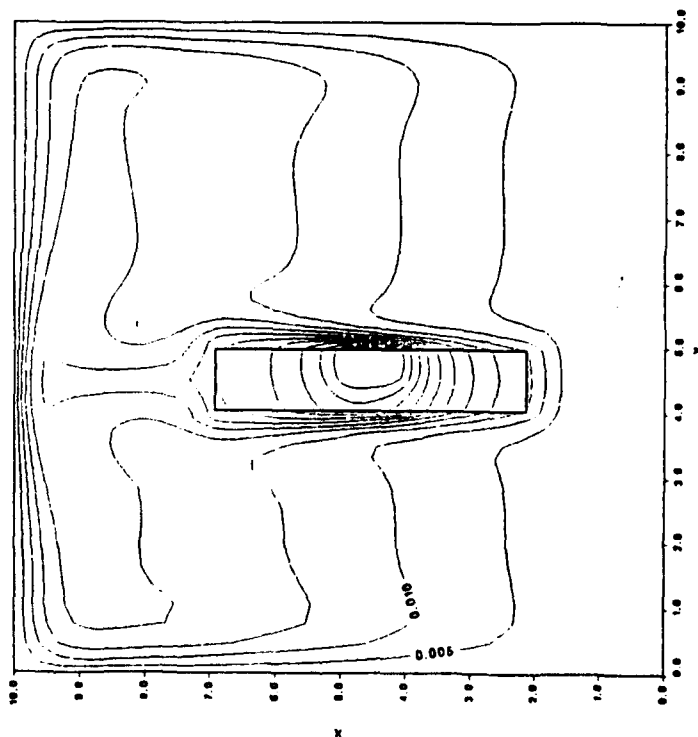
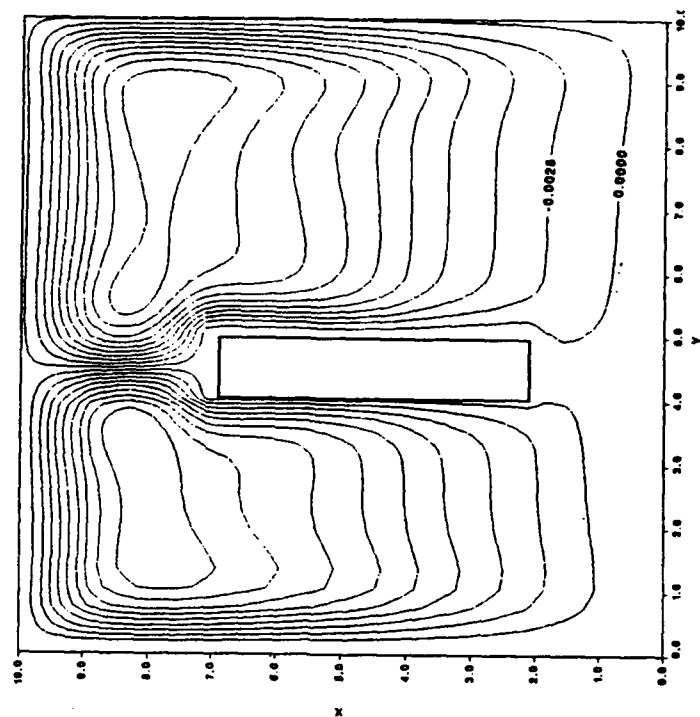


Figure 26(c). Temperature contours and streamlines for  $R_c=50$

Streamlines



Temperature Contours

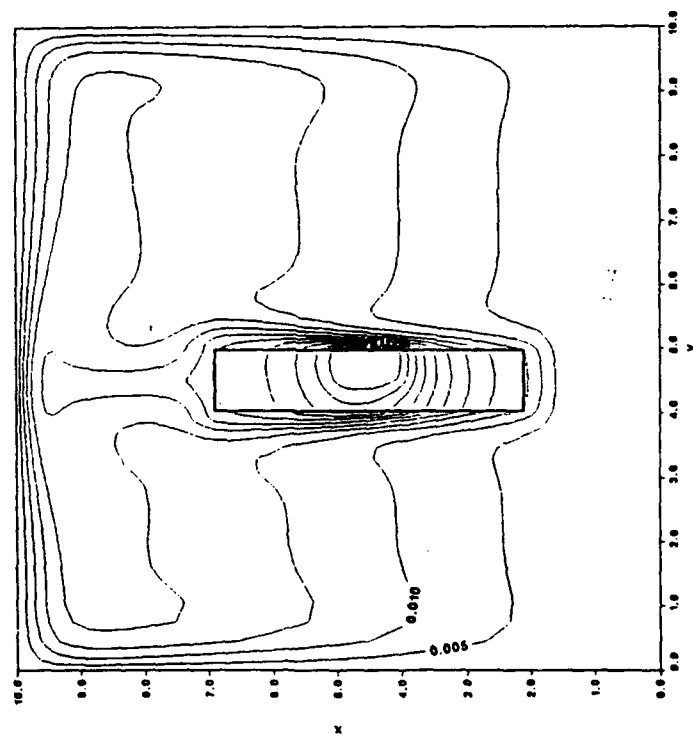


Figure 26(d). Temperature contours and streamlines for  $R_c=100$

component. For  $R_c=25$  the hot spot is towards the fluid face and the component is almost at a uniform temperature. For  $R_c=50$  and 100 the temperature contours look identical. There is a negligible change in the streamlines for the complete range of  $R_c$  studied.

Figure 27 shows the percent heat loss through the component faces. For  $R_c$  increasing from 1 to 25 there is a large decrease in the percent heat loss from the front face and a slight decrease from the back. A large increase in the percent heat loss from the bottom and a slight increase in the top face make up for the decrease at the front and back. With the increase in component conductivity, heat flows easier through the component and a greater percent can then go out the top and bottom. The substrate has a relatively high conductivity and the top and bottom substrate areas act like fins. For  $R_c$  increasing from 25 to 100 there is a slight increase in the bottom percent heat loss and a very slight decrease from the front and the back. The bottom face uses the substrate below as a fin to move the heat to the lower cooler region of the enclosure. The heat loss through the enclosure walls, shown in Fig. 28, changes insignificantly which is expected due to no change in the fluid flow or the temperature distribution in the fluid over the entire range of  $R_c$  studied.

The component surface heat flux, Fig. 29, shows for  $R_c=1$  a similar pattern for each face. Each face has a local maximum flux at the center with the largest maximum flux at the center of the back face at  $S1=2$ . The low conductivity of the component limits the movement of heat, so the greater flux is associated with the surfaces on the component that have the most volume of component around them. These locations on the component

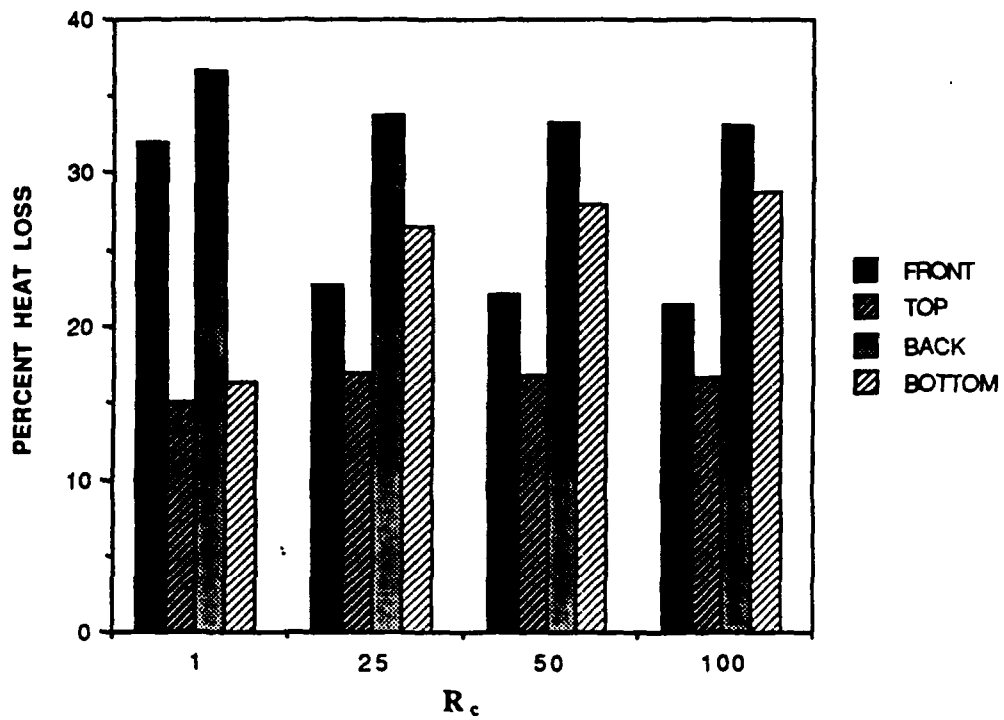


Figure 27. Heat loss through component faces for various  $R_c$ ,  $Ra=10^5$

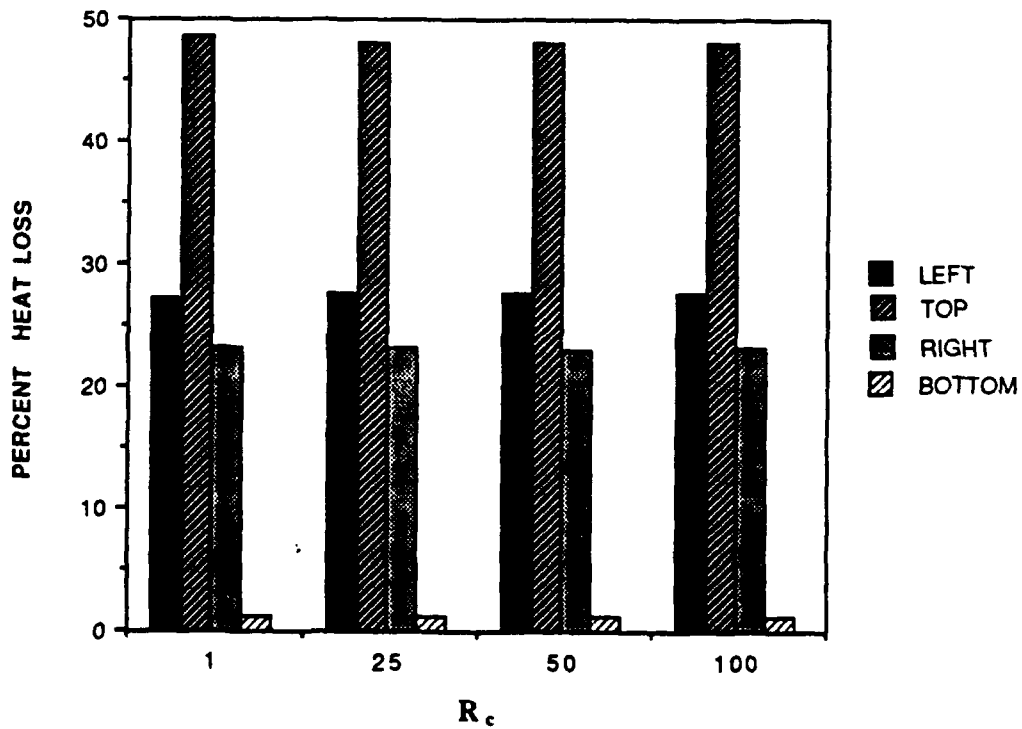


Figure 28. Heat loss through enclosure walls for various  $R_c$ ,  $Ra=10^5$

surfaces correspond to the center of each face. For  $25 \leq R_c \leq 100$ , the component surface heat fluxes are nearly identical with the greatest flux going through the bottom face near the fluid-component boundary. The flux is greatest here since the substrate extending below the component bottom surface acts like a fin. In addition there is induced flow over the substrate below the bottom of the component augments heat transfer from the front substrate surface below the heater.

The component surface temperatures for  $R_c=1$  vary widely with the maximum occurring at  $S1=0.7$  as seen in Fig. 30. For  $25 \leq R_c \leq 100$  the temperature over the surface is fairly uniform. The maximum temperature versus  $R_c$  in Fig. 31 shows little advantage in increasing  $R_c$  higher than 25.

#### **E. EFFECT OF COMPONENT TO SUBSTRATE WIDTH RATIO $w/d_t$**

Streamlines and the temperature contours in the liquid region in Figs. 32(a)-(d) show only minor changes when  $w/d_t$  is changed from 0.25 to 0.999. This occurs because the high  $R_s$  and  $R_c$  result in low solid thermal resistance, with the major temperature drop occurring in the fluid. In the component region the hot spot moves from the fluid surface to the component center as  $w/d_t$  increases from 0.25 to 0.999.

The percent heat loss through the component faces is shown in Fig. 33. For  $w/d_t$  increasing from 0.25 to 0.999 there is approximately a 10% increase of the heat loss from the top face and a 20% increase from the bottom face. Both the top and the bottom percent heat losses rise because of the increased heat transfer area as  $w/d_t$  increases and a greater volume of

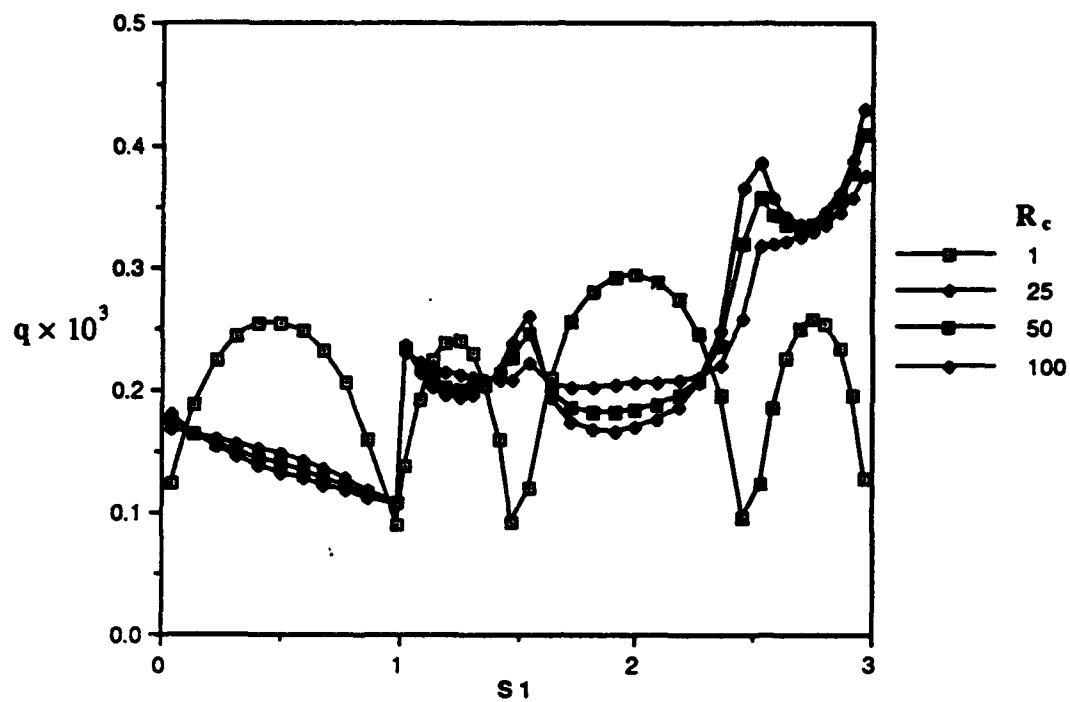


Figure 29. Component surface heat flux for various  $R_c$ ,  $Ra=10^5$

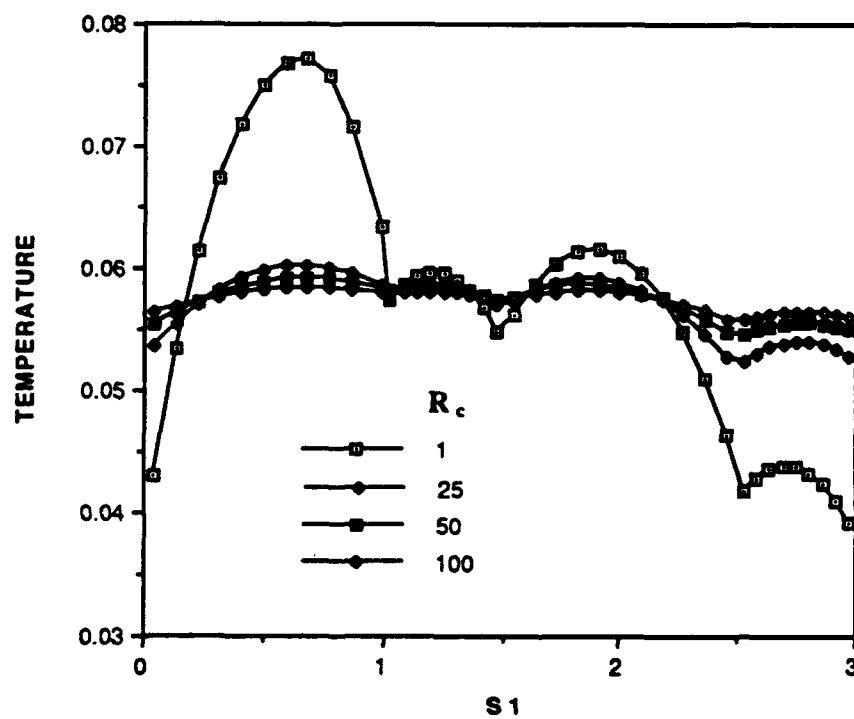


Figure 30. Component surface temperature for various  $R_c$ ,  $Ra=10^5$

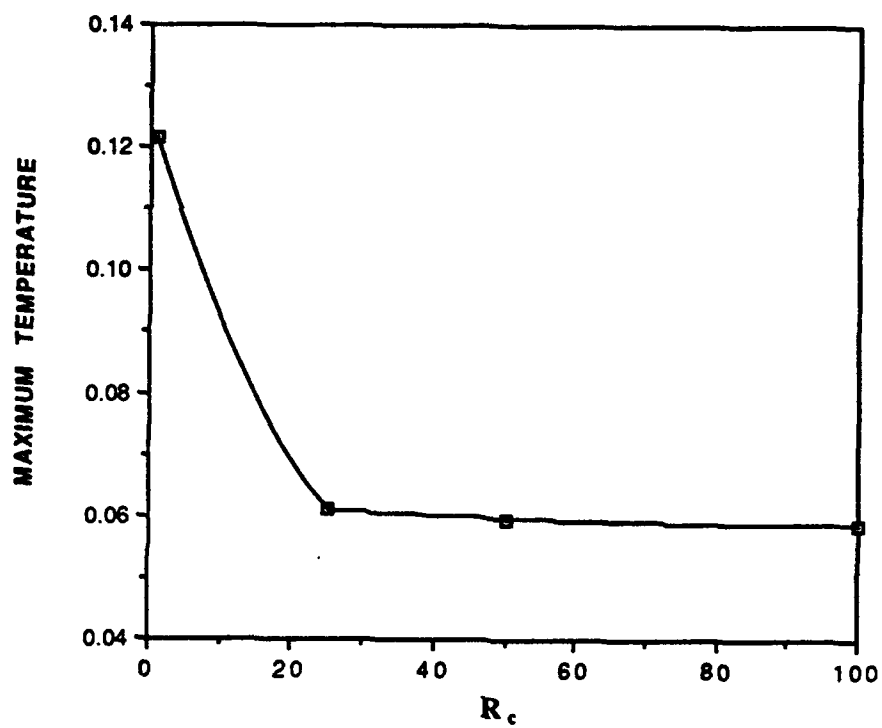
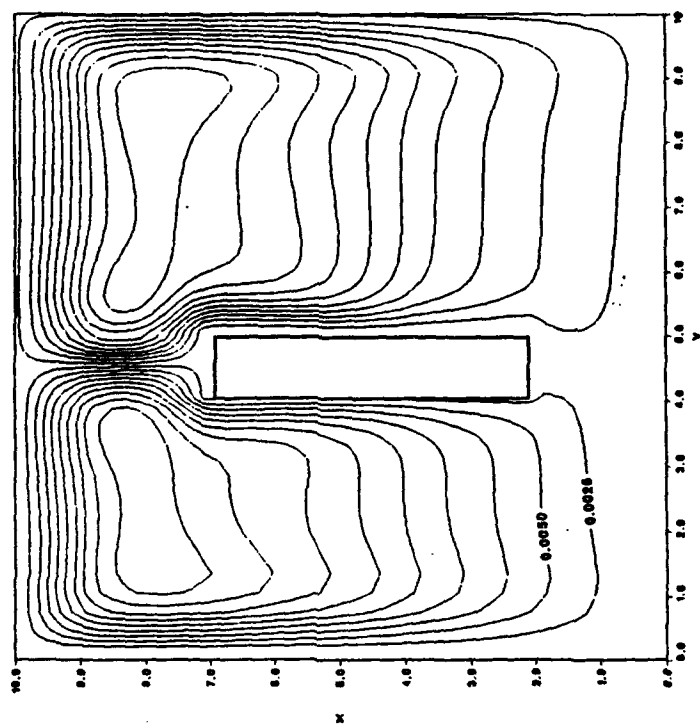


Figure 31. Maximum temperature versus  $R_c$ ,  $Ra=10^5$

Streamlines



Temperature Contours

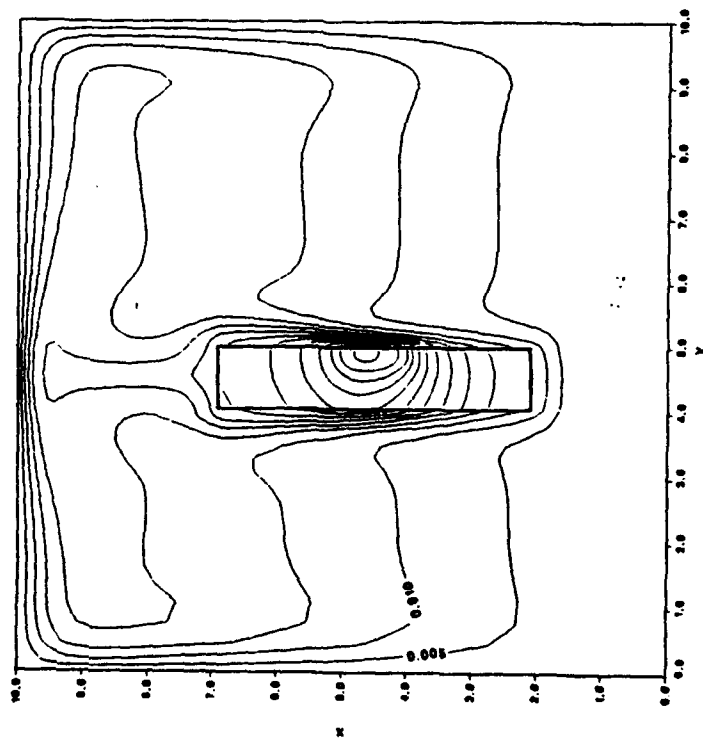
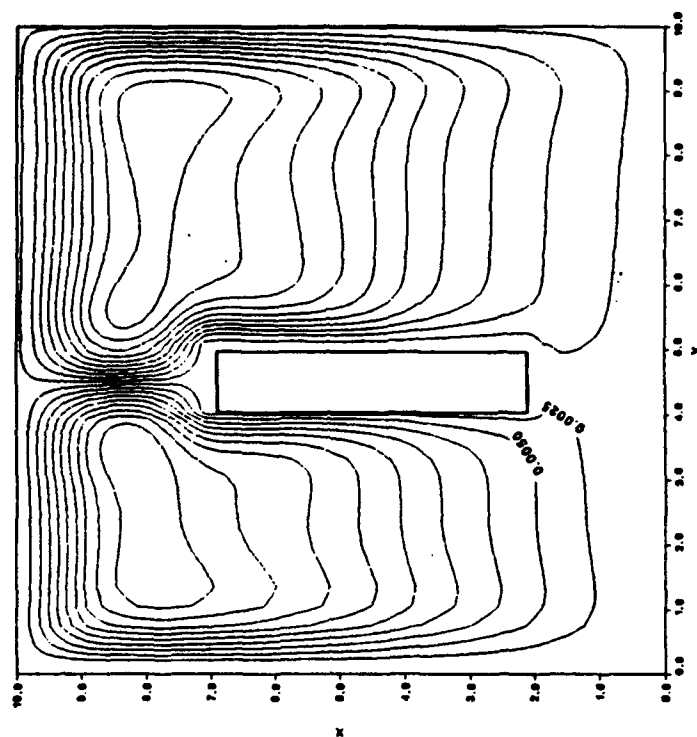


Figure 32(a). Temperature contours and streamlines for  $w/d_1=0.25$



Streamlines



Temperature Contours

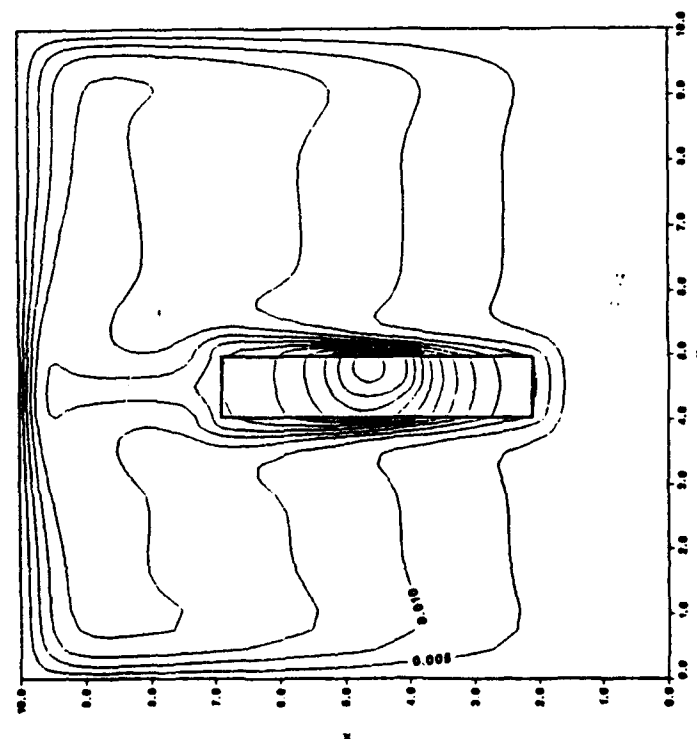
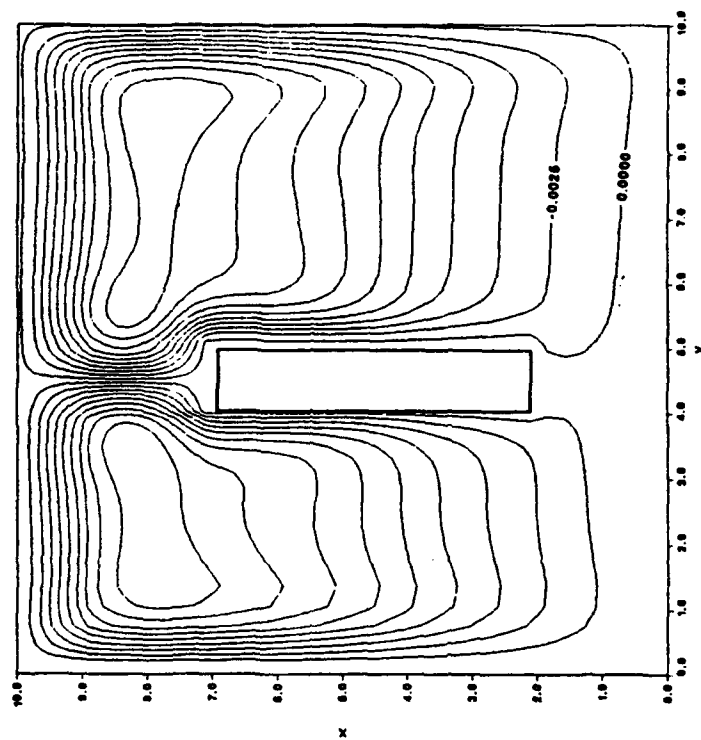


Figure 32(b). Temperature contours and streamlines for  $w/d_1=0.5$

Streamlines



Temperature Contours

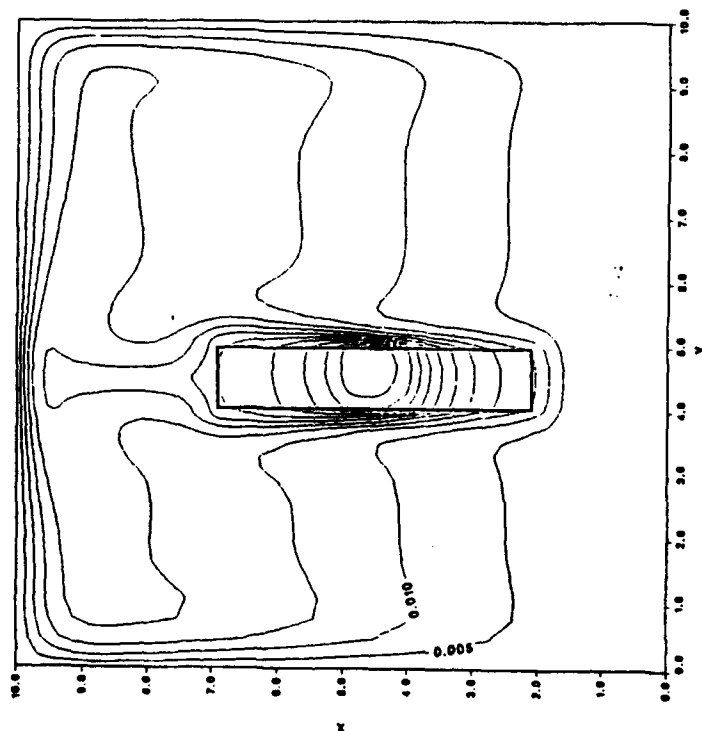
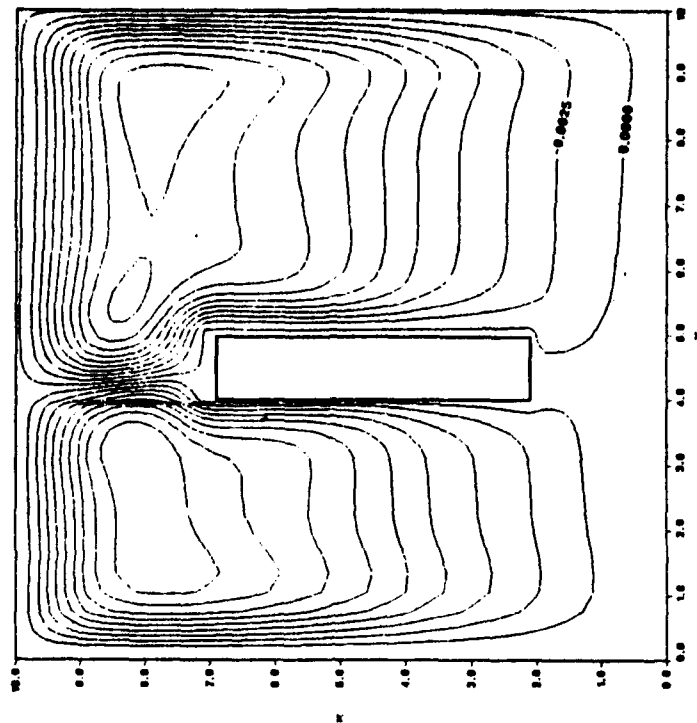


Figure 32(c). Temperature contours and streamlines for  $w/d_1=0.75$

Streamlines



Temperature Contours

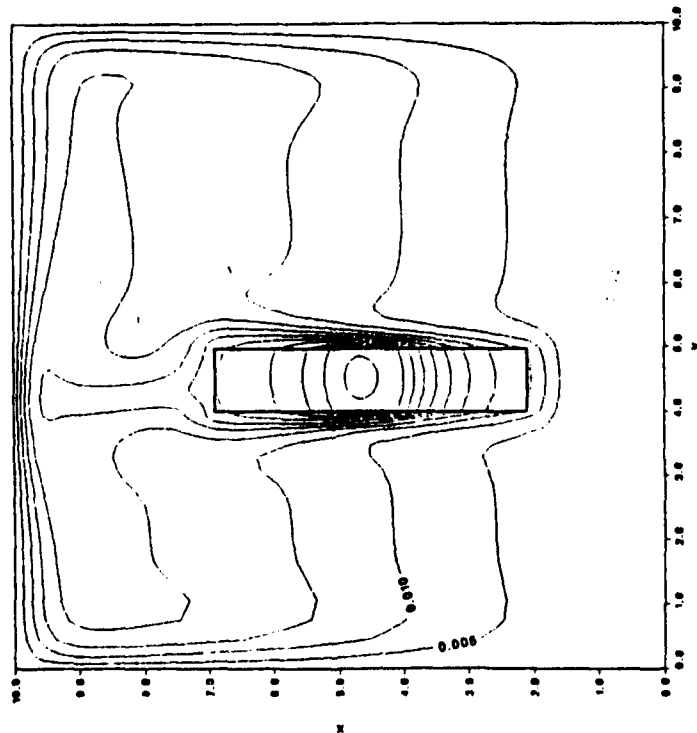


Figure 32(d). Temperature contours and streamlines for  $w/d_1=0.999$

the component next to them. There is approximately a 7% decrease in heat loss from the front face because more heat is being taken away from the top and bottom and the front is actually becoming less of the total surface area as  $w/d_t$  is increased. There is approximately a 23% decrease on the back face. The back face now is also less of the total percent area of the component surface and the back has less of the substrate acting as a fin as  $w/d_t$  increases until there is essentially no substrate at  $w/d_t = 0.999$ . There is no difference in the percent heat loss from the enclosure boundaries, Fig. 34, as was suggested from the temperature contours and streamlines.

Figure 35 shows the maximum temperature versus  $w/d_t$ . There is almost a linear decrease in maximum temperature with an increase in  $w/d_t$ . The same rate of heat is being dissipated by a larger volume which reduces the maximum temperature.

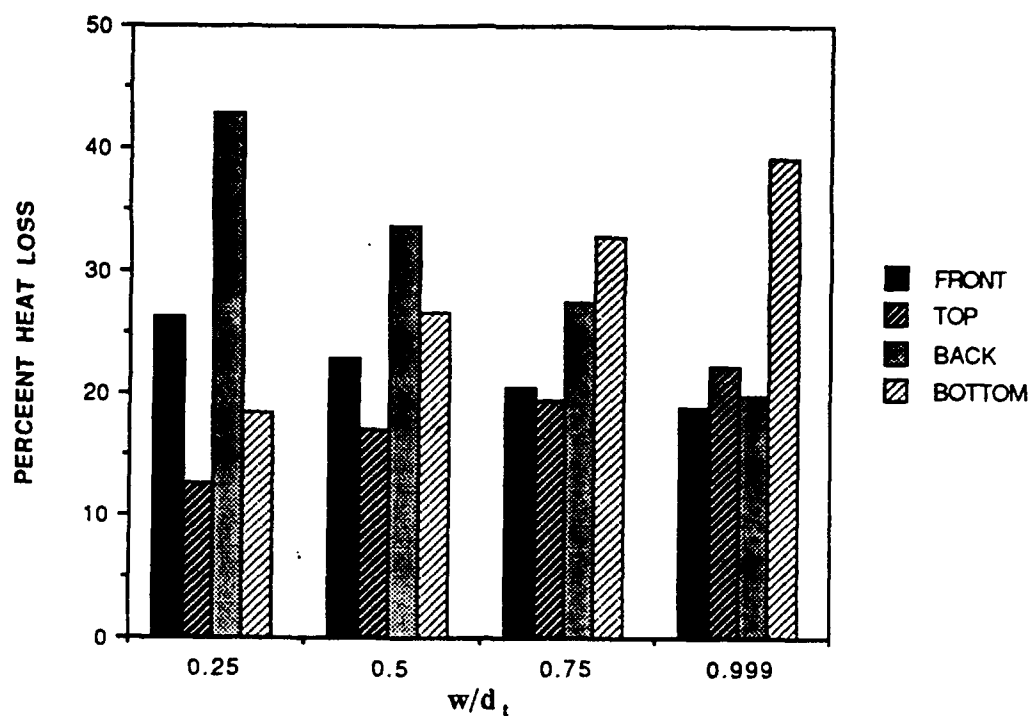


Figure 33. Heat loss through component faces for various  $w/d_t$ ,  $Ra=10^5$

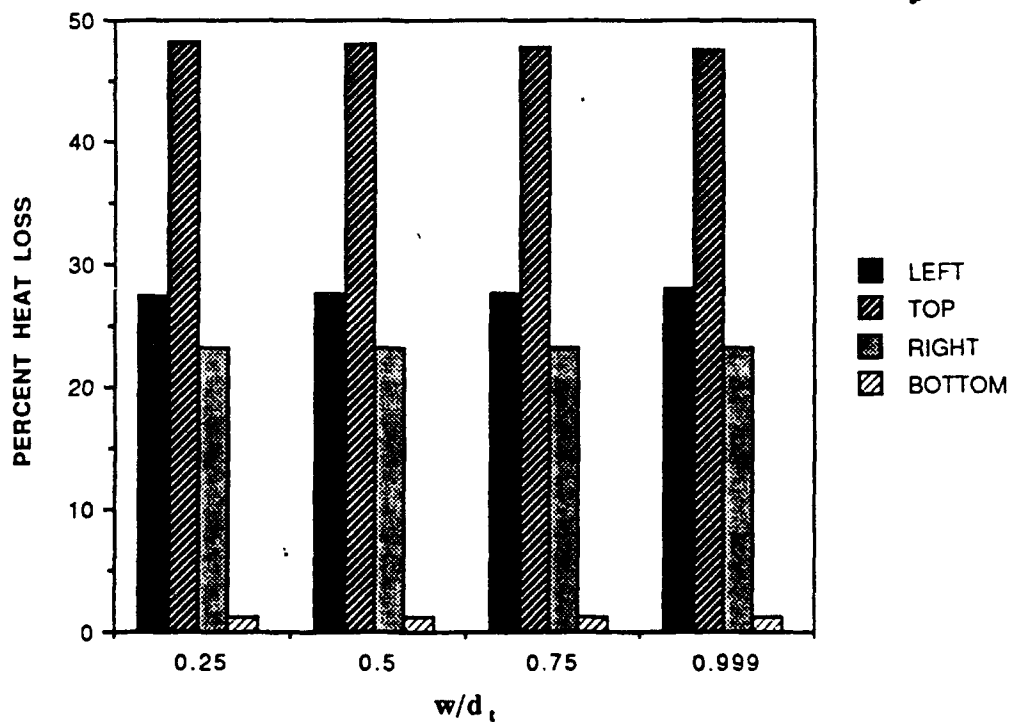


Figure 34. Heat loss through enclosure walls for various  $w/d_t$ ,  $Ra=10^5$

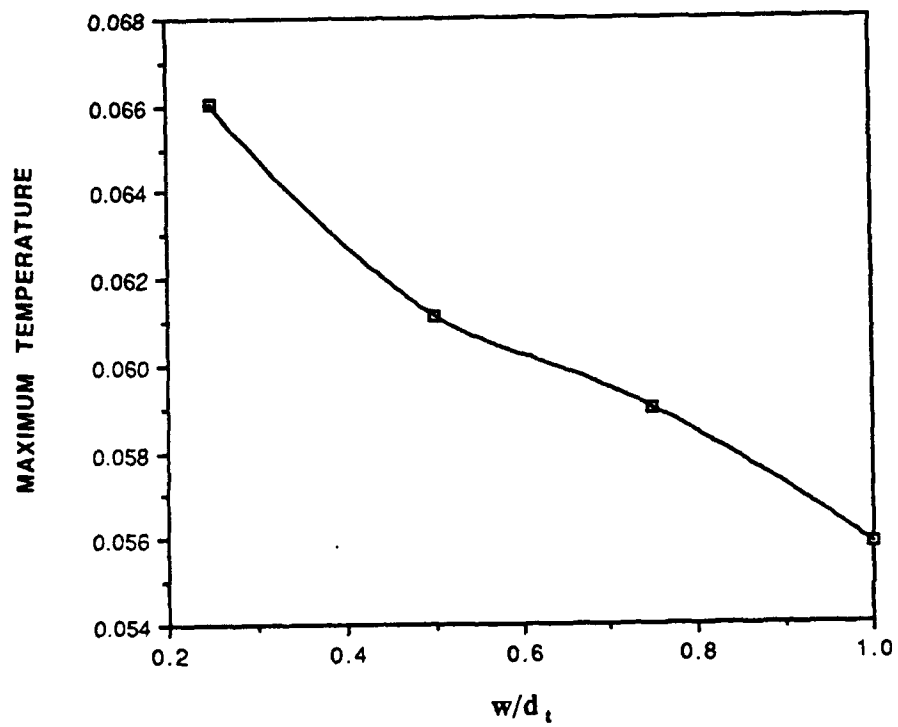


Figure 35. Maximum temperature versus  $w/d_t$ ,  $Ra=10^5$

## **IV. EXPERIMENTS**

### **A. EXPERIMENTAL APPARATUS**

#### **1. Additions**

The details of the experimental apparatus can be found in Gaiser [Ref. 6]. It consists of a test surface with 3 columns of flush heaters with 15 heaters per column as shown in Fig. 46. The test surface is immersed in a large plate glass tank filled with deionized water. Each heater has a thermocouple attached to the midpoint of the back. Voltages of the thermocouple and heater leads are taken by a data acquisition system and a HP(Hewlett Packard) computer determines the temperatures and power of the heaters. Further additions and changes done in the experimental setup are described below.

A 3-dimensional<sup>1</sup> traverse assembly with controller for the traverse motors and a deaerating system for the water were installed. The traverse controller interfaces with the HP computer in the two horizontal directions and a program was developed to move the traverse with the HP computer integrating the temperature acquisitions with a probe. The traverse must be manually moved in the vertical direction. See Appendix C for the traverse computer program. Deaeration was achieved by spraying water through a nozzle into a partially evacuated bottle. The water was then allowed to accumulate under the vacuum and pumped back into the tank at a rate similar to which it was being drawn out. Teflon sheets were placed over the tank's free surface to reduce the aeration of the water after it had

gone through this process. When the deaeration system was activated and a slight (3" or greater Hg) vacuum was drawn, the bottle would collapse leaving the system unoperable. A nonflexible container would be desirable for a better operation of the deaeration system.

## **2. Changes**

A change was made in the way the power input to the heaters was calculated. Upon taking over the apparatus it was noticed that the resistances of the various heaters varied by as much as 8% from the lowest resistance reading to the highest. The high density heater board was taken apart and the heaters with the resistances farthest from the norm were replaced. The new heaters were of a different batch than the original heaters and they all had a resistance of 10.4 ohms originally but when they were measured through the leads after they were installed the resistances again varied by as much as 6%, with the lowest value being the same as the heater before installation and the highest resistance being 6% above the original heater resistance. Since all the heaters were the same before being installed it was assumed that the excess resistance came from the leads. The excess resistance for all leads was then determined by subtracting the original heater resistance from the resistance of the heater and the leads and a computer program that took this into account was implemented. 1% and 5% precision resistors in parallel with the original 1% precision resistor were used to increase the current of the heaters that had less power due to the excess lead resistance. The following relation was used to determine the correct power:



$$P = \left( \frac{V_L(R_p + R_L) - VR_L}{R_p^2} \right) (V - V_L) \quad (9)$$

where the symbols are identified in the Nomenclature. Each heater and lead resistance had to be treated individually and in some cases extra line resistance had to be added to the leads to make the heaters have all the same power. A uniform and nonuniform power program were developed for the HP computer. The uniform power program was used when each heater was given the same power. The nonuniform power program was used when the power to the side columns was different than the center column of heaters. Also nonuniform and uniform data reduction programs were developed to obtain the temperatures and to reduce and store the data simultaneously for each case. See Appendixes D-H for computer programs utilized in the acquisition of experimental data.

## B. LIQUID CRYSTALS

Hallcrest thermochromic liquid crystals whose optical properties of the planar texture give rise to the selective reflection of bright colors that change with temperature [Ref. 13] were used in the experiment. The liquid crystals had to be kept refrigerated prior to usage. The first step in liquid crystal application was to obtain a clean dry surface. A black backing was then applied with an air brush. After the black backing had dried, the liquid crystals were mixed with a binder with 3 parts binder to 1 part liquid crystal slurry and the mixture was applied over the backing using the air brush. Care was taken to keep the layers very thin to reduce any interference with the heat transfer process. The water in the tank had to be

kept very clean and the water filtering system was run for two days constantly before placing the test surface with the liquid crystals on it in the water. If any contamination was present, only a dark blue color would show up which was difficult to see on the black backing. Even with the water being very pure, the liquid crystals deteriorated and could only be expected to last less than two weeks. It is believed that the crystals somehow react with the polar water molecule and become inactive. In dielectric fluid this had not been a problem, which was evident in past thesis research [Ref. 14].

The crystals were calibrated against temperatures using a platinum resistance standard (Rosemont Engineering Model 920A Commuting Bridge) and a Model 913A Calibration Bath. Two ranges of liquid crystal sensitivity to temperature were used. After standardization for the colors which appeared below 30 degrees C, the crystals compared within 0.5 degrees C with the thermocouple temperatures of the heaters, but at higher temperatures (greater than 40) it was difficult to determine the change from blue to black and an agreement between the crystals and the heater thermocouples was about 5 degrees C with the thermocouple temperature always higher than the color indicated.

A problem with working with the crystals was to photograph the resulting surface temperature color patterns. It is very difficult to shoot into a glass container filled with water. All light sources outside the tank must be turned off or all that will be seen in the picture is the reflection of the photographer. The correct light source was also an important consideration. Florescent lights do not have a complete spectrum of light

being emitted and the pictures taken under these conditions did not show the colors that were actually present. Taking pictures with a spot lamp on the face with a high speed film (ASA 1600) did not work because the area with the spot ended up being burned out in the picture and the surrounding area of the picture appeared black. The best method found was to obtain a light source that contained the wavelength band necessary. It was obtainable at a local photograph store and it was used with a film speed of 400 ASA or higher. Care had to be taken to keep the light source above the water and shining inside the tank. Shielding was placed so the bulb would only light up inside the tank staying away from the reflecting glass and lighting only the test surface. The light was only switched on when taking pictures to avoid setting up fluid variations by warming up the tank water.

Figure 36 shows the view that is shown in the pictures to follow. It also shows the shroud and the test surface. The shroud is a clear plastic that causes a constriction to the flow and simulates another circuit board or a wall in an actual situation in electronic equipment. At no power, the test surface appears black and corresponds to ambient temperature (18 degrees C). The first picture, Fig. 37 is a picture with no shroud and a power level of .5 watts per heater. The actual colors that were present are brown which appears at 24.0 degrees C, green which appears at 25.3 degrees C, and blue which appears at 28.3 degrees C and disappears at 44.0 degrees C where the surface returns to black. The black and white pictures can only be used to show higher temperature regions with the lighter regions on the photographs indicating where the hot spots are. The color patterns become more evident near the middle and top compared to the bottom of the heater

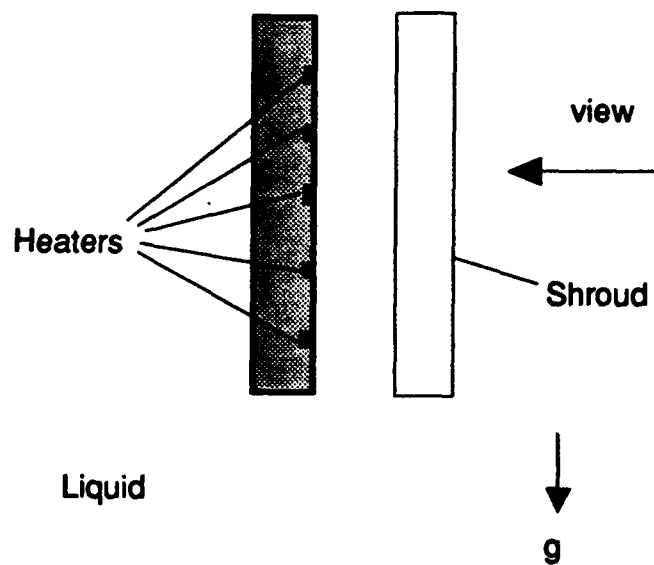


**Figure 36. Schematic of the view that is seen in the following pictures**

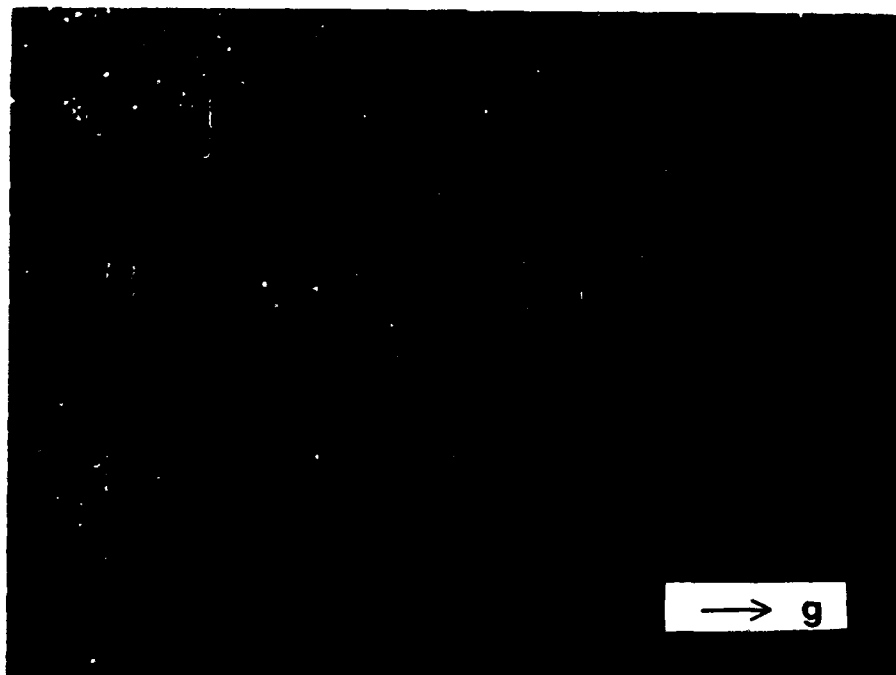


**Figure 37. No shroud case, .5 watts per heater power input**

columns. The temperature patterns seem symmetric for all three columns and there appears to be no thermal interaction between the three columns. Heat being brought up by natural convection is brought up the face and some is transferred back into the plexiglass substrate. As the power is increased with no shroud the color patterns become more evident at the bottom of the heater column. At three watts per heater power input, Fig. 38 shows again that there is no interaction between the columns. The color pattern above the top heater indicate higher temperatures in that region compared to the 0.5 watts per heater case.

A shroud is placed 6mm in front of the test surface in Fig. 39 and entrainment of the flow is evident by the shape of the temperature patterns. The shroud prevents entrainment flow from the front and water must come from the sides towards the center column. This actually enhances cooling of the outside top heaters for a shroud spacing of 6 mm as seen in Figs. 39 & 40, compared to when there is no shroud. The bottom heaters appear not to be effected by the shroud placement. In Fig. 41 the shroud spacing is 3 mm and the power input per heater is 0.2 watts. The color patterns now become visible at a much lower power level. The flow at the top is greatly constrained with the high temperature patterns actually merging over the center column. Temperatures are increased drastically at the 3mm shroud spacing and Fig. 42 shows that at a 0.5 watt power input per heater the temperatures are as high as with a 1 watt, 6 mm shroud spacing case or a 2 watt, no shroud case.

Nonuniform power levels for the side columns and center column at different power input were looked at for no shroud and 3mm shroud cases,

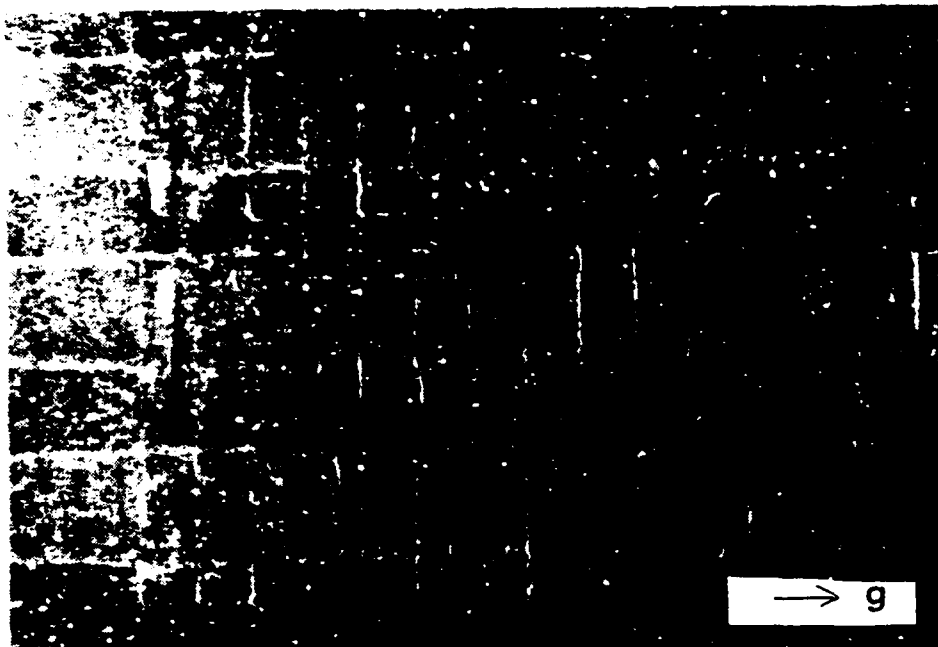


**Figure 38. No shroud case, 3 watts per heater power input**

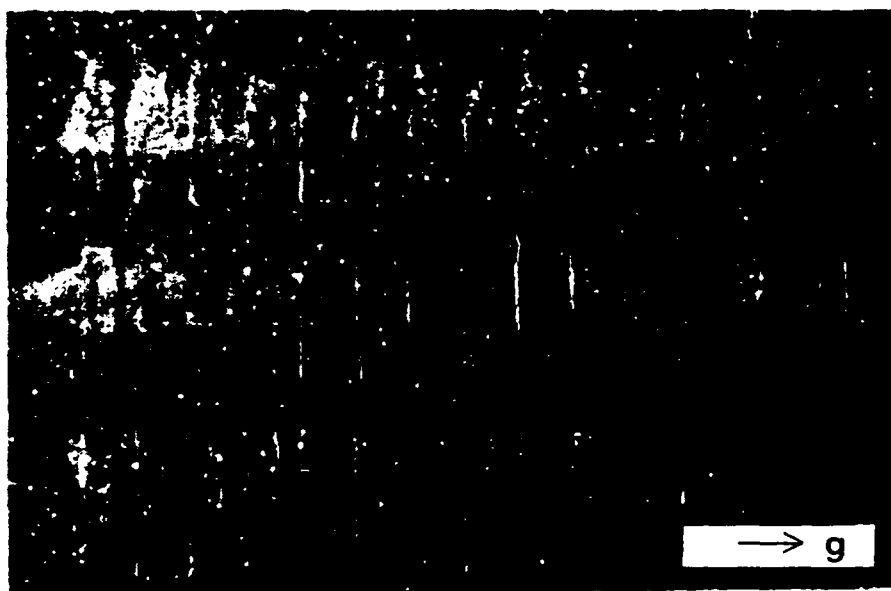


**Figure 39. 6 mm shroud spacing, .5 watt per heater power input**

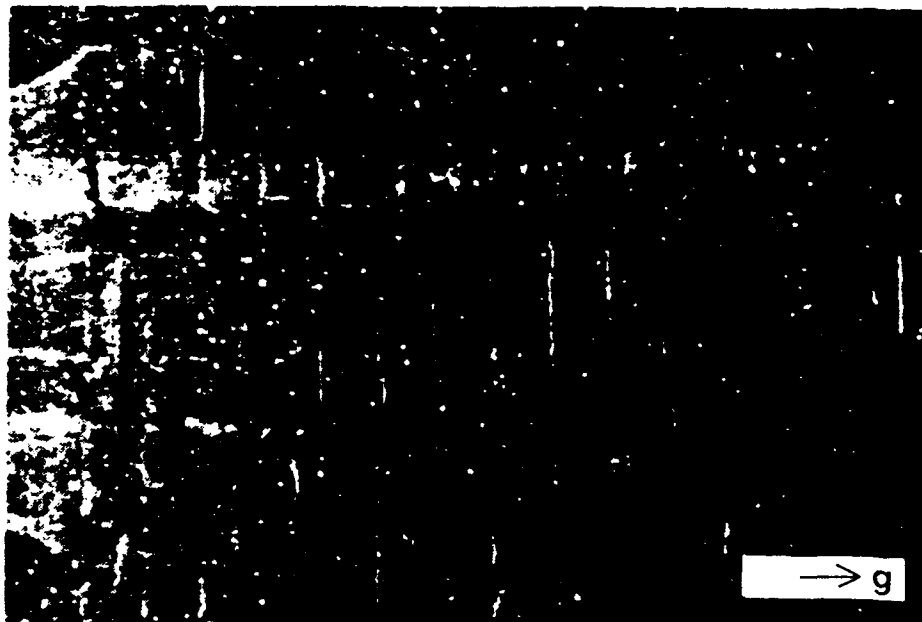


**Figure 40. 6 mm shroud spacing, 1 watt per heater power input**

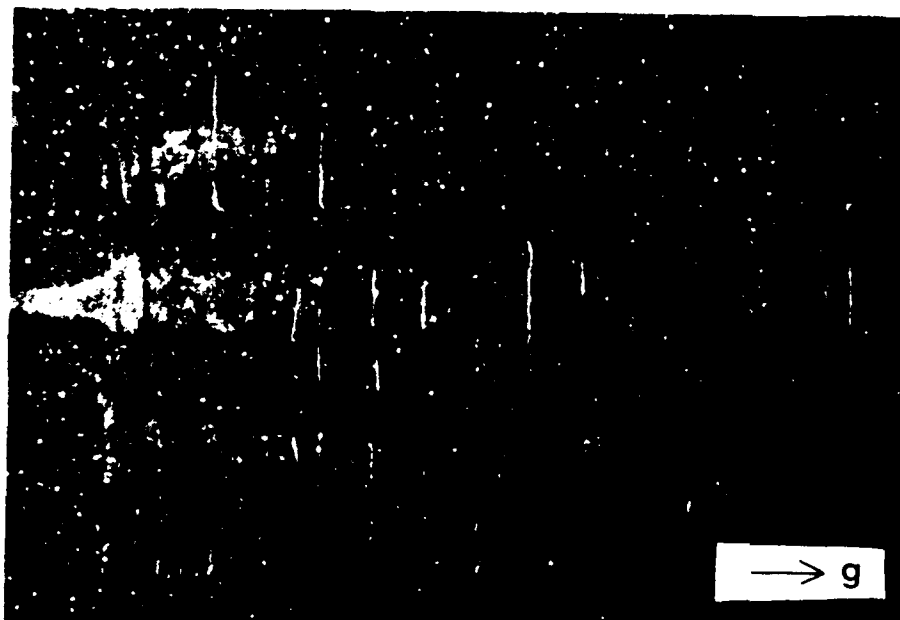


**Figure 41. 3 mm shroud spacing, .2 watt per heater power input**

Figs. 43-45 , and showed the same patterns as the uniform power cases. For the no shroud case there did not appear to be any interaction between the three columns. For the small shroud spacing cases there was considerable side entrainment . It was difficult to go to higher power levels in the low shroud spacing cases because air bubbles formed over the top center region and disrupted the flow and made the temperatures increase greatly even for power levels of the order of 0.5 watts per heater.

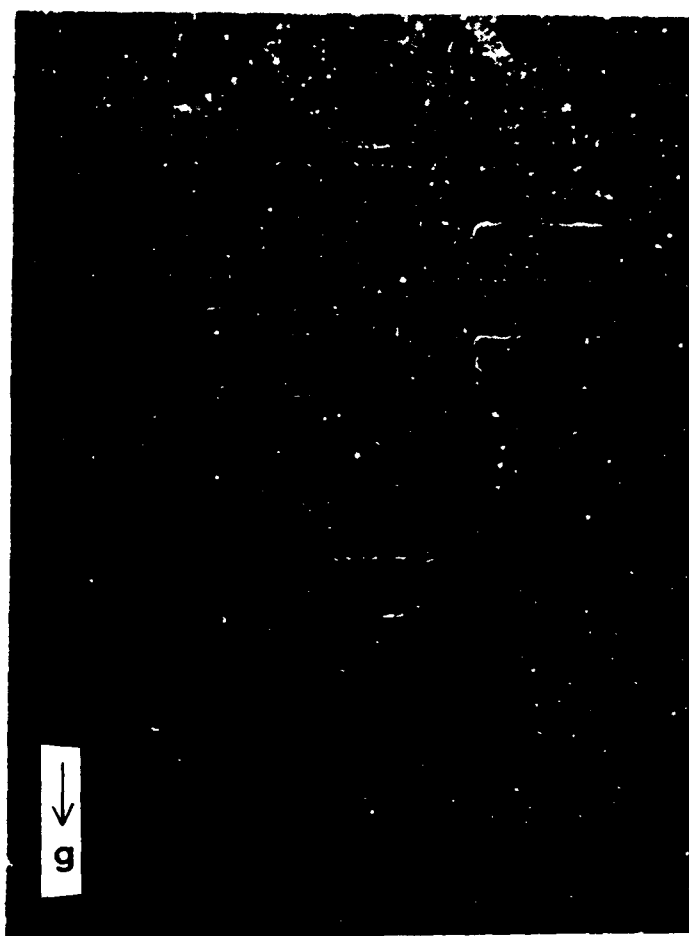


Figure 42. 3 mm shroud spacing, .5 watt per heater power input



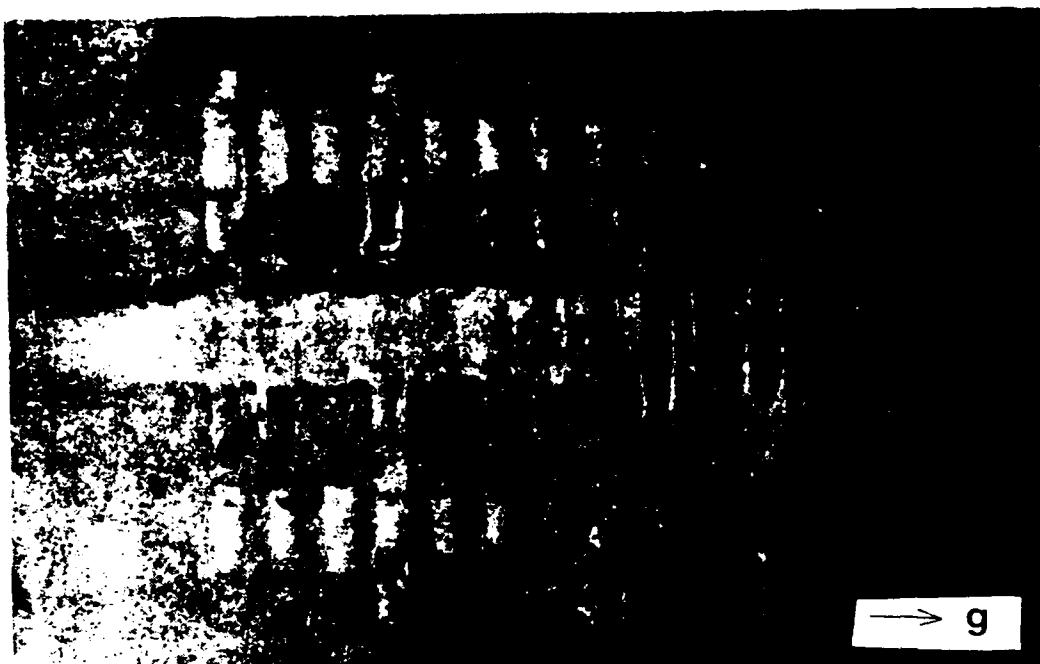


Figure 43. No shroud case, 0.5 & 0.2 watt per heater power input  
(center/sides)

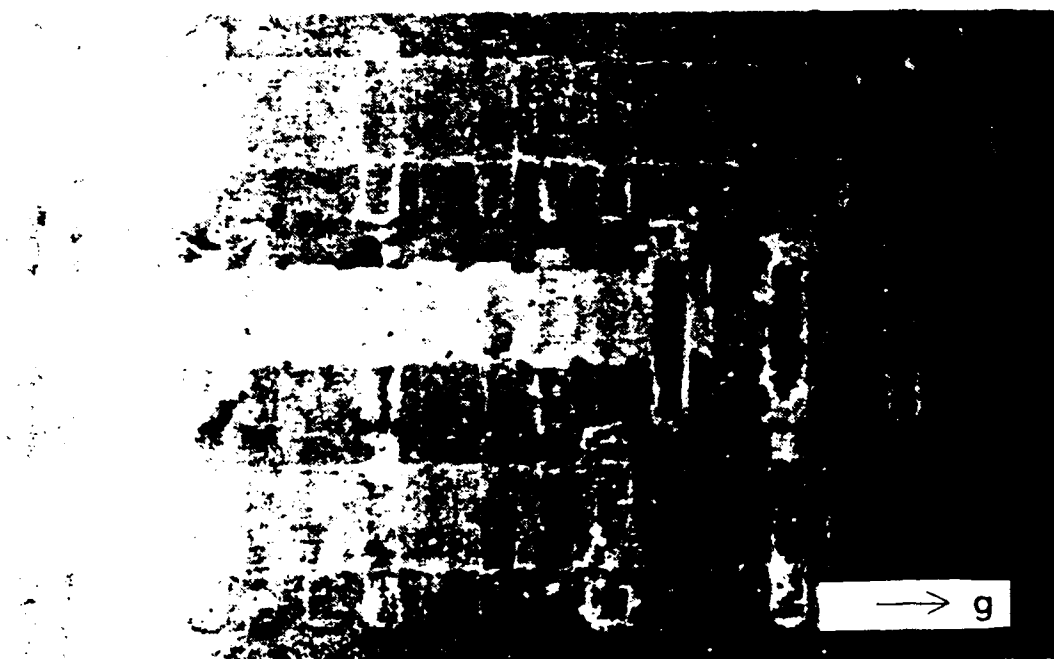


Figure 44. No shroud case, 0.5 & 1 watt per heater power input  
(center/sides)

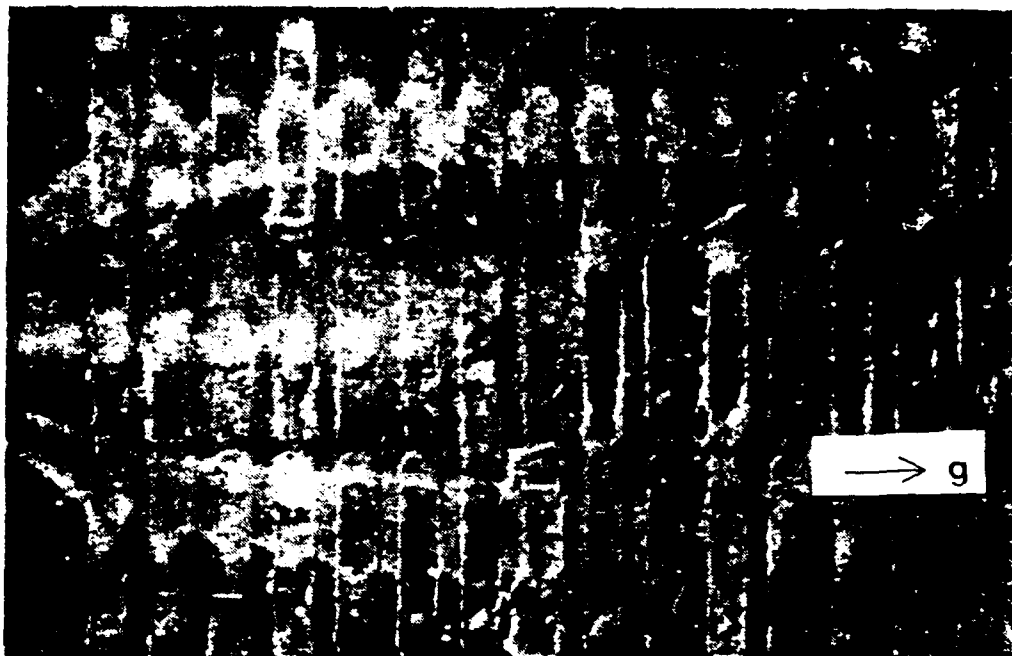


Figure 45. 6 mm shroud spacing, .2&.5 watt per heater input (center/side)

## **V. NUMERICAL COMPARISON WITH EXPERIMENT**

### **A. WHAT TO COMPARE ?**

The liquid crystal temperature patterns show that there are pronounced 3-dimensional effects in the flow and temperature patterns with low shroud spacings, especially near the top of the 3 columns of heaters. With no shroud and wider shroud spacings, the heat transfer and fluid flow problem is primarily 2-dimensional, especially at the lower center portion of the 3 columns and at the center of the heaters. The central plane of the bottom heater of the center column (section AA in Fig. 46) was chosen for a 2-dimensional numerical comparison.

### **B. 0.2 WATT NUMERICAL COMPARISON**

The first attempt to model the temperature measured with a thermocouple at the middle of the back of the heater for the 0.2 watt case agreed only by approximately 25%. Figure 47 shows the heater surface temperatures versus S1. S1, as in the parametric study, is the counter-clockwise contour distance around the heater starting at the lower right corner of the heater. The experimental value of the thermocouple is located at S1 slightly greater than 1.5. To get closer to the experimental temperature the numerical model was examined again. A two heater model was developed to account for the effect of upper heaters. Figure 48 shows the corresponding temperature contours and streamlines. With the two heater model the agreement was within approximately 13%, as seen in

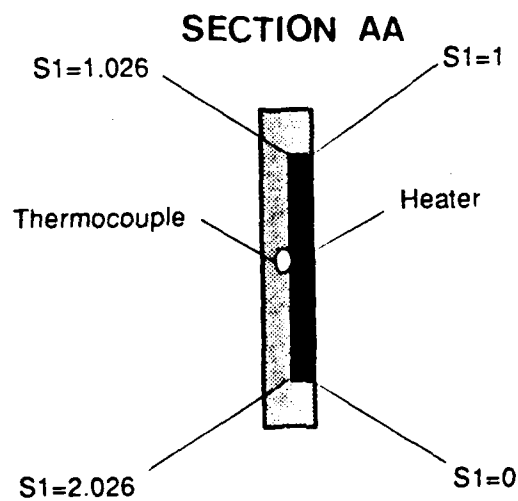
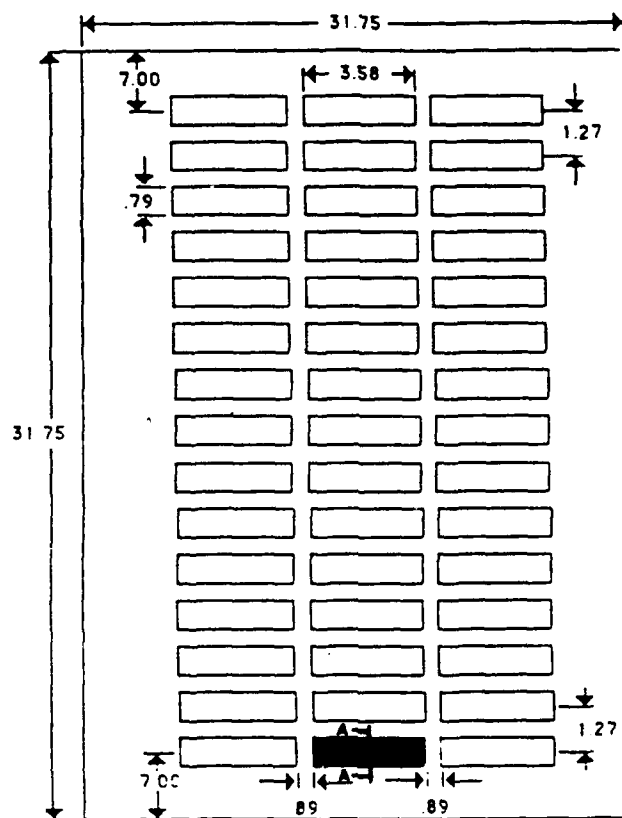


**Figure 46. Schematic diagram of the experimental heater studied**

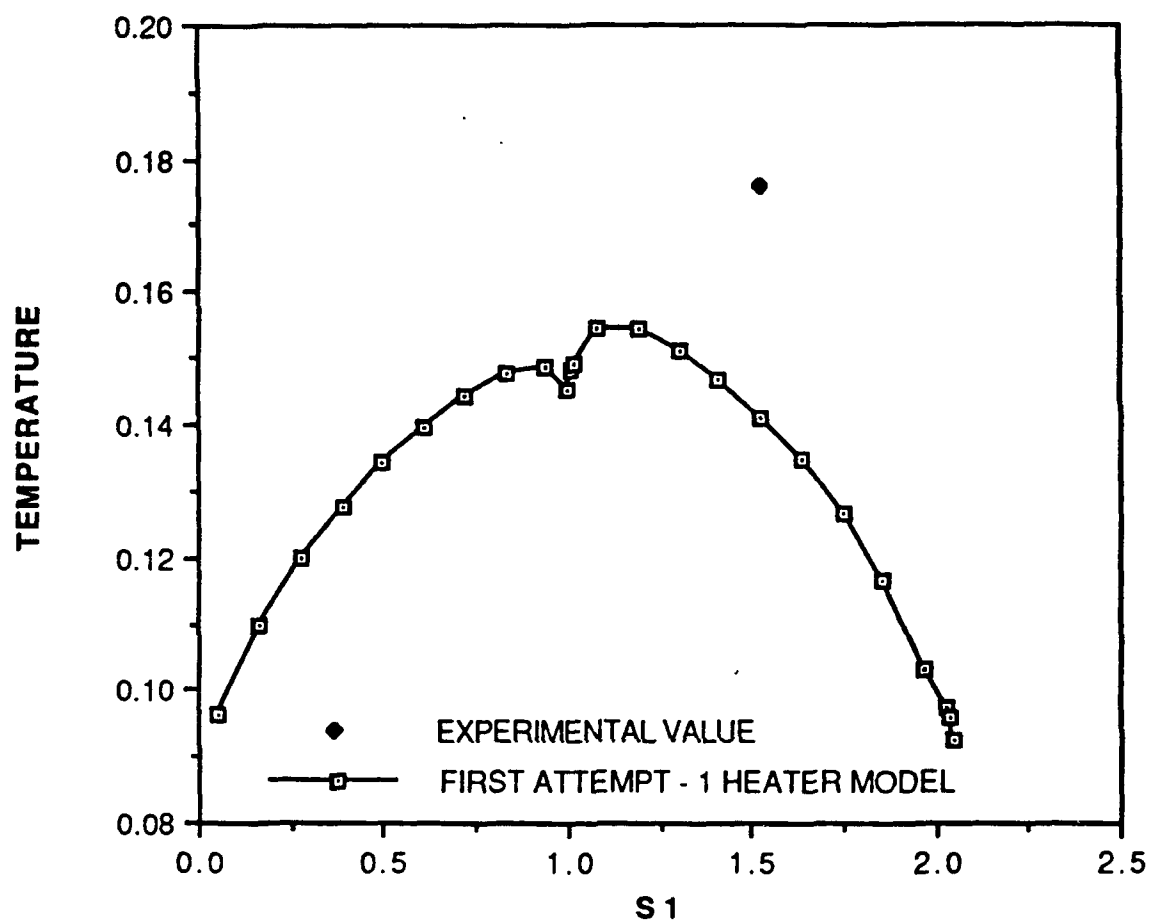


Figure 47. Initial 2W experimental/numerical comparison

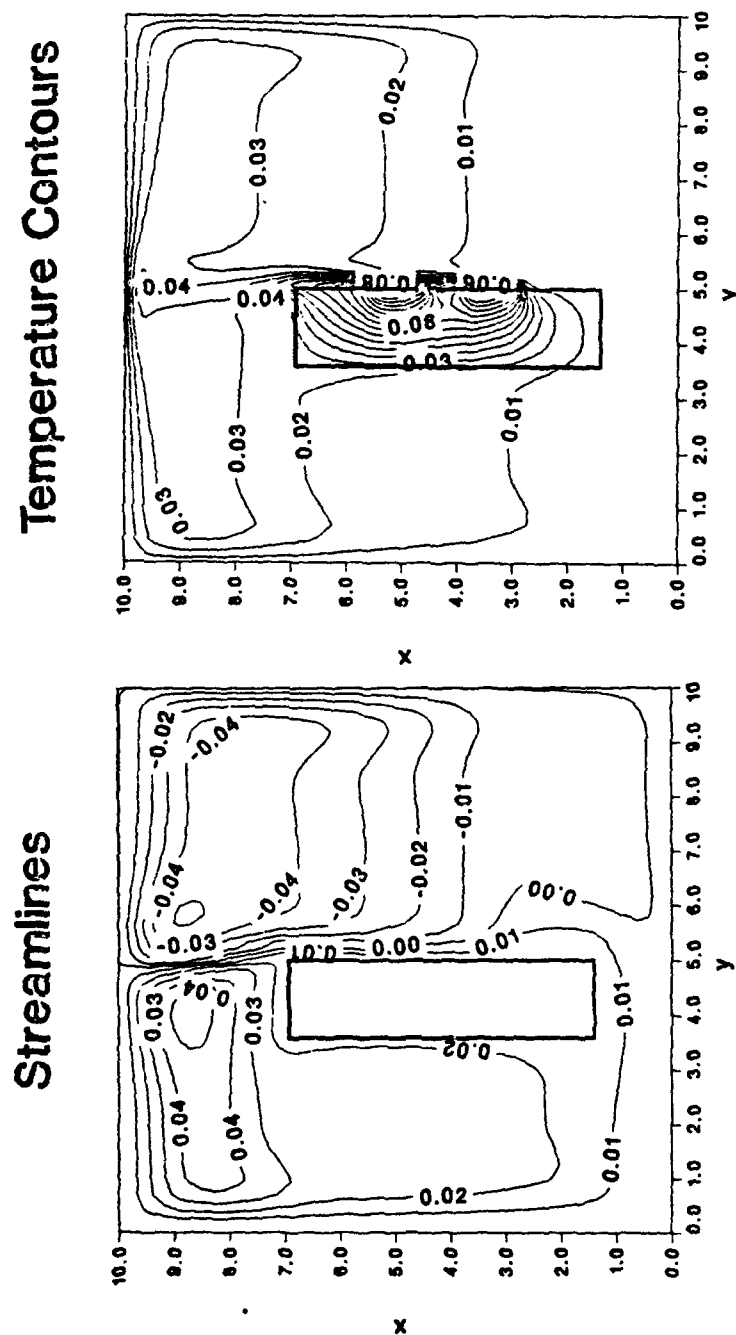


Figure 48. Temperature contours and streamlines for 2 heater model

Fig. 49. The heaters were placed within the grooves in the plexiglass test-surface using a low thermal conductivity epoxy. During the liquid crystal work it was observed that the epoxy thermal conductivity was lower than that of plexiglass, so, a thermal conductivity of  $1/2$  that of plexiglass was used in the numerical model to see what effect it would have on the comparison. It proved to be a slight improvement over the plexiglass thermal conductivity case but not as much of an improvement as the two heater model, as seen in Fig. 50. The dimensions of the heater were then looked at closely. The heater is made up of a Kapton sheet and an inconel sheet together. The dimensions of the Kapton were the dimensions of the heater that were being used but the inconel was actually the resistor that was causing the increase in temperature and its dimensions were smaller than the Kapton. The height of the region which contained the inconel was 0.0062 m and the width was 0.022 m. When these new smaller dimensions were used in the numerical model the agreement was much better as seen in Fig. 51. Temperatures for both thermal conductivities (0.14 W/m-K and 0.07 W/m-K) are plotted in Fig. 51 and the agreement with the experiment is within approximately 9% for the one heater model.

The heater was a layer of Kapton over a sheet of inconel as stated above. When the heater was modeled as two layers, the numerical prediction was within 7 % of the experimental measurement as shown in Fig. 52. When the two heater model was used with the smaller dimensions for the heater and the heater divided into two layers, as mentioned above, Fig 53 shows that the temperature variation for the two different substrate conductivities bracketed the experimental result, as was expected.

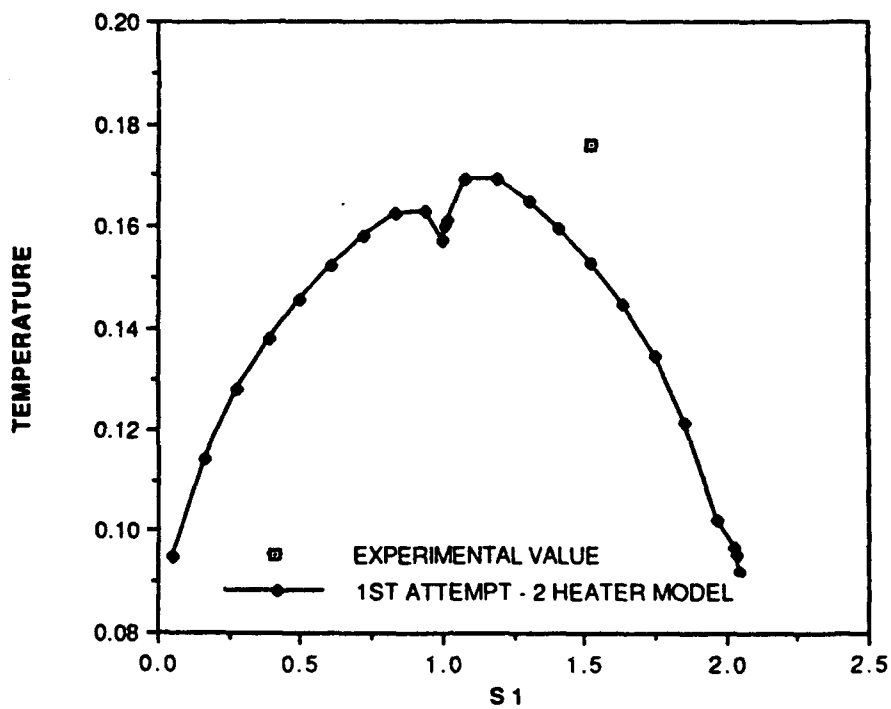


Figure 49. First attempt at 2 heater model

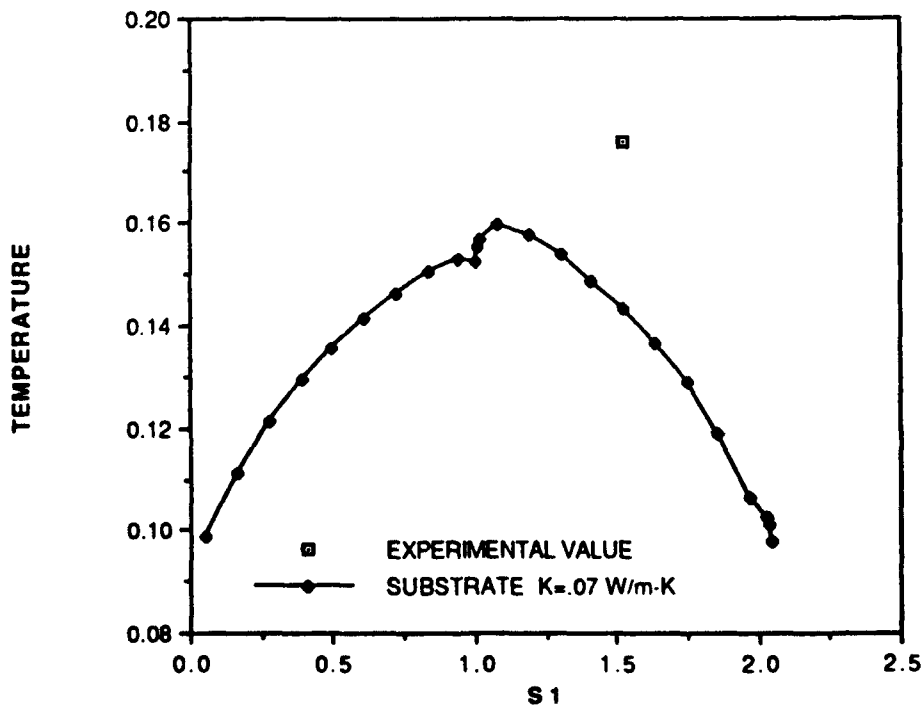


Figure 50. Thermal conductivity of plexiglass changed to .07 W/m-K, 1 heater model



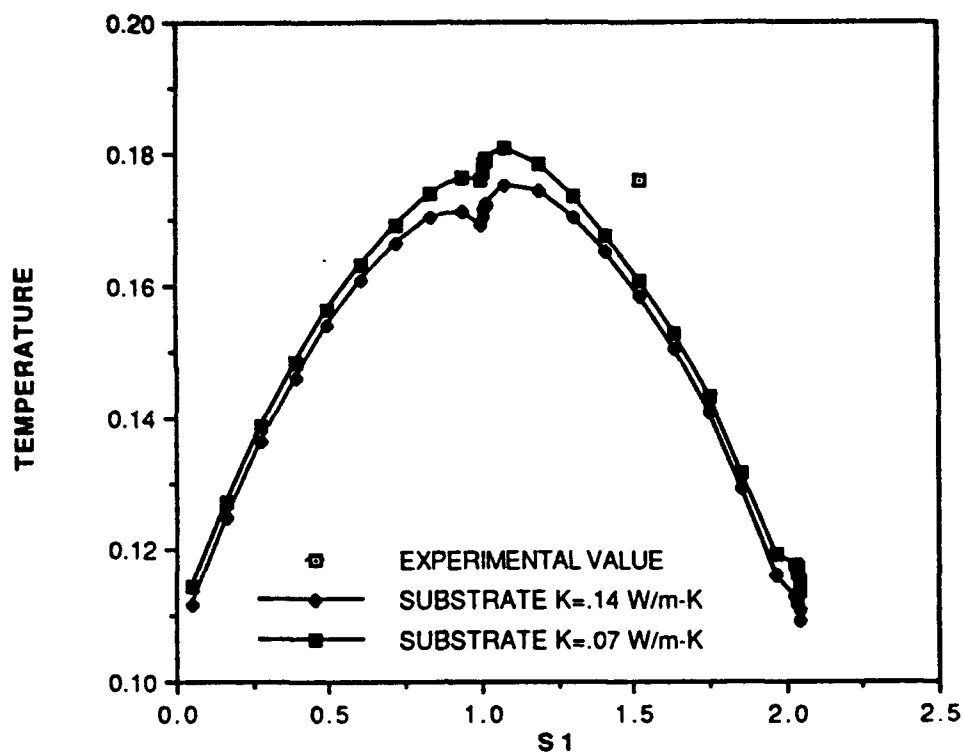


Figure 51. Dimensions of the heater changed to that of Inconel-1 heater

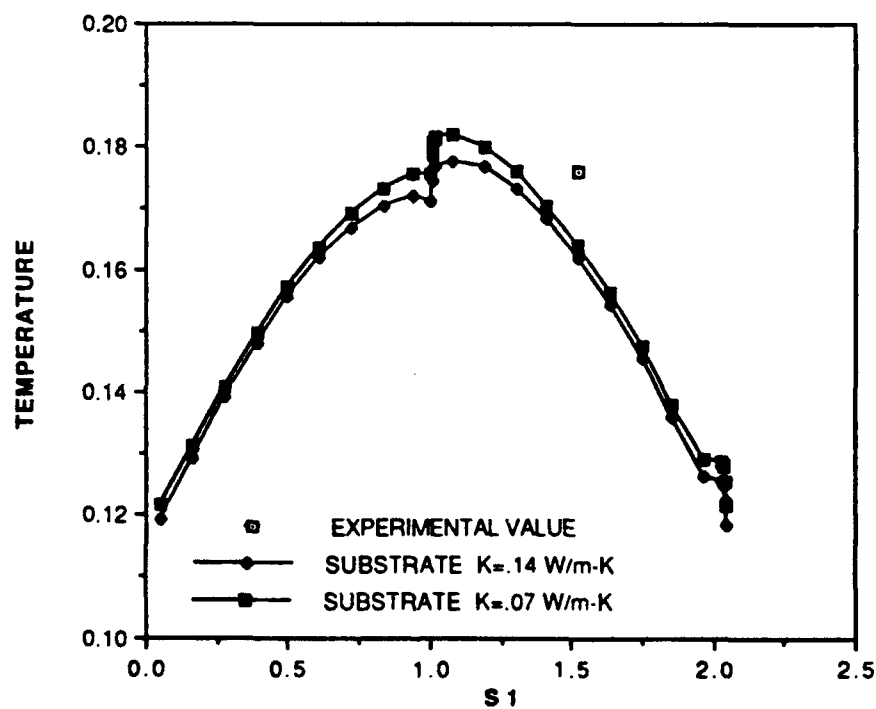


Figure 52. One heater model, heater split into a Kapton and Inconel layer

### **C. HIGHER POWER NUMERICAL COMPARISONS**

The measured component temperatures at higher power levels experimental values did not agree as closely as the 0.2 watt power case. Figure 54 shows that as the power input per heater is increased the disagreement between the numerical and experimental values increases. At 0.5 watt power input the percent difference is approximately 8 %. One possible reason for this is that as the power is increased, the downstream heaters have a greater effect on the upstream heater temperatures due to greater conduction through the substrate. Thus the experimentally measured temperatures are higher by a greater extent compared to the numerical model. Thus for comparison with higher power cases, additional heaters must be added both on the side and on the top in the model. Another possible reason for the percent difference increase with power is that the properties for the water used in the model were taken at the average temperature of the heater and the ambient water. Also, the inconel region of the heater was taken as a uniform heat source in the model but in reality is a ribbon that snakes up and down on the Kapton sheet. At higher power levels this could cause hotter areas near the ribbon and this could cause the numerical value to be slightly lower. Still another possibility is that there are 3-dimensional effects in reality that the 2-dimensional model cannot detect and these effects get larger with increased power. Entrainment of the warmer fluid from the sides columns into the center region of the heater could make the experimental value greater than the 2-dimensional model.

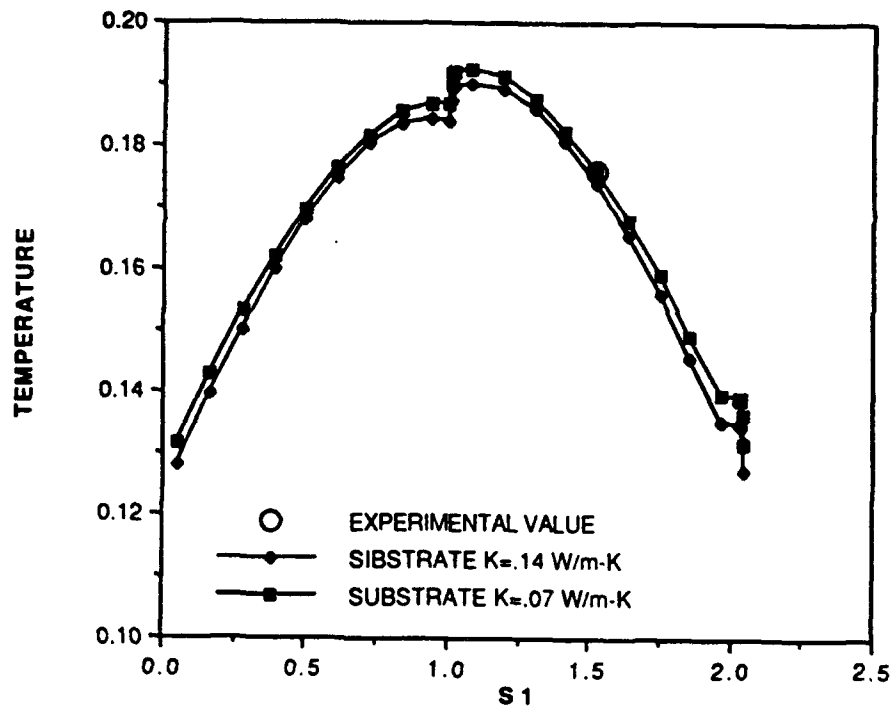


Figure 53. 2 heater model with heater divided into two layers

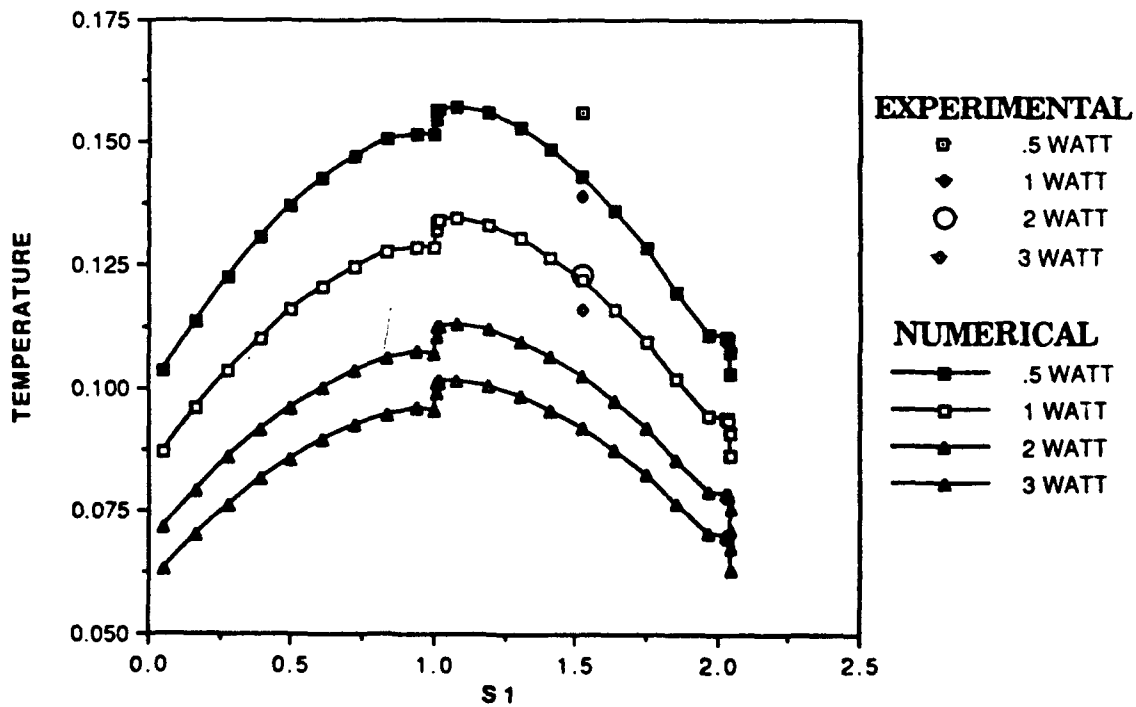


Figure 54. Higher power level two heater model results with heater divided

#### **D. UPPER/LOWER HEATER NUMERICAL EVALUATION**

The numerical model for two heaters provided the upper and lower heater temperatures. A study of the effects of the lower heater on the upper heater was conducted. Figures 55-59 show the progression of the top and bottom heater temperatures as the power is increased from 0.2 to 3 watts equally in both heaters. Figures 60-61 collect the temperature patterns at the various power levels studied for the two heaters. Similar patterns are observed as power level increases for all top heaters and all bottom heaters when compared with themselves. When comparing the lower heater to upper heater temperatures, there is a larger increase in the top heater's top face temperatures. The back face temperatures do not decrease as much on the top heater as the bottom heater. Also, the bottom face temperatures of the top heater do not decrease below the temperature of the bottom of the front face contrary to the bottom heater. It is more difficult for the upper heater to lose heat because of the natural convection bringing up the heat from the lower heater, thus the upper heater temperatures are higher than the lower heater temperatures. The front face temperatures of both heaters are always closer than the other faces. As power level increases, the top, back and bottom faces become farther from their counterparts on the bottom heater.

Figures 62-65 compare the heat loss through the heater face for increasing power levels. The only face that shows an increase for the top and the bottom heater is the front face. At low power levels the percent heat loss through the front face with increasing power is its largest. Both

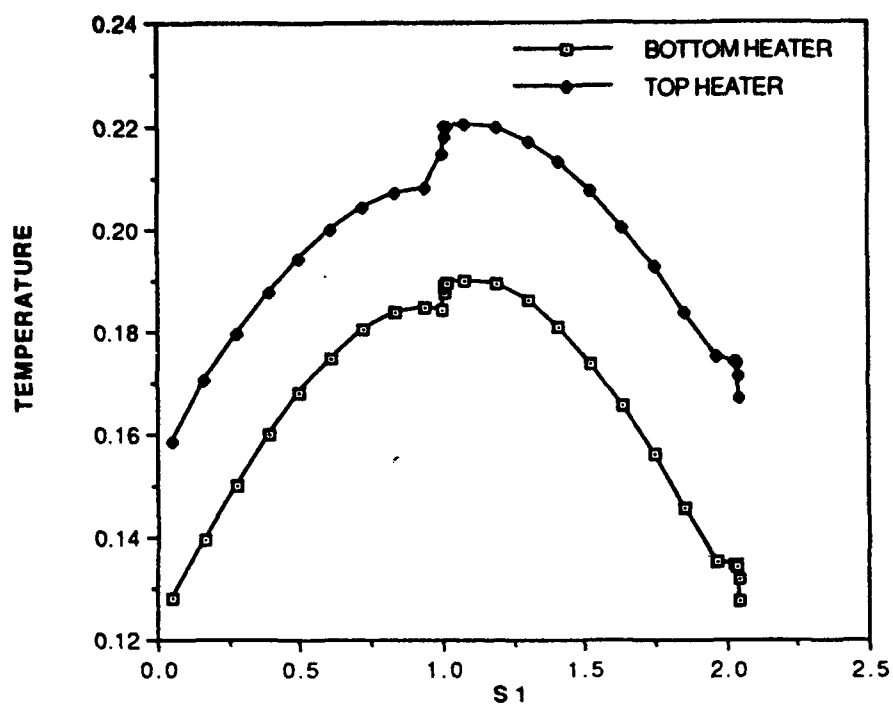


Figure 55. 0.2 watt case top and bottom heater surface temperatures

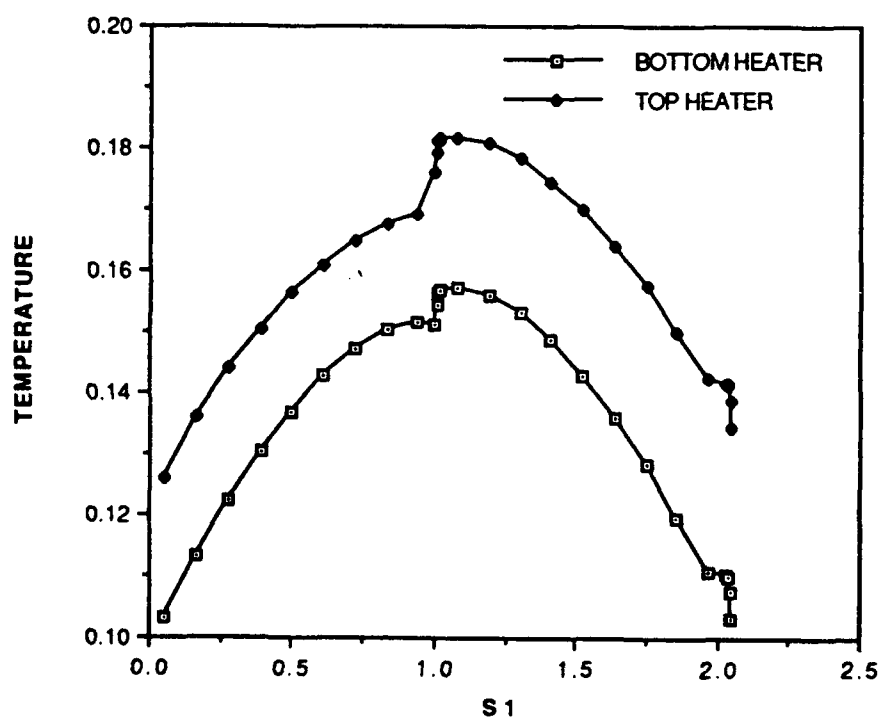


Figure 56. 0.5 watt surface temperatures for the top and bottom heater

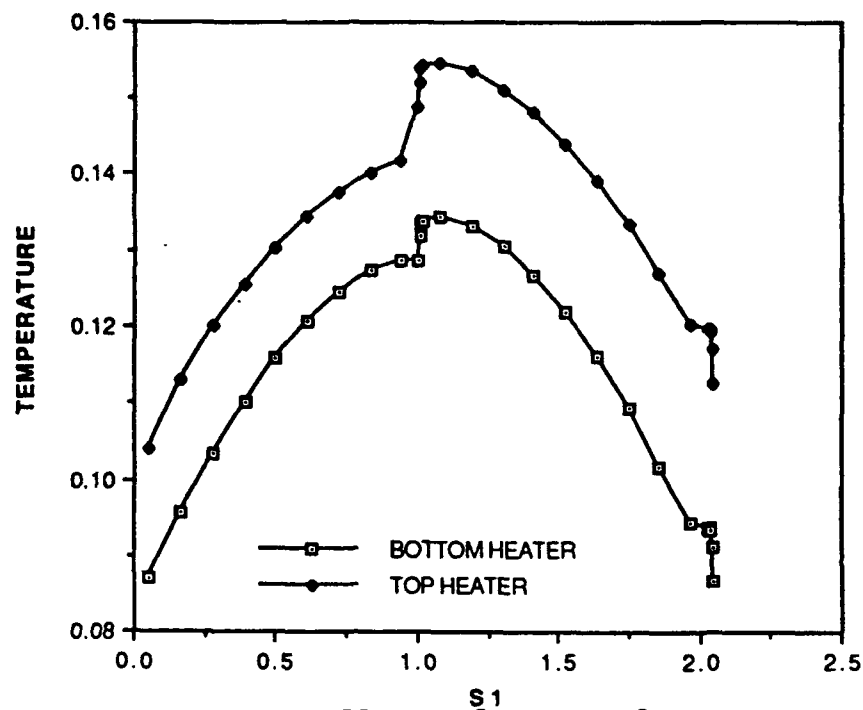


Figure 57. 1 watt per heater top and bottom heater surface temperatures

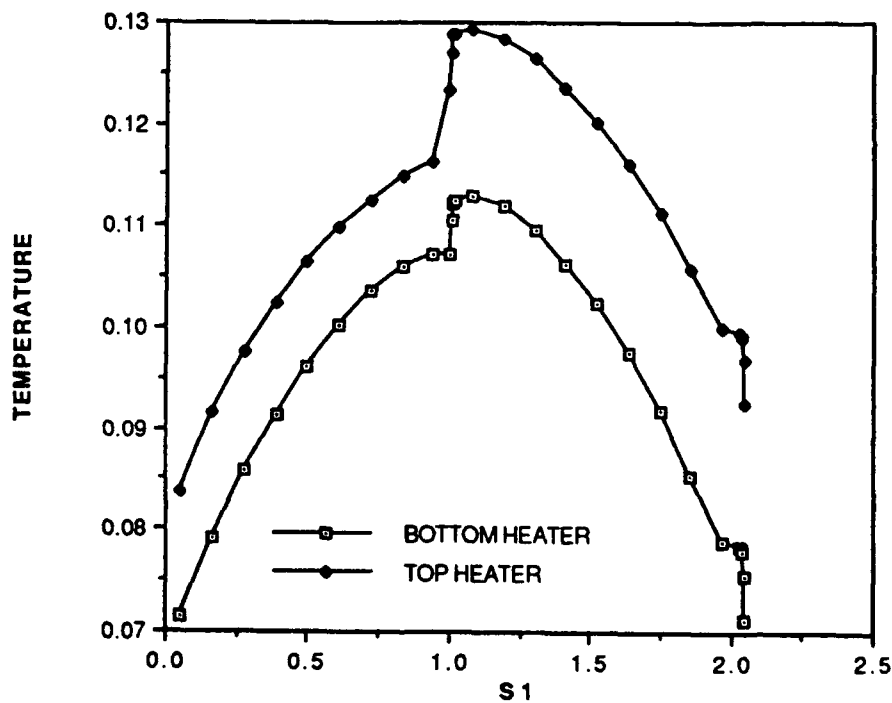
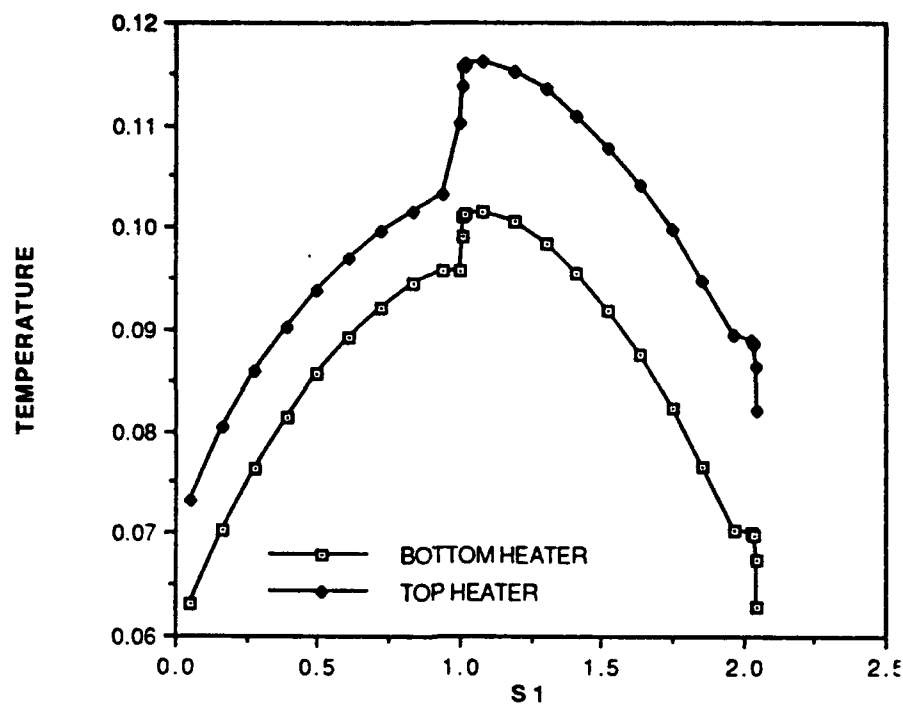
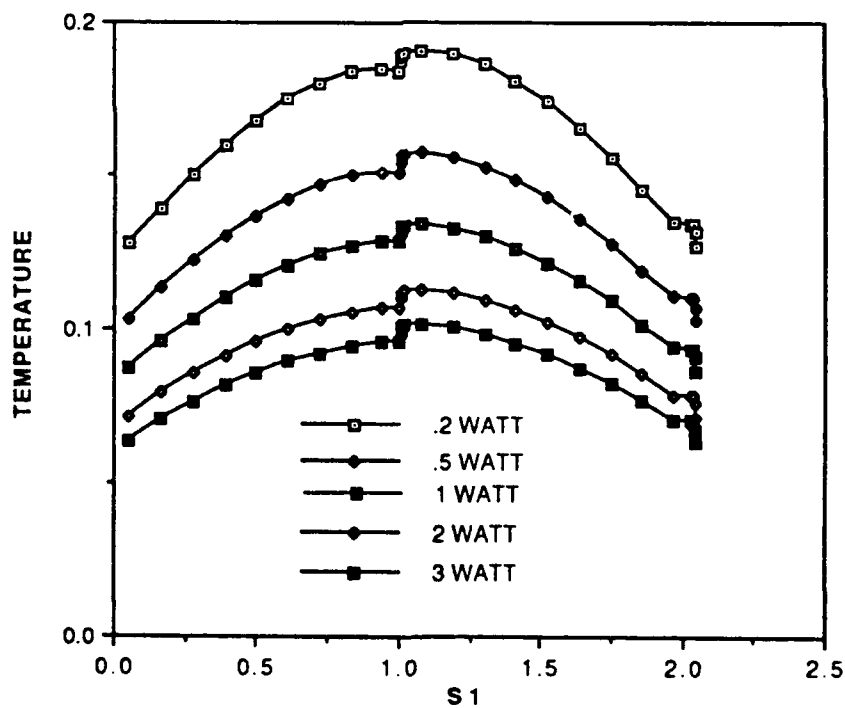


Figure 58. 2 watts per heater top and bottom surface temperatures



**Figure 59. 3 watt per heater top and bottom heater surface temperatures**



**Figure 60. 0.2-3 watts bottom heater surface temperatures**

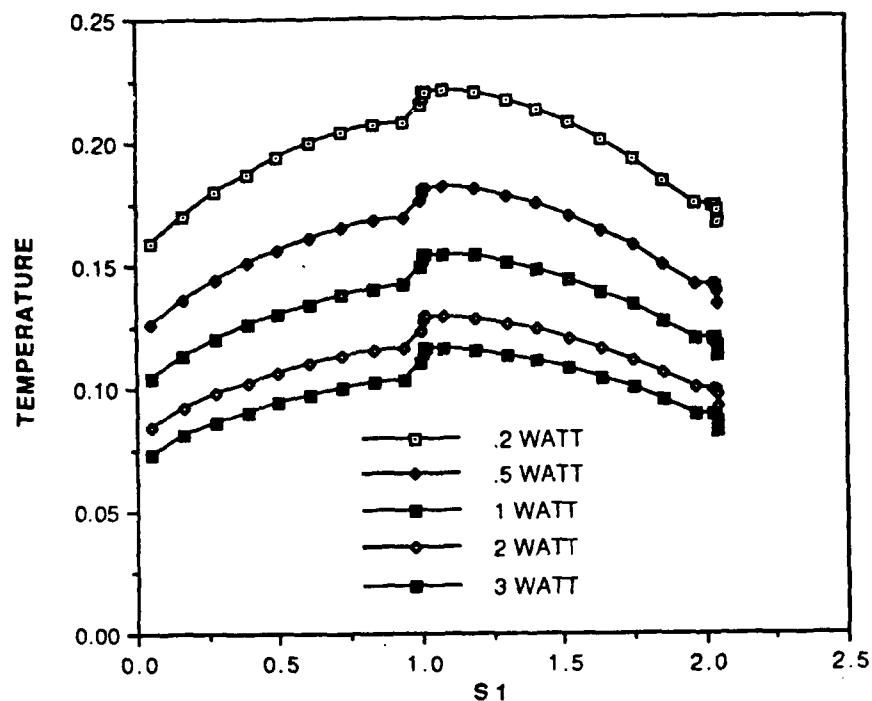


Figure 61. 0.2-3 watt top heater surface temperatures

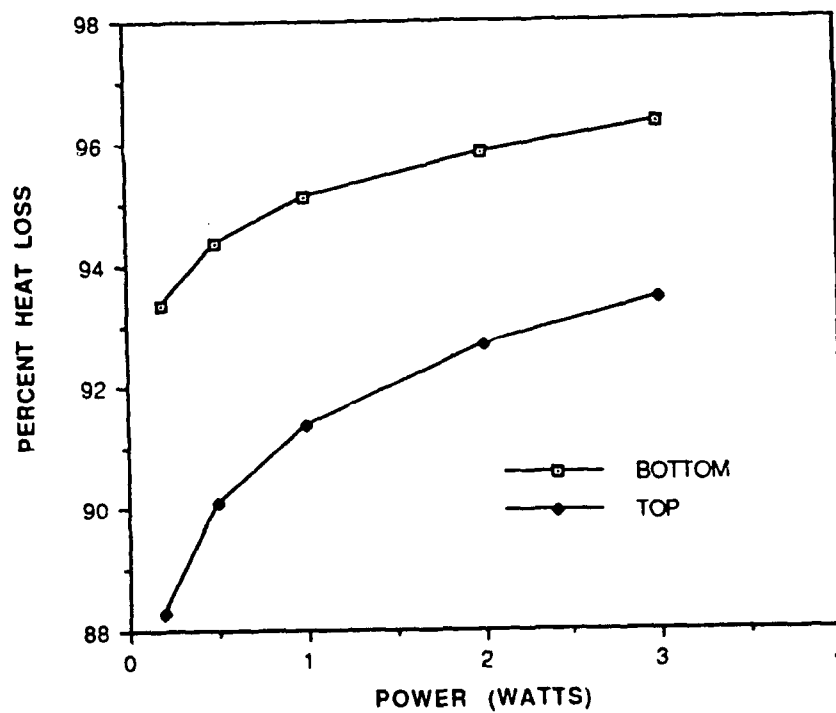
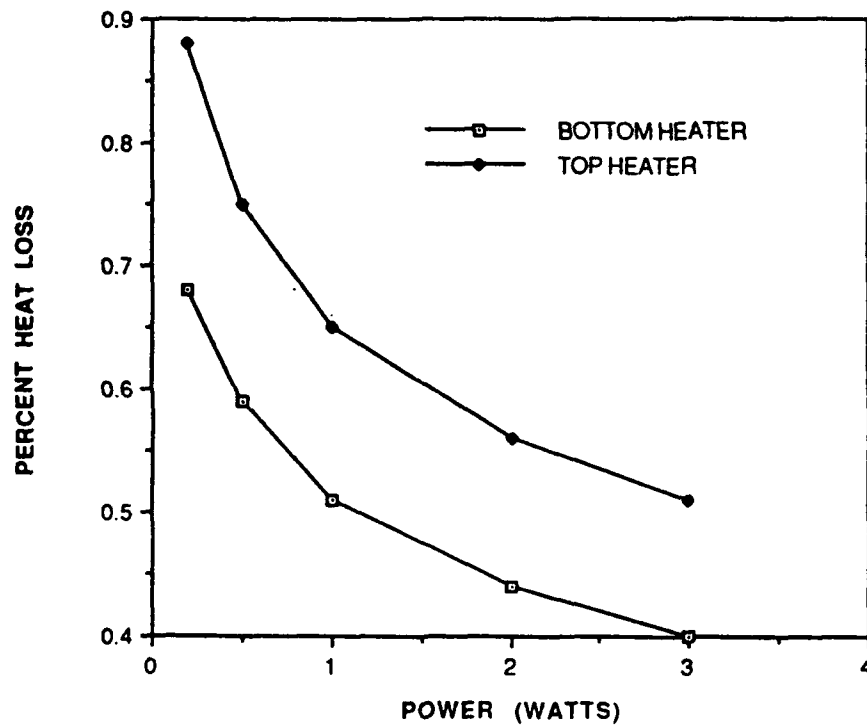
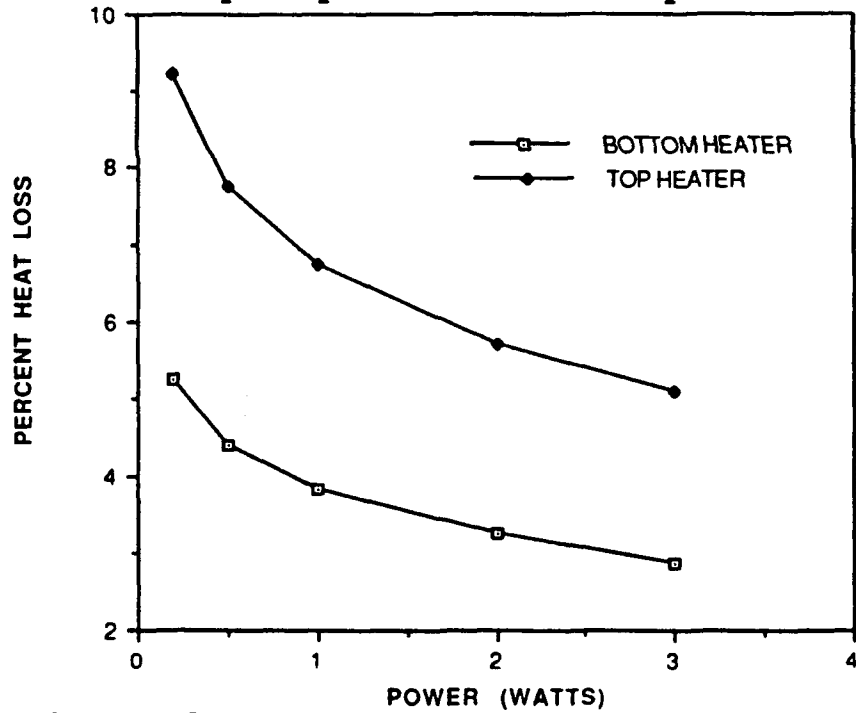


Figure 62. 0.2 -3 watt front face percent heat loss for top and bottom heater





**Figure 63. 0.2-3 watt top face percent heat loss for top and bottom heater**



**Figure 64. 0.2-3 watt back face percent heat loss for top and bottom heater**

heaters show a similar pattern. The back and bottom faces percent heat loss both decrease for increasing power levels

The effect on the lower heater of a heater above it is shown in Figs. 66-67. For 0.2 watt power input per heater shown in Fig. 66, the one heater model surface temperatures are all less than the corresponding 2 heater model surface temperatures for the bottom heater. For 3 watts power per heater, shown in Fig. 67 the opposite is true. The surface temperatures for the bottom heater of the 2 heater model are lower except at the top of the heaters where it is equal to the one heater model. The increased convection for the 2 heater model when the heat input is much higher causes lower temperatures at the bottom of the lower heater. Thus for 0.2 watts, conduction from the upper heater to the lower heater causes an increase in temperature of the bottom heater, whereas for a higher power input of 3 watts, the increased convection caused a cooling effect on the bottom heater.

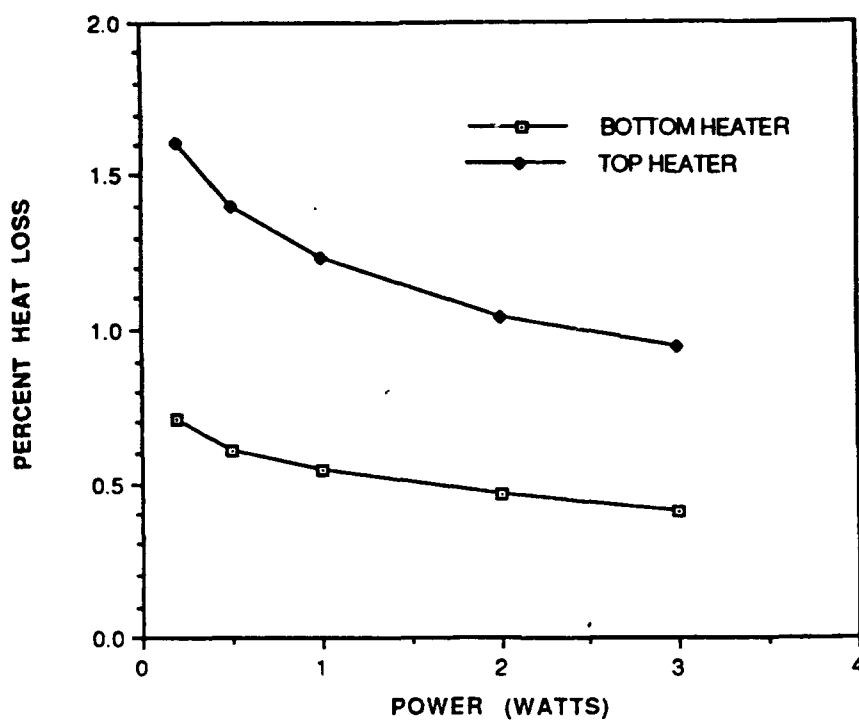


Figure 65. 0.2-3 watt bottom face percent heat loss for top and bottom heater

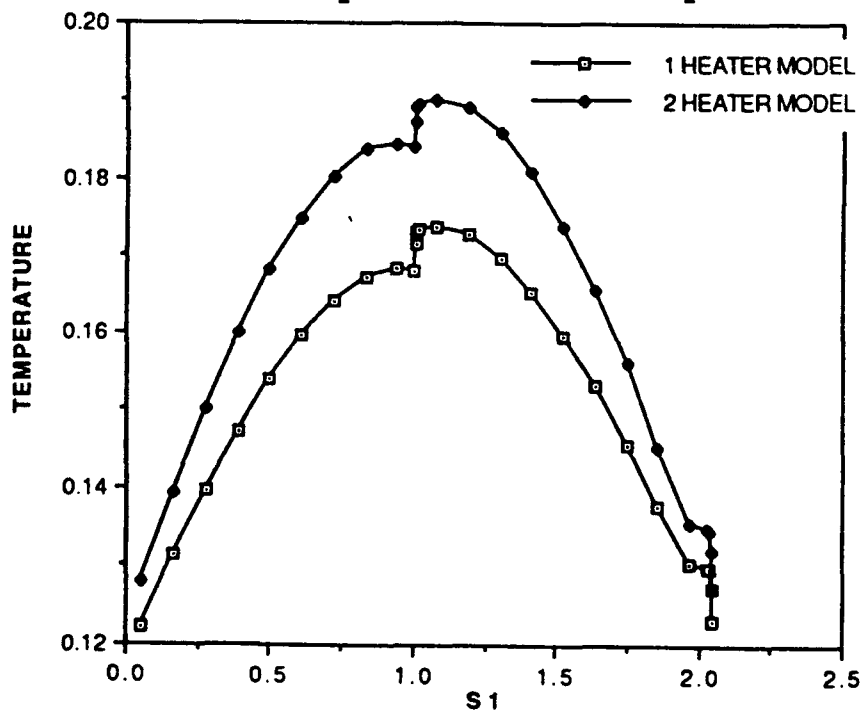
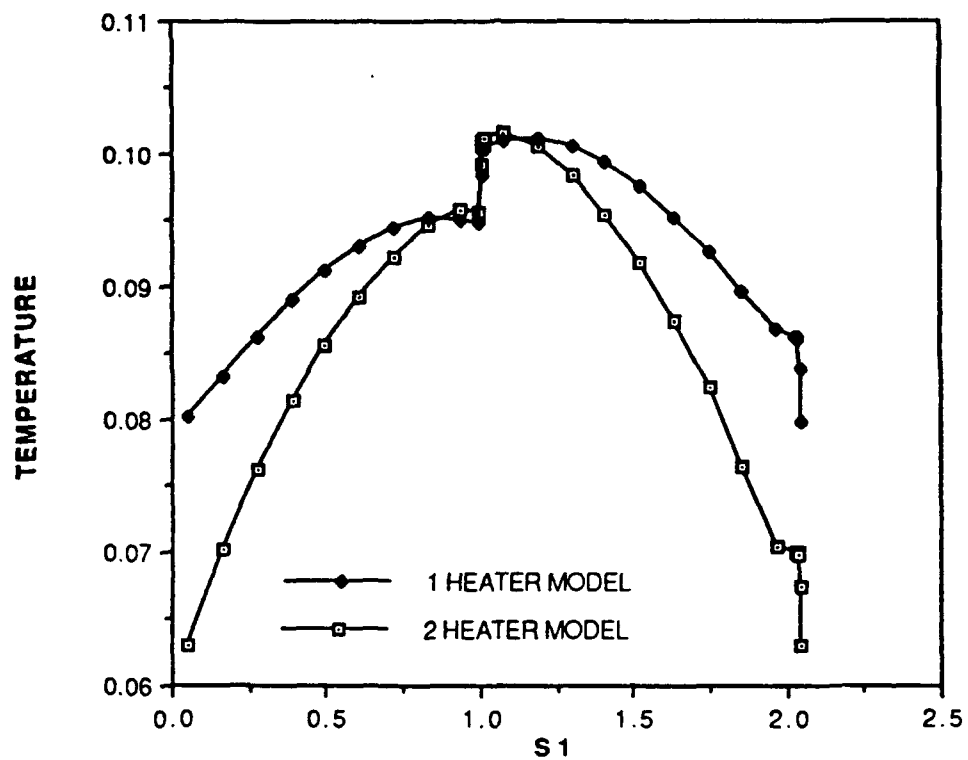


Figure 66. 0.2 watt surface temperatures for bottom heater for 1&2 heater models



**Figure 67. 3 watt surface temperatures for bottom heater for 1&2 heater models**

## VI. CONCLUSIONS

During the course of the numerical and experimental study, several important conclusions were drawn about the transfer of heat from a flush heat source. A constant flux of temperature boundary condition must be used carefully as the numerical study showed that it can be far from uniform when using the conjugate solution to solve the problem. With the advent of faster computers it seems that all heat transfer problems should be solved with a combined conduction/convection procedure to improve accuracy of the solution.

Changes in the  $Pr$  between 7 and 100 did not change the nondimensional temperatures. This was extremely important to this study because the experimental work has been done in water, with a  $Pr$  of 7 and most fluids that are currently being used for the immersion of electronic components are fluorinerts and have a  $Pr$  greater than 10 and less than 100. The experimental results should therefore be applicable to these fluids as well.

Increasing the  $R_s$  provides substantial cooling enhancement when  $R_s$  is less than 10 but increasing it past 10 only provides slight enhancement. For the designer of electronic equipment, this should help in the decision as to how high a conductivity the substrate should be. When a choice of more than one material is available, the cheapest material with an  $R_s$  of 10 or greater could be chosen.

An increase in  $R_c$  provides lower and more uniform component temperatures primarily for  $R_c$  less than 25. The designer can once again

look for the cheapest material that would do the job with an  $R_c$  of 25 or greater and optimize the cooling of the component as well.

There is almost a linear decrease in maximum temperature with increase in  $w/d_t$ . This would suggest that the component should be made as wide as the substrate if the design permits.

Finally, liquid crystals proved to be a valuable tool in determining the areas of the hot flow up the front of an experimental surface. The effect of the shroud spacing became very evident as the spacing decreased. Although at small shroud spacing the 3-D effects of the fluid flow were evident, at large spacing and no shroud conditions and near the bottom of the high density board always the heat transfer process could be modeled as 2-dimensional. Very good agreement of numerical and experimental results were seen, especially at the low power levels.

## **VII. RECOMMENDATIONS**

In continuation of this study, it is suggested that the same configuration of three high density heater columns be used, however it is recommend that the following aspects be further investigated:

- Utilize liquid crystals to determine the spacing where shroud effects are negligible

- Use a 3 heater model to determine what effects this would have on the lower heater at the higher power levels

- Analyse the effects of using non-steady power inputs on the heat transfer

- Utilize a 3-dimensional numerical model to see if 3-D effects are significant, especially at the high power levels

- A nonflexible container should be acquired for the deaeration system to allow the use of the test surface at higher power levels

- High power studies to determine the onset of turbulence could be looked at with the accompanying effects on the heat transfer

# APPENDIX A

## USER PORTION OF FINITE DIFFERENCE PROGRAMS

```

C *****THEESIS*****
C
      BLOCK DATA
      LOGICAL LSOLVE,LPRINT,LBLK,LSTOP
      COMMON F(75,75,5),P(75,75),RHO(75,75),GAM(75,75),CON(75,75),
1 AIP(75,75),AIM(75,75),AJP(75,75),AJM(75,75),AP(75,75),
2 X(75),XU(75),XDIF(75),XCV(75),XCVS(75),
3 Y(75),YV(75),YDIF(75),YCV(75),YCVS(75),
4 YCVR(75),YCVRS(75),ARX(75),ARXJ(75),ARXJP(75),
5 R(75),RMN(75),SX(75),SXMN(75),XCVI(75),XCVIP(75)
      COMMON DU(75,75),DV(75,75),FV(75),FVP(75),
1 FX(75),FXM(75),FY(75),FYM(75),PT(75),QT(75)
      COMMON/INDX/NF,NFMAX,NP,NRHO,NGAM,L1,L2,L3,M1,M2,M3,
1IST,JST,ITER,LAST,TITLE(13),RELAX(13),TIME,DT,XL,YL,
2IPREF,JPREF,LSOLVE(10),LPRINT(13),LBLK(11),MODE,NTIMES(10),
3RHOCON,ZERO
      COMMON/CNTL/LSTOP
      COMMON/SORC/SMAX,SSUM
      COMMON/COEF/FLOW,DIFF,ACOF,ALFA
      DIMENSION U(75,75),V(75,75),PC(75,75)
      EQUIVALENCE(F(1,1,1),U(1,1)),(F(1,1,2),V(1,1)),(F(1,1,3),
1PC(1,1))
      DIMENSION TH(75),THU(75),THDIF(75),THCU(75),THCVS(75)
      EQUIVALENCE(X(1),TH(1)),(XU(1),THU(1)),(XDIF(1),THDIF(1)),
1(XCV(1),THCV), (XCVS(1),THCVS(1)),(XL,THL)
      DATA NFMAX,NP,NRHO,NGAM/5,6,7,8/
      DATA LSTOP,LSOLVE,LPRINT/1*.FALSE.,10*.FALSE.,13*.FALSE./
      DATA MODE,TIME,ITER/1,0.,0/
      DATA RELAX,NTIMES/13*1.,10*1/
      DATA LBLK/11*.TRUE./
      DATA DT,IPREF,JPREF,RHOCON/1.E+10,1,1,1.0/
C *****
C  ENTER DATA INTO LABELED COMMONS USING DATA STATEMENTS
C *****
      DATA TITLE(1),TITLE(2),TITLE(3),TITLE(4),
1TITLE(6)/'VELU','VELV','STFN','TEMP',
2'PRES'/
      DATA (LSOLVE(I),I=1,4),LSOLVE(6),LPRINT(3)/6*.TRUE./
      DATA RELAX(1),RELAX(2),RELAX(4),RELAX(6),ALFA/.04,.04,.4,.4,.1/
      DATA LAST/5000/
C  DATA LAST/5/
      END
C *****
      SUBROUTINE USER
C *****

```



```

COMMON F(75,75,5),P(75,75),RHO(75,75),GAM(75,75),CON(75,75),
1 AIP(75,75),AIM(75,75),AJP(75,75),AJM(75,75),AP(75,75),
2 X(75),XU(75),XDIF(75),XCV(75),XCVS(75),
3 Y(75),YV(75),YDIF(75),YCV(75),YCVS(75),
4 YCVR(75),YCVRS(75),ARX(75),ARXJ(75),ARXJP(75),
5 R(75),RMN(75),SX(75),SXMN(75),XCVI(75),XCVIP(75)
COMMON DU(75,75),DV(75,75),FV(75),FVP(75),
1 FX(75),FXM(75),FY(75),FYM(75),PT(75),QT(75)
LOGICAL LSOLVE,LPRINT,LBLK,LSTOP
COMMON/INDX/NF,NFMAX,NP,NRHO,NGAM,L1,L2,L3,M1,M2,M3,
1IST,JST,ITER,LAST,TITLE(13),RELAX(13),TIME,DT,XL,YL,
2IPREF,JPREF,LSOLVE(10),LPRINT(13),LBLK(11),MODE,NTIMES(10),
3RHOCON,ZERO
COMMON/CNTL/LSTOP
COMMON/SORC/SMAX,SSUM
COMMON/COEF/FLOW,DIFF,ACOF,ALFA
DIMENSION U(75,75),V(75,75),PC(75,75)
EQUIVALENCE(F(1,1,1),U(1,1)),(F(1,1,2),V(1,1)),(F(1,1,3),
1PC(1,1))
DIMENSION TH(75),THU(75),THDIF(75),THCU(75),THCVS(75)
EQUIVALENCE(X(1),TH(1)),(XU(1),THU(1)),(XDIF(1),THDIF(1)),
1(XCV(1),THCV), (XCVS(1),THCVS(1)),(XL,THL)
DIMENSION T(75,75),STO(75,75),IBODY(75,75)
EQUIVALENCE (T(1,1),F(1,1,4))
LOGICAL LREAD,LWRITE
DIMENSION D(10),H(10),W(10),Q(10)
DIMENSION TTOP(75),TSIDES(2,75),TBOT(75),QTOP(75),QSIDES(2,75),
1QBOT(75),QHTR(75),THBSID(75),THTOP(75),THBOT(75)
CHARACTER*1 AREAD
C*****
ENTRY GRID
C*****
write(36,*) ' ks = 10 ,ra=10e6 '
WRITE(36,*)
C    SET UP THE GRID
N1X=11
N2X=6
N3X=9
N4X=11
N5X=17
N6X=8
N7X=10
N1Y=8
N2Y=12
N3Y=15
N4Y=15
N5Y=11
N6Y=12
C HEATER DIMENSIONS
WIDTH=.02
H1=.0078
DEPTH=.5*H1
C    SET UP THE DIMENSIONS OF THE ENCLOSURE
AL1=3*H1/H1
AL2=H1/H1
AL3=(H1-DEPTH)/H1
AL4=DEPTH/H1
AL5=2*H1/H1
AL6=2*H1/H1
AL7=H1/H1

```

```

BL1=2*H1/H1
BL2=2*H1/H1
BL3=H1/H1
BL4=2*H1/H1
BL5=2*H1/H1
BL6=H1/H1
DX1=AL1/N1X
DX2=AL2/N2X
DX3=AL3/N3X
DX4=AL4/N4X
DX5=AL5/N5X
DX6=AL6/N6X
DX7=AL7/N7X
DY1=BL1/N1Y
DY2=BL2/N2Y
DY3=BL3/N3Y
DY4=BL4/N4Y
DY5=BL5/N5Y
DY6=BL6/N6Y
C      MAKING OF THE GRID
      XU(2)=0
      FIRST=3
      LLAST=3-1+N1X
      DO 11 I=FIRST,LLAST
        XU(I)=XU(I-1)+DX1
11     CONTINUE
      FIRST=LLAST+1
      LLAST=LLAST+N2X
      DO 12 I=FIRST,LLAST
        XU(I)=XU(I-1)+DX2
12     CONTINUE
      FIRST=LLAST+1
      LLAST=LLAST+N3X
      DO 13 I=FIRST,LLAST
        XU(I)=XU(I-1)+DX3
13     CONTINUE
      FIRST=LLAST+1
      LLAST=LLAST+N4X
      DO 14 I=FIRST,LLAST
        XU(I)=XU(I-1)+DX4
14     CONTINUE
      FIRST=LLAST+1
      LLAST=LLAST+N5X
      DO 15 I=FIRST,LLAST
        XU(I)=XU(I-1)+DX5
15     CONTINUE
      FIRST=LLAST+1
      LLAST=LLAST+N6X
      DO 16 I=FIRST,LLAST
        XU(I)=XU(I-1)+DX6
16     CONTINUE
      FIRST=LLAST+1
      LLAST=LLAST+N7X
      DO 17 I=FIRST,LLAST
        XU(I)=XU(I-1)+DX7
17     CONTINUE
      L1=LLAST
      XL=XU(LLAST)
      YV(2)=0
      FIRST=3

```

```

        LLAST=FIRST-1+N1Y
        DO 19 I=FIRST,LLAST
            YV(I)=YV(I-1)+DY1
19      CONTINUE
        FIRST=LLAST+1
        LLAST=LLAST+N2Y
        DO 20 I=FIRST,LLAST
            YV(I)=YV(I-1)+DY2
20      CONTINUE
        FIRST=LLAST+1
        LLAST=LLAST+N3Y
        DO 21 I=FIRST,LLAST
            YV(I)=YV(I-1)+DY3
21      CONTINUE

        FIRST=LLAST+1
        LLAST=LLAST+N4Y
        DO 22 I=FIRST,LLAST
            YV(I)=YV(I-1)+DY4
22      CONTINUE
        FIRST=LLAST+1
        LLAST=LLAST+N5Y
        DO 23 I=FIRST,LLAST
            YV(I)=YV(I-1)+DY5
23      CONTINUE
        FIRST=LLAST+1
        LLAST=LLAST+N6Y
        DO 24 I=FIRST,LLAST
            YV(I)=YV(I-1)+DY6
24      CONTINUE
        M1=LLAST
        YL=YV(LLAST)
        RETURN

C      ENTRY START
C      CIRCUIT BOARD CORNERS
        NA=N1X+N2X+2
        NB=N1X+N2X+N3X+N4X+1
        NC=N1Y+2
        ND=N1Y+N2Y+N3Y+N4Y+1
C      TEMPERATURE PRINTOUT LOCATION
        ITL=INT(N3Y/2)+1
C      HEATER LOCATIONS
        NQX=NB
        NQY1=NC+N2Y
C      INITIAL CONDITIONS
        DO 100 J=1,M1
        DO 100 I=1,L1
            U(I,J)=0.
            V(I,J)=0.
            T(I,J)=0.
            STO(I,J)=0.
100      CONTINUE
C***RELAXATION FOR BOUYANT FORCE (NOW FOUND AT THE TOP)
C      ALFA=.1
        ALFAM=1.-ALFA
C      PROPERTY ENTRY POINT
        RA=1.E6
        PR=25
        CP=4185

```

```

      RHOF=999.0
      BETA=162.020E-6
      G=9.807
      CONFLD=.596
      CONPLX=10*CONFLD
      CONHTR=25*CONFLD
      DYNVIS=PR*CONFLD/CP
      XKK=CONFLD
      ALPHA=CONFLD/(RHOF*CP)
      Q1=RA*ALPHA*CONFLD*DYNVIS/(RHOF*G*BETA*H1*H1*H1)
      USTAR=SQRT(G*BETA*Q1*H1/CONFLD)
      AMU=(DYNVIS/(RHOF*H1*USTAR))
      DUMMY=CP*RHOF*H1*USTAR
C DUMMY1 USED FOR DIMENSIONAL HEAT FLUXES
      DUMMY1=Q1*DUMMY/(H1*CONFLD)
      AMUP=CONFLD/DUMMY
      GAM2=CONPLX/DUMMY
      GAM4=CONHTR/DUMMY
      XQ=Q1/(DEPTH*H1)
      EIN=Q1
      SOURCE=CONFLD/(CP*DEPTH*RHOF*USTAR)
C PRINT *, '1 IF WANT TO READ FILE, 2 IF STARTING FROM SCRATCH'
C READ *, IFREAD
      IFREAD=2
      IF(IFREAD.EQ.1)THEN
        PRINT*, 'READING DATA'
C
C***READ DATA***
C      NTIME=TOTAL NUMBER OF TIME STEPS
C      ITIME=CURRENT TIMESTEP
C      rewind(46)
C      NTIME=1
C      read(46) NTIME,M1,L1
C
C      PRINT DATA FOR GRID
C      read(46) (YV(J),J=2,M1)
C      read(46) (XU(I),I=2,L1)
C      read(46) (Y(J),J=1,M1)
C      read(46) (X(I),I=1,L1)
C
C      READ DATA FOR DEPENDENDT VARIABLES
C      ITIME=1
C      read(46) ITIME
C      DO 3000 I=1,M1
3000 read(46) (V(J,I),J=1,L1)
C      DO 3020 I=1,M1
3020 read(46) (U(J,I),J=1,L1)
C      DO 3030 I=1,M1
3030 read(46) (T(J,I),J=1,L1)
C      DO 3040 I=1,M1
3040 read(46) (P(J,I),J=1,L1)
C      DO 3050 I=1,M1
3050 read(46) (STO(J,I),J=1,L1)
C      DO 3060 I=1,M1
3060 read(46) (F(J,I,3),J=1,L1)
C      DO 3070 I=1,M1
3070 read(46) (IBODY(J,I),J=1,L1)
      close(46)
      ELSE
      ENDIF

```

```

RETURN

ENTRY DENSE
RETURN

ENTRY BOUND
DO 300 I=2,L2
    T(I,M1)=0
    T(I,1)=0
300 CONTINUE
DO 301 I=2,M2
    T(L1,I)=0
    T(1,I)=0
301 CONTINUE
RETURN

ENTRY OUTPUT
C    IF(ITER.NE.0)GO TO 400
C    PRINT 401
C 401 FORMAT('    ITER',6X,'SMAX',8X,'SSUM ',7X,'V(FRONT)',
C    1 6X,'T(HEATER)')
C 400 PRINT 403,ITER,SMAX,SSUM,V(NQX+1,NQY1+2),T(NQX,NQY1+2)
C 403 FORMAT(I6,1P5E12.3)
    IF(ITER.NE.0)GO TO 400
    write(36,401)
401 FORMAT('    ITER',6X,'SMAX',8X,'SSUM ',7X,'V(FRONT)',
1 6X,'T(THERMC)')
400 IF(INT(ITER/25)*25.NE.ITER)GOTO 404
    write(36,403)ITER,SMAX,SSUM,V(NQX+1,NQY1+ITL),T(NQX,NQY1+ITL)
403 FORMAT(I6,1P5E12.3)
404 CONTINUE
    IF(ITER.LT.LAST) RETURN
    CALL PRINT
    SSUM=0.
    NCOUNT=0
982 CONTINUE
    S2=(YV(3)-YV(2))*H1
    IF(NCOUNT.EQ.1)S2=(YV(M1)-YV(M2))*H1
    DO 983 I=2,L1-1
        S1=(XU(I+1)-XU(I))*H1
        POWER=2*XKK*S1*(T(I,2)*Q1/CONFLD)/S2
        IF(NCOUNT.EQ.1) POWER=2*XKK*S1*(T(I,M2)*Q1/CONFLD)/S2
        SSUM=POWER+SSUM
983 CONTINUE
    NCOUNT=NCOUNT+1
    IF(NCOUNT.LT.1.5) GO TO 982
    NCOUNT=0
984 CONTINUE
    S2=(XU(3)-XU(2))*H1
    IF(NCOUNT.EQ.1)S2=(XU(L1)-XU(L2))*H1
    DO 985 I=2,M1-1
        S1=(YV(I+1)-YV(I))*H1
        POWER=2*XKK*S1*(T(2,I)*Q1/CONFLD)/S2
        IF(NCOUNT.EQ.1) POWER=2*XKK*S1*(T(L2,I)*Q1/CONFLD)/S2
        SSUM=POWER+SSUM
985 CONTINUE
    NCOUNT=NCOUNT+1
    IF(NCOUNT.LT.1.5) GOTO 984
    write(36,*)
    write(36,*) 'ENERGY IN = ',EIN

```

```

write(36,*)
write(36,*) 'ENERGY OUT = ',SSUM
write(36,*) 'SURFACE TEMPERATURES'
write(36,*)
DO 987 I=1,75
    TTOP(I)=0
    TBOT(I)=0
    QTOP(I)=0
    QBOT(I)=0
    QHTR(I)=0
    THTOP(I)=0
    THBOT(I)=0
    THBSID(I)=0
DO 987 J=1,75
    TSIDES(1,75)=0
    TSIDES(2,75)=0
    QSIDES(1,75)=0
    QSIDES(2,75)=0
987 CONTINUE
C
* CALCULATION OF SUBSTRATE SURFACE TEMPERATURES
DO 988 I=NA,NB
    TTOP(I)=(T(I,ND)*.5*YCV(ND+1)/CONFLD+T(I,ND+1)*.5*YCV(ND)/CONPLX)/
    1(.5*(YCV(ND+1)/CONFLD+YCV(ND)/CONPLX))
    TBOT(I)=(T(I,NC)*.5*YCV(NC-1)/CONFLD+T(I,NC-1)*.5*YCV(NC)/CONPLX)/
    1(.5*(YCV(NC-1)/CONFLD+YCV(NC)/CONPLX))
988 CONTINUE
DO 989 I=ND,NC,-1
    TSIDES(1,I)=(T(NA,I)*.5*XCV(NA-1)/CONFLD+T(NA-1,I)*.5*XCV(NA)
    1/CONPLX)/(.5*(XCV(NA-1)/CONFLD+XCV(NA)/CONPLX))
    TSIDES(2,I)=(T(NB,I)*.5*XCV(NB+1)/CONFLD+T(NB+1,I)*.5*XCV(NB)
    1/CONPLX)/(.5*(XCV(NB+1)/CONFLD+XCV(NB)/CONPLX))
    IF((I.LT.NQY1).OR.(I.GT.NQY1+N3Y-1))GOTO989
    TSIDES(2,I)=(T(NB,I)*.5*XCV(NB+1)/CONFLD+T(NB+1,I)*.5*XCV(NB)
    1/CONHTR)/(.5*(XCV(NB+1)/CONFLD+XCV(NB)/CONHTR))
989 CONTINUE
write(36,*) 'TOP'
write(36,4000) (TTOP(I),I=NA,NB)
write(36,*) 'BACK', 'FRONT'
DO 990 I=ND,NC,-1
990 write(36,4001) TSIDES(1,I),TSIDES(2,I)
write(36,*) 'BOTTOM'
write(36,4000) (TBOT(I),I=NA,NB)
4000 FORMAT(1X,6E11.4 / 1X,6E11.4)
4001 FORMAT(1X,E11.4,20X,E11.4)
C
C SUBSTRATE SURFACE HEAT FLUXES
write(36,*)
write(36,*) 'SURFACE HEAT FLUXES-NONDIMENSIONAL'
write(36,*)
DO 994 I=NA,NB
    QTOP(I)=(T(I,ND)-T(I,ND+1))/(.5*YCV(ND)/GAM2+.5*YCV(ND+1)
    1/AMUP)
    QBOT(I)=(T(I,NC)-T(I,NC-1))/(.5*YCV(NC)/GAM2+.5*YCV(NC-1)
    1/AMUP)
994 CONTINUE
write(36,4000) (QTOP(I),I=NA,NB)
DO 995 I=ND,NC,-1
    QSIDES(1,I)=(T(NA,I)-T(NA-1,I))/(.5*XCV(NA)/GAM2+.5*XCV(NA-1;

```

```

1/AMUP)
  QSIDES(2,I)=(T(NB,I)-T(NB+1,I))/(.5*XCV(NB)/GAM2+.5*XCV(NB+1)
1/AMUP)
  IF((I.LT.NQY1).OR.(I.GT.NQY1+N3Y-1))GOTO995
  QSIDES(2,I)=(T(NB,I)-T(NB+1,I))/(.5*XCV(NB)/GAM4+.5*XCV(NB+1)
1/AMUP)
995 CONTINUE
  DO 996 I=ND,NC,-1
996 write(36,4001) QSIDES(1,I),QSIDES(2,I)
  write(36,4000) (QBOT(I),I=NA,NB)
C
  write(36,*)
  write(36,*) 'DIMENSIONAL SUBSTRATE HEAT FLUXES'
  write(36,*)
  write(36,4000) (QTOP(I)*DUMMY1,I=NA,NB)
  DO 1050 I=ND,NC,-1
1050 write(36,4001) QSIDES(1,I)*DUMMY1,QSIDES(2,I)*DUMMY1
  write(36,4000) (QBOT(I)*DUMMY1,I=NA,NB)
C
  write(36,*)
  write(36,*) 'LOCATION OF SUBSTRATE TEMPERATURES AND FLUXES'
  write(36,*)
  write(36,*) 'TOP ROW ', '1 Y', ' & X'S'
  write(36,*) '(1X,E11.4 / 6E11.4 / 6E11.4)' YV(ND+1),(X(I),I=NA,NB)
  write(36,*)
  write(36,*) 'BACK AND FRONT X'S'
  write(36,*) '(1X,E11.4,2X,E11.4)' XU(NA),XU(NB+1)
  write(36,*) 'Y POSITIONS'
  DO 1020 I=ND,NC,-1
1020 write(36,*) '(5X,E11.4)' Y(I)
  write(36,*) 'BOTTOM ROW Y AND X'S'
  write(36,*) '(1X,E11.4 / 6E11.4 / 6E11.4)' YV(NC),(X(I),I=NA,NB)
  write(36,*)
  write(36,*) 'HEATER SURFACE TEMPERATURES'
  DO 1021 I=NA+N3X,NB
    THTOP(I)=(T(I,NQY1+N3Y)*.5*YCV(NQY1)/CONHTR+T(I,NQY1+N3Y-1)*.5*
1YCV(NQY1+N3Y)/CONPLX)/(.5*(YCV(NQY1)/CONHTR+YCV(NQY1+N3Y)/CONPLX))
    THBOT(I)=(T(I,NQY1)*.5*YCV(NQY1-1)/CONPLX+T(I,NQY1-1)*.5*
1YCV(NQY1)/CONHTR)/(.5*(YCV(NQY1-1)/CONPLX+YCV(NQY1)/CONHTR))
1021 CONTINUE
  DO 1022 I=ND,NC,-1
    THBSID(I)=(T(NA+N3X,I)*.5*XCV(NB-N4X)/CONPLX+T(NB-N4X,I)*.5
1*XCV(NA+N3X)/CONHTR)/(.5*(XCV(NB-N4X)/CONPLX+XCV(NA+N3X)/CONHTR))
1022 CONTINUE
  write(36,*) 'HEATER TOP'
  write(36,4000) (THTOP(I),I=NA+N3X,NB)
  write(36,*) 'BACK', 'FRONT'
  DO 1025 I=NQY1+N3Y-1,NQY1,-1
1025 write(36,4001) THBSID(I),TSIDES(2,I)
  write(36,*) 'BOTTOM'
  write(36,4000) (THBOT(I),I=NA+N3X,NB)
C
C HEATER SUFACE HEAT FLUXES
  write(36,*)
  write(36,*) 'HEATER SURFACE HEAT FLUXES - NONDIMENSIONAL'
  write(36,*)
  IHTRC=1
  DO 997 I=NQX-N4X+1,NQX
    QHTR(IHTRC)=(T(I,NQY1+N3Y-1)-T(I,NQY1+N3Y))/(.5*YCV(NQY1+N3Y-1)

```

```

1 /GAM4+.5*YCV(NQY1+N3Y)/GAM2)
  IHTRC=IHTRC+1
997 CONTINUE
  DO 998 I=NQX-N4X+1,NQX
    QHTR(IHTRC)=(T(I,NQY1)-T(I,NQY1-1))/(.5*YCV(NQY1)
1 /GAM4+.5*YCV(NQY1-1)/GAM2)
    IHTRC=IHTRC+1
998 CONTINUE
  DO 999 I=NQY1+N3Y-1,NQY1,-1
    QHTR(IHTRC)=(T(NQX-N4X+1,I)-T(NQX-N4X,I))/(.5*XCV(NQX-N4X+1)
1 /GAM4+.5*XCV(NQX-N4X)/GAM2)
    IHTRC=IHTRC+1
999 CONTINUE
  write(36,4000) (QHTR(I),I=1,N4X)
  HFTOT=0
  DO 1001 I=1,N3Y
    write(36,4002) QHTR(2*N4X+I),QSIDES(2,NQY1+N3Y-I)
    HFTOT=HFTOT+QSIDES(2,NQY1+N3Y-I)*YCV(NQY1+N3Y-I)
1001 CONTINUE
  write(36,4000) (QHTR(N4X+I),I=1,N4X)
4002 FORMAT(1X,E11.4,10X,E11.4)
  write(36,*)
  write(36,*) 'HEAT GOING DIRECTLY TO FLUID = ',HFTOT*DUMMY1*H1
  write(36,*)
  write(36,*) 'DIMENSIONAL HEATER HEAT FLUXES'
  write(36,*)
  write(36,4000) (QHTR(I)*DUMMY1,I=1,N4X)
  DO 1051 I=1,N3Y
1051 write(36,4002) QHTR(2*N4X+I)*DUMMY1,QSIDES(2,NQY1+N3Y-I)*DUMMY1
  write(36,4000) (QHTR(N4X+I)*DUMMY1,I=1,N4X)
  write(36,*)
  write(36,*) 'LOCATION OF HEATER TEMPERATURES AND FLUXES'
  write(36,*)
  write(36,*) 'TOP ROW ','1 Y',' & X''S'
  write(36,*(1X,E11.4/6E11.4/6E11.4))YV(NQY1+N3Y),
1(X(I),I=NA+N3X,NB)
  write(36,*)
  write(36,*) 'BACK AND FRONT X''S'
  write(36,*(1X,E11.4,2X,E11.4))XU(NA+N3X),XU(NB+1)
  write(36,*) 'Y POSITIONS'
  DO 1030 I=NQY1+N3Y-1,NQY1,-1
1030 write(36,*(5X,E11.4))Y(I)
  write(36,*) 'BOTTOM ROW Y AND X''S'
  write(36,*(1X,E11.4/6E11.4/6E11.4))YV(NQY1),(X(I),I=NA+N3X,NB)
  write(36,*)
  HPTOP=0
  HPBOT=0
  DO 1002 I=1,N4X
    HPTOP=HPTOP+QHTR(I)*XCV(NQX-N4X+I)
    HPBOT=HPBOT+QHTR(N4X+I)*XCV(NQX-N4X+I)
1002 CONTINUE
  HPBACK=0
  DO 1003 I=2*N4X+1,2*N4X+N3Y
    HPBACK=HPBACK+QHTR(I)*YCV(NQY1)
1003 CONTINUE
  HTRTOT=HFTOT+HPTOP+HPBOT+HPBACK
  PHTRF=100*HFTOT/HTRTOT
  PHTRT=100*HPTOP/HTRTOT
  PHTRL=100*HPBACK/HTRTOT

```



```

      PHTRB=100*HPBOT/HTRTOT
      PHTOT=PHTRF+PHTRT+PHTRL+PHTRB
C
C  MAXIMUM TEMPERATURE
      write(36,*)
      write(36,*) 'HEATER TEMPERATURES'
      write(36,*)
      TMAX=0
      IXX=0
      JYY=0
      DO 1005 J=N3Y,1,-1
        write(36,4000) (T(NQX-N4X+I,NQY1-1+J),I=1,N4X)
        DO 1005 K=1,N4X
          IF(TMAX.LT.T(NQX-N4X+K,NQY1-1+J)) THEN
            TMAX=T(NQX-N4X+K,NQY1-1+J)
            IXX=K
            JYY=J
          ELSE
            ENDIF
1005  CONTINUE
      write(36,*)
      write(36,*(1X,A,3X,E11.4)) 'MAX TEMPERATURE IS',TMAX
      write(36,*)
      write(36,*) 'POSITION FROM LOWER LEFT IS'
      write(36,*) 'RIGHT',IXX
      write(36,*) 'UP',JYY
      write(36,*)
      write(36,*) 'PERCENT HEATER ENERGY LOST TO FLUID = ',PHTRF
      write(36,*) 'PERCENT HEATER ENERGY LOST TO TOP = ',PHTRT
      write(36,*) 'PERCENT HEATER ENERGY LOST TO BACK = ',PHTRL
      write(36,*) 'PERCENT HEATER ENERGY LOST TO BOTTOM = ',PHTRB
      write(36,*) '-----'
      write(36,*) 'TOTAL PERCENTAGE = ',PHTOT
      write(36,*)
      write(36,*)
      write(36,*) 'ENERGY BALANCE'
      write(36,*)
      QLEFT=0
      DO 1010 I=2,M2
1010  QLEFT=QLEFT+T(2,I)*Q1*YCV(I)/XDIF(2)
      QUPPER=0
      DO 1012 I=2,L2
1012  QUPPER=QUPPER+T(1,M2)*Q1*XCV(I)/YDIF(M1)
      QRIGHT=0
      DO 1014 I=2,M2
1014  QRIGHT=QRIGHT+T(L2,I)*Q1*YCV(I)/XDIF(L1)
      QLOWER=0
      DO 1016 I=2,L2
1016  QLOWER=QLOWER+T(1,2)*Q1*XCV(I)/YDIF(2)
      QOUT=QLEFT+QUPPER+QRIGHT+QLOWER
      PLEFT=QLEFT*100/QOUT
      PUPPER=QUPPER*100/QOUT
      PRIGHT=QRIGHT*100/QOUT
      PLOWER=QLOWER*100/QOUT
      PTOT=PLEFT+PUPPER+PRIGHT+PLOWER
      write(36,*)
      write(36,*) 'ENERGY IN EQUALS',EIN
      write(36,*)
      write(36,*) 'ENERGY OUT EQUALS',QOUT
      write(36,*)

```

```

write(36,*)
write(36,*) 'PERCENTAGE OF HEAT LOSS THRU ENCLOSURE WALLS'
write(36,*)
write(36,*) 'LEFT WALL',PLEFT
write(36,*) 'TOP WALL',PUPPER
write(36,*) 'RIGHT WALL',PRIGHT
write(36,*) 'BOTTOM WALL',FLOWER
write(36,*) '-----'
write(36,*) 'TOTAL EQUALS',PTOT
write(36,*)
write(36,*) 'PARAMETERS'
write(36,*)
write(36,*) 'H/H1 = ',BL1+BL2+BL3+BL4+BL5+BL6
write(36,*) 'D/H1 = ',BL2
write(36,*) 'L/H1 = ',BL4
write(36,*) 'ST/H1 = ',BL5+BL6
write(36,*) 'SB/H1 = ',BL1
write(36,*) 'DT/H1 = ',AL3+AL4
write(36,*)
write(36,*) 'RA = ',RA
write(36,*) 'PR = ',PR
write(36,*) 'RS = ',CONPLX/CONFLD
write(36,*) 'RC = ',CONHTR/CONFLD
write(36,*) 'W/H1 = ',DEPTH/H1
write(36,*)

C
C***PREPARE PLOTTING DATA***
C      NTIME=TOTAL NUMBER OF TIME STEPS
C      ITIME=CURRENT TIMESTEP
C      NTIME=1
C      write(46) NTIME,M1,L1

C
C      PRINT DATA FOR GRID
C      write(46) (YV(J),J=2,M1)
C      write(46) (XU(I),I=2,L1)
C      write(46) (Y(J),J=1,M1)
C      write(46) (X(I),I=1,L1)

C
C      PRINT DATA FOR DEPENDENDT VARIABLES
C      ITIME=1
C      write(46) ITIME
C      DO 3001 I=1,M1
3001 write(46) (V(J,I),J=1,L1)
C      DO 3021 I=1,M1
3021 write(46) (U(J,I),J=1,L1)
C      DO 3031 I=1,M1
3031 write(46) (T(J,I),J=1,L1)
C      DO 3041 I=1,M1
3041 write(46) (P(J,I),J=1,L1)
C      DO 3051 I=1,M1
3051 write(46) (STO(J,I),J=1,L1)
C      DO 3061 I=1,M1
3061 write(46) (F(J,I,3),J=1,L1)
C      DO 3071 I=1,M1
3071 write(46) (IBODY(J,I),J=1,L1)
C      close(46)

C
C      RETURN

C
C      ENTRY GAMSOR

```

```

      IF(NF.EQ.3) RETURN
      DO 500 J=1,M1
      DO 500 I=1,L1
      GAM(I,J)=AMU
      IBODY(I,J)=1
      IF(NF.NE.4) GO TO 500
      GAM(I,J)=AMUP
500  CONTINUE
      DO 501 I=NA,NB
      DO 501 J=NC,ND
      GAM(I,J)=1.0E5
      IBODY(I,J)=0
      IF(NF.NE.4) GO TO 501
      GAM(I,J)=GAM2
501  CONTINUE
      IF(NF.NE.2) GO TO 503
      DO 502 J=2,M2
      DO 502 I=2,L2
      IF(J.EQ.2)GO TO 502
      TM=(FY(J)*T(I,J)+FYM(J)*T(I,J-1))
      CON(I,J)=ALFA*TM+ALFAM*STO(I,J)
      STO(I,J)=TM
502  CONTINUE
503  CONTINUE
      IF(NF.EQ.4) THEN
      DO 505 J=1,N4X
      DO 505 I=0,N3Y-1
      GAM(NQX-N4X+J,NQY1+I)=GAM4
      CON(NQX-N4X+J,NQY1+I)=SOURCE
505  CONTINUE
      ELSE
      ENDIF
      RETURN
      END

```

```

***** PLOTTING ROUTINE FOR A SERIES OF CONTOUR PLOTS *****
K .... CURRENT NUMBER OF TIME STEP BEING READ
NT .... TOTAL NUMBER OF TIME-STEPS ON DATA FILE
NPTS ... TOTAL NUMBER OF POINTS (INPUT)
NTYP ... CURVE-TYPE
      1 ... PRESSURE
      2 ... STREAMFUNCTION
      3 ... U-VELOCITY
      4 ... V-VELOCITY
      5 ... PRESSURE

```

---

```

COMMON /INDATA/ X(102),Y(102),Z(102,102)
COMMON /GRIDII/ XX(200),YY(200)
COMMON /PLOTDT/ XPAGE,YPAGE,XPLOT,YPLOT
COMMON /BODCTR/ XCT(102),YCT(102),XBL(102),YBL(102),NCT
COMMON WRK (20000)
DIMENSION X1(10404),Y1(10404),Z1(10404),ZZ(200,200)
DIMENSION U(102,102),V(102,102),T(102,102),P(102,102),
2       IBODY(102,102),ST1(102,102),ST2(102,102)
DIMENSION XU(101),YV(101)
REAL*8 XARRAY(102)
CHARACTER*1 IDECI
LOGICAL ZERO,CONT,ZERI,CONTI

```

---

```

C *** DEFINE SOME FUNCTIONS ***
ZERO(II,JJ) = ABS(U(II,JJ)).LT.0.1E-10 .AND.
2       ABS(V(II,JJ)).LT.0.1E-10
CONT(II,JJ) = (ZERO(II+1,JJ+1).AND.ZERO(II+1,JJ-1).AND.
2       ZERO(II-1,JJ+1).AND.ZERO(II-1,JJ-1))
3       .NEQV. (ZERO(II+1,JJ+1).OR.ZERO(II+1,JJ-1).OR.
4       ZERO(II-1,JJ+1).OR.ZERO(II-1,JJ-1))
ZERI(II,JJ) = IBODY(II,JJ).EQ.0
CONTI(II,JJ) = (ZERI(II+1,JJ+1).AND.ZERI(II+1,JJ-1).AND.
2       ZERI(II-1,JJ+1).AND.ZERI(II-1,JJ-1))
3       .NEQV. (ZERI(II+1,JJ+1).OR.ZERI(II+1,JJ-1).OR.
4       ZERI(II-1,JJ+1).OR.ZERI(II-1,JJ-1))
C *** DEFINE PAGESIZE AND PLOTSIZE ***
XPAGE = 9.5
YPAGE = 11.0
XPLOT = 6.5
YPLOT = 6.5

```

---

```

C *** READ DATA FOR GRID ***
870 REWIND (3)
READ (3) NT,L1,M1
READ (3) (XARRAY(I),I=2,L1)
DO 8002 I=2,L1
8002 XU(I) = SNGL(XARRAY(I))
READ (3) (XARRAY(J),J=2,M1)
DO 8004 J=2,M1
8004 YV(J) = SNGL(XARRAY(J))
READ (3) (XARRAY(I),I=1,L1)
DO 8006 I=1,L1
8006 X(I) = SNGL(XARRAY(I))
READ (3) (XARRAY(J),J=1,M1)
DO 8008 J=1,M1
8008 Y(J) = SNGL(XARRAY(J))

```

---

```

C PREPARE THE GRID-DATA FOR THE CONTOUR PLOTTING
NPTS = L1*M1
DO 1300 J=1,M1
DO 1300 I=1,L1
J1=L1*(J-1)+I
1300 X1(J1) = X(I)
DO 1310 J=1,M1
DO 1310 I=1,L1
J1=L1*(J-1)+I

```

```

1310 Y1(J1) = Y(J)
C *** NOMINATE DEVICE ***
C
  WRITE (*,930)
930 FORMAT (1H1,34(1H*)/1X,'PLEASE, SELECT PLOTTING DEVICE'/1X,34(1H*)
2      //5X,'TEKTRONIX 618 SCREEN .... (1)'/
3      5X,'PRINTABLE SHERPA FILE ... (2)'/
4      5X,'IBM COLOR MONITOR ..... (3)'/
5      5X,'COMPRESSED METAFILE ..... (4)'/
6      5X,'EXIT PLOTTING ..... (99)')
  READ (*,*) IPLOT
  IF ((IPLOT.LT.1).OR.(IPLOT.GT.4)) GOTO 180
  IF (IPLOT.EQ.1) CALL TEK618
  IF (IPLOT.EQ.2) CALL SHERPA ('CONTOUR ', 'T', 2)
  IF (IPLOT.EQ.3) CALL IBM79
  IF (IPLOT.EQ.4) CALL COMPRS
C
C *** GET THE NUMBER OF TIME-STEPS TO BE PLOTTED AND THE INCREMENT ***
  WRITE (*,910) NT
910 FORMAT (1H1,39(1H*)/,
2      1X,'YOUR INPUT FILE INCLUDES ',13,' TIME-STEPS'/1X,39(1H*)//
3      1X,'CHOOSE A METHOD FOR CONSTRUCTING A REGULAR MATRIX: '/
4      5X,'UNIFORM GRID/NO REFINEMENT (102*102)..... (0)'/
5      5X,'DISSPLA'S GETMAT ALGORITHM (102*102)..... (1)'/
6      5X,'CUBIC SPLINE INTERPOLATION (102*102)..... (2)'/
7      5X,'LINEAR INTERPOLATION (200*200)..... (3)')
  READ (*,*) IMAT
  IF (IMAT.NE.0) GOTO 202
  LL = L1
  MM = M1
  GOTO 204
202 WRITE (*,911)
911 FORMAT (1X,'ENTER THE DIMENSIONS OF THE MATRIX TO BE CONSTRUCTED: '
2      , ' (1XDIM,1YDIM)')
  READ (*,*) LL,MM
C GENERATE AN EQUALLY SPACED GRID
204 DELX = X(L1)-X(1)
  DELY = Y(M1)-Y(1)
  DO 206 I=1,LL
206 XX(I) = X(1) + DELX*FLOAT(I-1)/FLOAT(LL-1)
  DO 208 J=1,MM
208 YY(J) = Y(1) + DELY*FLOAT(J-1)/FLOAT(MM-1)
C
C *** LOOP OVER A SERIES OF PLOTS *** BEGIN OF "200-LOOP"
C
  DO 200 N=1,NT
  READ (3) K
  WRITE (*,912) K
912 FORMAT (//1X,'DO YOU WANT ANY PLOTS FOR THE ',13,
2      '-TH TIME-STEP? (Y/N)')
  READ (*,914) IDECL
914 FORMAT (A1)
  IF (IDECL.EQ.'Y') GOTO 212
C ADVANCE BY 1 TIME-STEP
  DO 210 I=1,6
210 READ (3)
  GOTO 200
C READ DEPENDENT VARIABLES FROM FILE 3
212 DO 213 I=1,L1
  READ (3) (XARRAY(J),J=1,M1)
  DO 213 J=1,M1
213 U(I,J) = SNGL(XARRAY(J))
  DO 214 I=1,L1
  READ (3) (XARRAY(J),J=1,M1)
  DO 214 J=1,M1
214 V(I,J) = SNGL(XARRAY(J))
  DO 215 I=1,L1
  READ (3) (XARRAY(J),J=1,M1)
  DO 215 J=1,M1
215 T(I,J) = SNGL(XARRAY(J))
  DO 216 I=1,L1
  READ (3) (XARRAY(J),J=1,M1)

```

```

DO 216 J=1,M1
216 P(I,J) = SNGL(XARRAY(J))
DO 217 I=1,L1
READ (3) (XARRAY(J),J=1,M1)
DO 217 J=1,M1
217 ST1(I,J) = SNGL(XARRAY(J))
DO 218 I=1,L1
READ (3) (XARRAY(J),J=1,M1)
DO 218 J=1,M1
218 ST2(I,J) = SNGL(XARRAY(J))
DO 219 I=1,L1
219 READ (3) (IBODY(I,J),J=1,M1)
IF (N.NE.1) GOTO 890
WRITE (*,939)
939 FORMAT (/1X,'SHOULD THE CONTOUR OF THE BODY BE IDENTIFIED VIA:'/
2      6X,'THE VELOCITIES ..... (1)'/
3      6X,'THE INPUT DATA ..... (2)')
READ (*,*) ICONT
IF (ICONT.EQ.2) GOTO 1500
C
C *** FIND THE CONTOUR OF THE BODY VIA THE VELOCITIES ***
C
C LOCATE A CONVEX CORNER OF THE BODY
DO 1320 J=4,M1-3
DO 1320 I=4,L1-3
IF (ZERO(I,J)) GOTO 1322
1320 CONTINUE
1322 ICT = 1
XCT(ICT) = X(I)
YCT(ICT) = Y(J)
IP = 1
JP = 0
DO 1340 ICT=2,102
DO 1324 IDUM=1,MAX(L1,M1)
IF (ZERO(I+IP,J+JP).AND.CONT(I+IP,J+JP)) GOTO 1330
IF (IP.EQ.0) THEN
JP = 0
DO 1326 IP=-1,1,2
1326 IF (ZERO(I+IP,J+JP).AND.CONT(I+IP,J+JP)) GOTO 1332
ELSE
IP = 0
DO 1328 JP=-1,1,2
1328 IF (ZERO(I+IP,J+JP).AND.CONT(I+IP,J+JP)) GOTO 1332
ENDIF
C ANOTHER CONTOUR POINT HAS BEEN FOUND
1330 I = I+IP
J = J+JP
1324 CONTINUE
C THE PREVIOUSLY FOUND POINT IS A CORNER
1332 XCT(ICT) = X(I)
YCT(ICT) = Y(J)
IF (ABS(XCT(ICT)-XCT(1)).LT.0.1E-6.AND.
2 ABS(YCT(ICT)-YCT(1)).LT.0.1E-6) GOTO 1350
I = I+IP
J = J+JP
1340 CONTINUE
1350 ICT = ICT
GOTO 1400
C
C *** FIND THE CONTOUR OF THE BODY VIA INPUT ***
C
C LOCATE A CONVEX CORNER OF THE BODY
1500 DO 1520 J=4,M1-3
DO 1520 I=4,L1-3
IF (ZERI(I,J)) GOTO 1522
1520 CONTINUE
1522 ICT = 1
XCT(ICT) = X(I)
YCT(ICT) = Y(J)
IP = 1
JP = 0
DO 1540 ICT=2,102

```

```

DO 1524 IDUM=1,MAX(L1,M1)
IF (ZERI(I+IP,J+JP).AND.CONTI(I+IP,J+JP)) GOTO 1530
IF (IP.EQ.0) THEN
  JP = 0
DO 1526 IP=-1,1,2
1526 IF (ZERI(I+IP,J+JP).AND.CONTI(I+IP,J+JP)) GOTO 1532
ELSE
  IP = 0
DO 1528 JP=-1,1,2
1528 IF (ZERI(I+IP,J+JP).AND.CONTI(I+IP,J+JP)) GOTO 1532
ENDIF
C ANOTHER CONTOUR POINT HAS BEEN FOUND
1530 I = I+IP
J = J+JP
1524 CONTINUE
C THE PREVIOUSLY FOUND POINT IS A CORNER
1532 XCT(ICT) = X(I)
YCT(ICT) = Y(J)
IF (ABS(XCT(ICT)-XCT(1)).LT.0.1E-6.AND.
2 ABS(YCT(ICT)-YCT(1)).LT.0.1E-6) GOTO 1550
I = I+IP
J = J+JP
1540 CONTINUE
1550 NCT = ICT
C
C COMPUTE THE COORDINATES FOR BLANKING (IN INCHES FROM PHYSOR)
1400 DO 1410 ICT=1,NCT
XBL(ICT) = (XCT(ICT)-X(1))/(X(L1)-X(1))*XPLOT
1410 YBL(ICT) = (YCT(ICT)-Y(1))/(Y(M1)-Y(1))*YPLOT
C
C *** FIND OUT WHICH CURVES TO PLOT ***
890 WRITE (*,900)
900 FORMAT (1H1,'WHAT WOULD YOU LIKE TO PLOT?'/
2 5X,'TEMPERATURE..... (1)'/
3 5X,'STREAMLINES..... (2)'/
4 5X,'U-VELOCITY ..... (3)'/
5 5X,'V-VELOCITY ..... (4)'/
6 5X,'PRESSURE ..... (5)'/
7 5X,'NEXT TIMESTEP ..... (0)'/
8 5X,'RE-INITIALISE ..... (-99)'/
9 5X,'EXIT PLOTTING ..... (99)')
READ (*,*) NTYP
IF (NTYP.EQ.99) GOTO 180
IF (NTYP.EQ.-99) GOTO 870
IF (NTYP.EQ.0) GOTO 200
C
C ASSIGN THE VALUES OF THE Z-FUNCTION WITH THE CHOSEN DATA
GOTO (1100,1102,1104,1106,1108) NTYP
C
C TEMPERATURE
1100 DO 1101 J=1,M1
DO 1101 I=1,L1
1101 Z(I,J) = T(I,J)
GOTO 1120
C STREAMFUNCTION
1102 DO 1103 J=1,M1
DO 1103 I=1,L1
1103 Z(I,J) = ST2(I,J) + .0005222
GOTO 1120
C U-VELOCITY
1104 DO 1105 J=1,M1
DO 1105 I=1,L1
1105 Z(I,J) = U(I,J)
GOTO 1120
C V-VELOCITY
1106 DO 1107 J=1,M1
DO 1107 I=1,L1
1107 Z(I,J) = V(I,J)
GOTO 1120
C PRESSURE
1108 DO 1109 J=1,M1
DO 1109 I=1,L1

```





```

      IF (NTYP.EQ.1) CALL HEADIN ('(T)EMPERATURE (C)ONTOURS$',
1    100,1.5,1)
      IF (NTYP.EQ.2) CALL HEADIN ('(S)TREAMLINES$',
1    100,1.5,1)
      IF (NTYP.EQ.3) CALL HEADIN ('(U-V)ELOCITY (C)ONTOURS$',
1    100,1.5,1)
      IF (NTYP.EQ.4) CALL HEADIN ('(V-V)ELOCITY (C)ONTOURS$',
1    100,1.5,1)
      IF (NTYP.EQ.5) CALL HEADIN ('(P)RESSURE (C)ONTOURS$',
1    100,1.5,1)
      CALL RESET ('HEIGHT')
      CALL SETCLR ('BLUE')
C
C *** SET UP AXES ***
      CALL XNAME ('Y $',100)
      CALL YAXANG (0.0)
      CALL YNAME ('X $',100)
      XINC = 0.1*(X(L1)-X(1))
      YINC = 0.1*(Y(M1)-Y(1))
      CALL GRAF (Y(1),YINC,Y(M1),X(1),XINC,X(L1))
      CALL GRID (0,0)
      CALL BCOMON (20000)
C  DRAW A GRID (IF REQUESTED)
      IF (LGRID.EQ.'N') GOTO 90
      DO 30 I=1,L1
30    CALL RLVEC (Y(1),X(I),Y(M1),X(I),0000)
      DO 32 J=1,M1
32    CALL RLVEC (Y(J),X(1),Y(J),X(M1),0000)
C
C *** PREPARE CONTOURS PLOTS ***
C
      90 GOTO (100,200,300) IMAT
C
C *** INPUT MATRIX IS REGULAR / NO GRID REFINEMENT REQUIRED ***
C
      DO 10 J=1,MM
      DO 10 I=1,LL
10    ZZ(I,J) = Z(J,I)
      GOTO 400
C
C *** CONSTRUCT THE MATRIX BY DISSPLA'S ALGORITHM GETMAT ***
C
C  TRANSFORM THE Z 2-D FUNCTION TO 1-D FUNCTION
100 DO 110 J=1,M1
      DO 110 I=1,L1
      J1=LL*(J-1)+I
110 Z1(J1) = Z(I,J)
C
C  CONSTRUCT A REGULAR MATRIX
      CALL BGNMAT(MM,LL)
      CALL GETMAT(Y1,X1,Z1,NPTS,0)
      CALL ENDMAT(ZZ,0)
      GOTO 400
C
C *** CONSTRUCT THE MATRIX BY CUBIC SPLINE INTERPOLATION ***
C
200 DO 210 J=1,M1
      DO 212 I=1,L1
212 C(1,I) = Z(I,J)
      CALL CUBSPL (X,C,L1,0,0)
      DO 214 I=1,LL
214 Z1(I,J) = PPVALU (X,C,L1,4,XX(I),0)
210 CONTINUE
C
      DO 220 I=1,LL
      DO 222 J=1,M1
222 C(1,J) = Z1(I,J)
      CALL CUBSPL (Y,C,M1,0,0)
      DO 224 J=1,MM
224 ZZ(J,I) = PPVALU (Y,C,M1,4,YY(J),0)
220 CONTINUE
      GOTO 400

```



```

C (C SERVES AS A TEMPORARY STORAGE)
DO 10 M=2,N
  C(3,M) = TAU(M) - TAU(M-1)
  10 C(4,M) = (C(1,M) - C(1,M-1))/C(3,M)
C
C *** CONSTRUCT FIRST EQUATION FROM FIRST BOUNDARY CONDITION ***
C
  IF (IBCBEG-1) 11,15,16
  11 IF (N.GT.2) GOTO 12
C NOT-A-KNOT COND AT LEFT END, AND N.EQ.2
  C(4,1) = 1.0
  C(3,1) = 1.0
  C(2,1) = 2.0*C(4,2)
  GOTO 25
C NOT-A-KNOT COND AT LEFT END, AND N.GT.2
  12 C(4,1) = C(3,3)
  C(3,1) = C(3,2) + C(3,3)
  C(2,1) = ((C(3,2)+2.0*C(3,1))*C(4,2)*C(3,3)+C(3,2)**2*C(4,3))
    2 /C(3,1)
  GOTO 19
C
C SLOPE PRESCRIBED AT LEFT END
  15 C(4,1) = 1.0
  C(3,1) = 0.0
  GOTO 18
C
C SECOND DERIVATIVE PRESCRIBED AT LEFT END
  16 C(4,1) = 2.0
  C(3,1) = 1.0
  C(2,1) = 3.0*C(4,2) - C(3,2)/2.0*C(2,1)
  18 IF (N.EQ.2) GOTO 25
C
C IN CASE OF INTERIOR KNOTS SET UP EQU, EXECUTE FORWARD PASS OF GAUSS
  19 DO 20 M=2,L
    G = -C(3,M+1)/C(4,M-1)
    C(2,M) = G*C(2,M-1) + 3.0*(C(3,M)*C(3,M+1)+C(3,M+1)*C(4,M))
    20 C(4,M) = G*C(3,M-1) + 2.0*(C(3,M) + C(3,M+1))
C
C *** CONSTRUCT LAST EQUATION FROM SECOND BOUNDARY CONDITION
C
  IF (IBCEM-1) 21,30,24
C FOR PRESCRIBED SLOPE ENTER DIRECTLY THE BACK SUBSTITUTION
  21 IF ((N.EQ.3).AND.(IBCBEG.EQ.0)) GOTO 22
C
C NOT-A-KNOT COND AT RIGHT END, AND N.GE.3,
C AND ((N.GT.3) .OR. (NOT-A-KNOT COND AT LEFT END))
  G = C(3,N-1) + C(3,N)
  C(2,N) = ((C(3,N)+2.0*G)*C(4,N)*C(3,N-1)
    2 + C(3,N)**2*(C(1,N-1)-C(1,N-2))/C(3,N-1))/G
  G = -G/C(4,N-1)
  C(4,N) = C(3,N-1)
  GOTO 29
C NOT-A-KNOT COND AT RIGHT END, AND ((N.EQ.3).AND.(NOT-A-KNOT AT LEFT)
C .OR. ((N.EQ.2).AND.(NOT-A-KNOT COND AT LEFT END))
  22 C(2,N) = 2.0*C(4,N)
  C(4,N) = 1.0
  GOTO 28
C
C SECOND DERIVATIVE PRESCRIBED AT RIGHT END
  24 C(2,N) = 3.0*C(4,N) + C(3,N)/2.0*C(2,N)
  C(4,N) = 2.0
  GOTO 28
  25 IF (IBCEM-1) 26,30,24
  26 IF (IBCBEG.GT.0) GOTO 22
C
C NOT-A-KNOT COND AT RIGHT AND LEFT END, AND N.EQ.2
  C(2,N) = C(4,N)
  GOTO 30
  28 G = -1.0/C(4,N-1)
C
C *** SOLVE TRIDIAGONAL SYSTEM FOR THE SLOPES C(2,J) ***
C

```

```

C FORWARD PASS (=ELIMINATION OF LOWER DIAGONAL)
29 C(4,N) = G*C(3,N-1) + C(4,N)
   C(2,N) = (G*C(2,N-1) + C(2,N))/C(4,N)
C BACKWARD PASS (=BACK SUBSTITUTION)
30 DO 40 J=L,1,-1
40 C(2,J) = (C(2,J) - C(3,J)*C(2,J+1))/C(4,J)

C
C *** GENERATE CUBIC COEFFICIENTS IN EACH INTERVAL
C
   DO 50 I=2,N
     DTAU = C(3,I)
     DIVDF1 = (C(1,I) - C(1,I-1))/DTAU
     DIVDF3 = C(2,I-1) + C(2,I) - 2.0*DIVDF1
     C(3,I-1) = 2.0*(DIVDF1-C(2,I-1)-DIVDF3)/DTAU
50 C(4,I-1) = (DIVDF3/DTAU)*(6.0/DTAU)
C
   RETURN
   END
CCCCCCCCCCCCCCCCCCCCCCCCCCCCCCCCCCCCCCCCCCCCCCCCCCCCCCCCCCCCCCCC
C
   REAL FUNCTION PPVALU (BREAK,COEF,L,K,X,JDERIV)
C
C   THIS FUNCTION CALCULATES THE VALUE OF THE JDERIV-TH DERIVATIVE
C   OF A PIECEWISE POLYNOMIAL FUNCTION.
C   SOURCE: CARL DE BOOR, A PRACTICAL GUIDE TO SPLINES
C
CCCCCCCCCCCCCCCCCCCCCCCCCCCCCCCCCCCCCCCCCCCCCCCCCCCCCCCCCCCCCCCC
C
   BREAK ..... ABSCISSAE OF BREAKPOINTS
   COEF ..... COEFFICIENTS OF PIECEWISE POLYNOMIAL INTERPOLANT
   L ..... NUMBER OF BREAKPOINTS
   K ..... ORDER OF POLYNOMIAL FUNCTIONS
   X ..... ABSCISSA AT WHICH TO EVALUATE
   JDERIV ..... ORDER OF DERIVATIVE (0 = FUNCTION)
C
C   _____
C   DIMENSION BREAK(L),COEF(K,L)
C
C   _____
C
   PPVALU = 0.0
   FMMJDR = K - JDERIV
C   DERIVATIVES OF ORDER K OR HIGHER ARE IDENTICALLY ZERO
   IF (FMMJDR.LE.0.0) GOTO 99
C
   IF (L.EQ.1) THEN
C     SINGLE POLYNOMIAL FUNCTION
     I = 1
   ELSE
C     FIND INDEX I OF LARGEST BREAKPOINT TO THE LEFT OF X
     CALL INTERV (BREAK,L,X,I,NDUMMY)
   ENDIF
   H = X - BREAK(I)
C
C   EVALUATE JDERIV-TH DERIVATIVE OF I-TH POLYNOMIAL PIECE AT X
   DO 10 M=K,JDERIV+1,-1
     PPVALU = (PPVALU/FMMJDR)*H + COEF(M,I)
10 FMMJDR = FMMJDR - 1.0
C
99 RETURN
   END
CCCCCCCCCCCCCCCCCCCCCCCCCCCCCCCCCCCCCCCCCCCCCCCCCCCCCCCCCCCCCCCC
C
   SUBROUTINE INTERV (XT,LXT,X,LEFT,MFLAG)
C
C   THIS SUBROUTINE DETERMINES THE INTERVAL INDEX WITH RESPECT
C   TO THE BREAKPOINT SEQUENCE.
C   SOURCE: CARL DE BOOR, A PRACTICAL GUIDE TO SPLINES
C
CCCCCCCCCCCCCCCCCCCCCCCCCCCCCCCCCCCCCCCCCCCCCCCCCCCCCCCCCCCCCCCC
C
   XT ..... ABSCISSAE OF BREAKPOINTS

```

```

C      LXT ..... NUMBER OF BREAKPOINTS
C      X ..... ABSCISSA WHOSE INTERVAL INDEX IS TO BE DETERMINED
C      LEFT ..... INDEX OF THE LARGEST BREAKPOINT TO THE LEFT OF X
C      MFLAG ..... RETURN CODE: MFLAG = -1: X.LT.XT(1)
C                               MFLAG = 0: XT(1).LE.X.LT.XT(LXT)
C                               MFLAG = 1: X.GE.XT(LXT)
C
C      _____
C      DIMENSION XT(LXT)
C      _____
C
C      RECALL THE INDEX OF THE PREVIOUS CALL TO THIS SUBROUTINE
C      SAVE ILO
C      DATA ILO/1/
C      IHI = ILO + 1
C      IF (IHI.LT.LXT) GOTO 20
C      IF (X.GT.XT(LXT)) GOTO 110
C      IF (LXT.LE.1) GOTO 90
C      ILO = LXT - 1
C      IHI = LXT
C
C      20 IF (X.GE.XT(IHI)) GOTO 40
C      IF (X.GE.XT(ILO)) GOTO 100
C
C      DECREASE ILO TO CAPTURE
C      ISTEP = 1
C      31 IHI = ILO
C      ILO = IHI - ISTEP
C      IF (ILO.LE.1) GOTO 35
C      IF (X.GE.XT(ILO)) GOTO 50
C      ISTEP = ISTEP*2
C      GOTO 31
C      35 ILO = 1
C      IF (X.LT.XT(1)) GOTO 90
C      GOTO 50
C
C      INCREASE IHI TO CAPTURE X
C      40 ISTEP = 1
C      41 ILO = IHI
C      IHI = ILO + ISTEP
C      IF (IHI.GE.LXT) GOTO 45
C      IF (X.LT.XT(IHI)) GOTO 50
C      ISTEP = ISTEP*2
C      GOTO 41
C      45 IF (X.GE.XT(LXT)) GOTO 110
C      IHI = LXT
C
C      NARROW THE INTERVAL (XT(ILO),XT(IHI))
C      50 MIDDLE = (ILO + IHI)/2
C      IF (MIDDLE.EQ.ILO) GOTO 100
C
C      IF (X.LT.XT(MIDDLE)) GOTO 53
C      ILO = MIDDLE
C      GOTO 50
C      53 IHI = MIDDLE
C      GOTO 50
C
C      *** SET OUTPUT AND ASSIGN RETURN CODES ***
C
C      X LIES TO THE LEFT OF THE SMALLEST BREAKPOINT
C      90 MFLAG = -1
C      LEFT = 1
C      RETURN
C
C      REGULAR RETURN FROM THIS SUBROUTINE
C      100 MFLAG = 0
C      LEFT = ILO
C      RETURN
C
C      X LIES TO THE RIGHT OF THE LARGEST BREAKPOINT
C      110 MFLAG = 1
C      LEFT = LXT-1
C      RETURN
C      END

```

# APPENDIX C

## TRAVERSE PROGRAM

```

10  !!!!!!!!!!!!!!!!!!!!!!!!!!!!!!!!!!!!!!!!!!!!!!!!!!!!!!!!!!!!!!!!!!!!!!!!!!!!!!!
20  !! PROGRAM TRAV
30  !! PROGRAM USED TO MOVE TRAVERSE
31  !!
32  !!
40  !!!!!!!!!!!!!!!!!!!!!!!!!!!!!!!!!!!!!!!!!!!!!!!!!!!!!!!!!!!!!!!!!!!!!!!!!!!!!!!
42  Isc=9
43  ASSIGN @Datacomm TO Isc
44  ASSIGN @Terminal TO 1
46  CONTROL Isc,3:1200
47  CONTROL Isc,4:2+4+0+16
49  CONTROL Isc,5:10
50  COM /Path/ @Datacomm
52  OUTPUT @Datacomm;"EZT"
53  OUTPUT @Datacomm;"C S1000,SM2000,I1500,IM1500,R"
54  END

```

# APPENDIX D

## TEMPERATURE ACQUISITION PROGRAM

```

10  !!!!!!!!!!!!!!!!!!!!!!!!!!!!!!!!!!!!!!!!!!!!!!!!!!!!!!!!!!!!!!!!!!!!!!!!!!!!!!!
20  !!                                TEMPERATURE ACQUISITION PROGRAM                                !!
30  !!                                (STEADY STATE)                                                !!
31  !! PROGRAM PERFORMS THE REQUIRED FUNCTIONS NEEDED TO OBTAIN DATA !!
32  !! FROM THE ACQUISITION SYSTEM AND CONVERT THE THERMOCOUPLE OUT- !!
33  !! PUT VOLTAGES INTO TEMPERATURE VALUES. THE TEMPERATURES ARE !!
34  !! STORED INTO DATA FILES FOR FURTHER REDUCTION. !!
35  !!                                VARIABLE DEFINITIONS                                        !!
36  !!                                VOLTS : THERMOCOUPLE OUTPUT                                !!
37  !!                                TEMP  : HEATER TEMPERATURES                                !!
40  !!!!!!!!!!!!!!!!!!!!!!!!!!!!!!!!!!!!!!!!!!!!!!!!!!!!!!!!!!!!!!!!!!!!!!!!!!!!!!!
50  REAL Volts(50)
60  REAL Temp(50)
70  !CREATE BDAT "THRED15:,700,1",45
80  !ASSIGN @Path3 TO "THRED15:,700,1"
81  PRINT DATE$(TIMEDATE)
82  PRINT " "
83  PRINT " 1.0 WATT INPUT POWER"
84  PRINT " 45 STRIPS NO SHROUD"
85  PRINT " BDAT FILE THRED15:,700,1"
87  PRINT " "
89  PRINT " "
89  PRINT " "
93  !!!!!!!!!!!!!!!!!!!!!!!!!!!!!!!!!!!!!!!!!!!!!!!!!!!!!!!!!!!!!!!!!!!!!!!!!!!!!!! SURFACE #1-20
95  OUTPUT 709;"CONFMEAS DCV, 100-119,USE 0"
96  FOR I=1 TO 20
98  ENTER 709;Volts(I)
99  Temp(I)=.0006797+(25825.1328*Volts(I))-(607789.2467*(Volts(I)+Volts(I)))-
21952034.3364*(Volts(I)^3)+(8370910996.1874*(Volts(I)^4))+.039
100 NEXT I
530 !!!!!!!!!!!!!!!!!!!!!!!!!!!!!!!!!!!!!!!!!!!!!!!!!!!!!!!!!!!!!!!!!!!!!!!!!!!!!!! SURFACE #21-40
550 OUTPUT 709;"CONFMEAS DCV,200-219,USE 0"
550 FOR I=21 TO 40
570 ENTER 709;Volts(I)
580 Temp(I)=.0006797+(25825.1328*Volts(I))-(607789.2467*(Volts(I)+Volts(I)))-
21952034.3364*(Volts(I)^3)+(8370910996.1874*(Volts(I)^4))+.039
590 NEXT I
600 !!!!!!!!!!!!!!!!!!!!!!!!!!!!!!!!!!!!!!!!!!!!!!!!!!!!!!!!!!!!!!!!!!!!!!!!!!!!!!! SURFAC #41-45
610 OUTPUT 709;"CONFMEAS DCV,300-304,USE 0"
620 FOR I=41 TO 45
655 ENTER 709;Volts(I)
657 Temp(I)=.0006797+(25825.1328*Volts(I))-(607789.2467*(Volts(I)+Volts(I)))-
21952034.3364*(Volts(I)^3)+(8370910996.1874*(Volts(I)^4))+.039
669 NEXT I
878 !!! PRINT OUTPUT TEMPERATURES
879 PRINT " "
880 FOR I=1 TO 45
881 PRINT "HEATER #";I," TEMPERATURE IN DEG. C =";Temp(I)
882 NEXT I
883 !OUTPUT @Path3;Temp(*)
884 PRINT " "
885 PRINT " "

```

```

990 PRINT "
990 PRINT "          BATH TEMPERATURES (TOP TO BOTTOM)"
1000 PRINT "
1010 OUTPUT 709;"CONFMEAS DCU,317-319,USE 0"
1020 FOR I=57 TO 59
1030 ENTER 709;Volts(I)
1040 Temp(I)=.0005797+(25525.1328*Volts(I))-1507789.2467*(Volts(I)*Volts(I))-
21952034.3364*(Volts(I)^3)+(8370510996.1874*(Volts(I)^4))+.035
1050 PRINT "TEMP. DEG. C ";Temp(I)
1060 NEXT I
1070 END

```



## APPENDIX E

### UNIFORM POWER PROGRAM

```

1  !!!!!!!!!!!!!!!!!!!!!!!!!!!!!!!!!!!!!!!!!!!!!!!!!!!!!!!!!!!!!!!!!!!!!!!!!!!!!
2  !!!          POWER INPUT PROGRAM          !!!
4  !!!!!!!!!!!!!!!!!!!!!!!!!!!!!!!!!!!!!!!!!!!!!!!!!!!!!!!!!!!!!!!!!!!!!!!!!!!!!
5  !OUTPUT 709;"LOCAL CLR"
7  OUTPUT 709;"RST"
10 REAL Volts(51)
20 REAL Pow(51)
30 REAL Ptot,Pavg,Perdif
920 OUTPUT 709;"CONFMEAS DCV,308-315,USE 0"
930 FOR I=1 TO 8
931 J=9-I
940 ENTER 709;Volts(J)
950 PRINT " "
952 NEXT I
953 OUTPUT 709;"RST"
954 OUTPUT 709;"CONFMEAS DCV,316,USE 0"
955 ENTER 709;Volts(46)
956 OUTPUT 709;"RST"
971 OUTPUT 709;"CONFMEAS DCV,403-417,USE 0"
972 FOR I=9 TO 23
973 ENTER 709;Volts(I)
977 NEXT I
978 OUTPUT 709;"RST"
979 OUTPUT 709;"CONFMEAS DCV,400-401,USE 0"
980 FOR I=47 TO 48
981 ENTER 709;Volts(I)
982 NEXT I
983 OUTPUT 709;"RST"
985 OUTPUT 709;"CONFMEAS DCV,503-517,USE 0"
986 FOR I=24 TO 38
987 ENTER 709;Volts(I)
989 NEXT I
990 OUTPUT 709;"RST"
991 OUTPUT 709;"CONFMEAS DCV,500-501,USE 0"
992 FOR I=49 TO 50
993 ENTER 709;Volts(I)
994 NEXT I
996 OUTPUT 709;"RST"
997 OUTPUT 709;"CONFMEAS DCV,602-608,USE 0"
998 FOR I=39 TO 45
999 ENTER 709;Volts(I)
1000 NEXT I
1001 OUTPUT 709;"RST"
1002 OUTPUT 709;"CONFMEAS DCV,600,USE 0"
1003 ENTER 709;Volts(51)
1004 OUTPUT 709;"RST"
1005 PRINT " "
1006 PRINT " "
1050 PRINT "INPUT VOLTAGE D.C. VOLTS PAN 1";Volts(46)
1051 PRINT "INPUT VOLTAGE D.C. VOLTS PAN 2";Volts(47)
1052 PRINT "INPUT VOLTAGE D.C. VOLTS PAN 3";Volts(48)
1053 PRINT "INPUT VOLTAGE D.C. VOLTS PAN 4";Volts(49)

```

```

1054 PRINT "INPUT VOLTAGE D.C. VOLTS PAN 5";Volts(50)
1055 PRINT "INPUT VOLTAGE D.C. VOLTS PAN 6";Volts(51)
1060 PRINT " "
1070 PRINT " "
1080 Resist=2.0
1109 R2=Resist*Resist
1119 Pow(2)=(Volts(46)-Volts(2))*(Volts(2)*(Resist+.4)-Volts(46)*.4)/R2
1149 Pow(5)=(Volts(46)-Volts(5))*(Volts(5)*(Resist+.2)-Volts(46)*.2)/R2
1179 Pow(9)=(Volts(47)-Volts(9))*(Volts(9)*(Resist+.3)-Volts(47)*.3)/R2
1189 Pow(10)=(Volts(47)-Volts(10))*(Volts(10)*(Resist+.45)-Volts(47)*.45)/R2
1194 Pow(18)=(Volts(48)-Volts(18))*(Volts(18)*(Resist+.55)-Volts(48)*.55)/R2
1197 Pow(23)=(Volts(48)-Volts(23))*(Volts(23)*(Resist+.55)-Volts(48)*.55)/R2
1198 Pow(24)=(Volts(49)-Volts(24))*(Volts(24)*(Resist+.1)-Volts(48)*.1)/R2
1199 Pow(25)=(Volts(49)-Volts(25))*(Volts(25)*(Resist+.3)-Volts(48)*.3)/R2
1238 Pow(29)=(Volts(49)-Volts(29))*(Volts(29)*(Resist+.45)-Volts(49)*.45)/R2
1241 Pow(32)=(Volts(50)-Volts(32))*(Volts(32)*(Resist+.6)-Volts(50)*.6)/R2
1243 Pow(34)=(Volts(50)-Volts(34))*(Volts(34)*(Resist+.3)-Volts(50)*.3)/R2
1244 Pow(35)=(Volts(50)-Volts(35))*(Volts(35)*(Resist+.6)-Volts(50)*.6)/R2
1245 Pow(36)=(Volts(50)-Volts(36))*(Volts(36)*(Resist+.6)-Volts(50)*.6)/R2
1246 Pow(37)=(Volts(50)-Volts(37))*(Volts(37)*(Resist+.6)-Volts(50)*.6)/R2
1247 Pow(39)=(Volts(51)-Volts(39))*(Volts(39)*(Resist+.3)-Volts(51)*.3)/R2
1248 Pow(40)=(Volts(51)-Volts(40))*(Volts(40)*(Resist+.3)-Volts(51)*.3)/R2
1250 Pow(42)=(Volts(51)-Volts(42))*(Volts(42)*(Resist+.55)-Volts(51)*.55)/R2
1251 Pow(43)=(Volts(51)-Volts(43))*(Volts(43)*(Resist+.45)-Volts(51)*.45)/R2
1252 Pow(44)=(Volts(51)-Volts(44))*(Volts(44)*(Resist+.55)-Volts(51)*.55)/R2
1281 Pow(2)=(Volts(46)-Volts(2))*(Volts(2)*(Resist+.4)-Volts(46)*.4)/R2
1284 Pow(5)=(Volts(46)-Volts(5))*(Volts(5)*(Resist+.2)-Volts(46)*.2)/R2
1290 Pow(4)=(Volts(46)-Volts(4))*(Volts(4)*(Resist+.1)-Volts(46)*.1)/R2
1294 Pow(9)=(Volts(47)-Volts(9))*(Volts(9)*(Resist+.3)-Volts(47)*.3)/R2
1295 Pow(25)=(Volts(49)-Volts(25))*(Volts(25)*(Resist+.3)-Volts(49)*.3)/R2
1297 Pow(29)=(Volts(49)-Volts(29))*(Volts(29)*(Resist+.2)-Volts(49)*.2)/R2
1298 Resist=1.972
1299 R2=Resist*Resist
1300 Pow(15)=(Volts(47)-Volts(15))*(Volts(15)*(Resist+.2)-Volts(47)*.2)/R2
1301 Resist=1.9184
1302 R2=Resist*Resist
1303 Pow(14)=(Volts(47)-Volts(14))*(Volts(14)*(Resist+.1)-Volts(47)*.1)/R2
1304 Resist=1.886
1305 R2=Resist*Resist
1306 Pow(4)=(Volts(46)-Volts(4))*(Volts(4)*(Resist+.1)-Volts(46)*.1)/R2
1307 Pow(6)=(Volts(46)-Volts(6))*(Volts(6)*(Resist+.1)-Volts(46)*.1)/R2
1308 Pow(30)=(Volts(49)-Volts(30))*(Volts(30)*(Resist+.4)-Volts(49)*.4)/R2
1309 Resist=1.862
1310 R2=Resist*Resist
1311 Pow(27)=(Volts(49)-Volts(27))*(Volts(27)*(Resist+.5)-Volts(49)*.5)/R2
1312 Pow(28)=(Volts(49)-Volts(28))*(Volts(28)*(Resist+.0)-Volts(49)*.0)/R2
1313 Pow(31)=(Volts(50)-Volts(31))*(Volts(31)*(Resist+.65)-Volts(50)*.65)/R2
1314 Pow(38)=(Volts(50)-Volts(38))*(Volts(38)*(Resist+.3)-Volts(50)*.3)/R2

```

```

1315 Resist=1.852
1316 R2=Resist*Resist
1317 Pow(24)=(Volts(49)-Volts(24))*(Volts(24)*(Resist+.1)-Volts(49)*.1)/R2
1318 Pow(33)=(Volts(50)-Volts(33))*(Volts(33)*(Resist+.7)-Volts(50)*.7)/R2
1319 Resist=1.8333
1320 R2=Resist*Resist
1321 Pow(11)=(Volts(47)-Volts(11))*(Volts(11)*(Resist+.5)-Volts(47)*.5)/R2
1322 Pow(12)=(Volts(47)-Volts(12))*(Volts(12)*(Resist+.1)-Volts(47)*.1)/R2
1323 Pow(13)=(Volts(47)-Volts(13))*(Volts(13)*(Resist+.2)-Volts(47)*.2)/R2
1325 Pow(41)=(Volts(51)-Volts(41))*(Volts(41)*(Resist+.1)-Volts(51)*.1)/R2
1326 Pow(45)=(Volts(51)-Volts(45))*(Volts(45)*(Resist+.6)-Volts(51)*.6)/R2
1327 Resist=1.8182
1328 R2=Resist*Resist
1329 Pow(21)=(Volts(48)-Volts(21))*(Volts(21)*(Resist+.7)-Volts(48)*.7)/R2
1330 Resist=1.8
1331 R2=Resist*Resist
1332 Pow(8)=(Volts(46)-Volts(8))*(Volts(8)*(Resist+.2)-Volts(46)*.2)/R2
1333 Pow(19)=(Volts(48)-Volts(19))*(Volts(19)*(Resist+.2)-Volts(48)*.2)/R2
1334 Pow(20)=(Volts(48)-Volts(20))*(Volts(20)*(Resist+.7)-Volts(48)*.7)/R2
1335 Pow(22)=(Volts(48)-Volts(22))*(Volts(22)*(Resist+.2)-Volts(48)*.2)/R2
1336 Resist=1.6667
1337 R2=Resist*Resist
1338 Pow(1)=(Volts(46)-Volts(1))*(Volts(1)*(Resist+.3)-Volts(46)*.3)/R2
1339 Pow(3)=(Volts(46)-Volts(3))*(Volts(3)*(Resist+.7)-Volts(46)*.7)/R2
1340 Pow(7)=(Volts(46)-Volts(7))*(Volts(7)*(Resist+.2)-Volts(46)*.2)/R2
1341 Pow(16)=(Volts(48)-Volts(16))*(Volts(16)*(Resist+.4)-Volts(48)*.4)/R2
1342 Pow(17)=(Volts(48)-Volts(17))*(Volts(17)*(Resist+.4)-Volts(48)*.4)/R2
1343 Pow(26)=(Volts(49)-Volts(26))*(Volts(26)*(Resist+.2)-Volts(49)*.2)/R2
1344 FOR I=1 TO 45
1345 PRINT "BLOCK # ";I," POWER = ";Pow(I)," WATTS"
1346 WAIT .5
1347 NEXT I
1348 Ptot=0
1349 FOR I=1 TO 45
1350 Ptot=Ptot+Pow(I)
1351 NEXT I
1352 Pavg=Ptot/45
1353 PRINT " "
1354 PRINT "AVERAGE POWER = ";Pavg," WATTS"
1355 PRINT " "
1356 FOR I=1 TO 45
1357 Perdif=ABS((Pavg-Pow(I))/Pavg)*100
1358 PRINT "HEATER #";I," PERCENT DEVIATION ";Perdif
1359 WAIT .5
1360 NEXT I
1361 END

```

# APPENDIX F

## UNIFORM DATA REDUCTION PROGRAM

```

10  !!!!!!!!!!!!!!!!!!!!!!!!!!!!!!!!!!!!!!!!!!!!!!!!!!!!!!!!!!!!!!!!!!!!!!!!!!!!!!!
20  !!          TEMPERATURE ACQUISITION AND REDUCTION PROGRAM          !!
30  !!          (STEADY STATE)                                          !!
31  !!  PROGRAM PERFORMS THE REQUIRED FUNCTIONS NEEDED TO OBTAIN DATA  !!
32  !!  FROM THE ACQUISITION SYSTEM AND CONVERT THE THERMOCOUPLE OUT-  !!
33  !!  PUT VOLTAGES INTO TEMPERATURE VALUES. THE TEMPERATURES ARE  !!
34  !!  PRINTED OUT AND THEN REDUCED TO COMPARE WITH THEORETICAL VALUES !!
40  !!!!!!!!!!!!!!!!!!!!!!!!!!!!!!!!!!!!!!!!!!!!!!!!!!!!!!!!!!!!!!!!!!!!!!!!!!!!!!!
50  REAL Volts(60)
60  REAL T(60)
65  REAL Ndt(45),Ndt1(45),Lnu(45),Lgr(45)
66  REAL Power,Tamb,G,Kpg,Delx,As,Per,Ta,Qconv,Lbar
67  REAL Qflux,Delt,Tfilm,Beta,Spvol,Dynvisc,Qcond
68  REAL Kinvisc,Kf,Pr,Theta,Hx,Grm,Hux
69  PRINTER IS CRT
70  PRINT "ENTER OUTPUT DATA FILE NAME"
71  INPUT Filename$
72  PRINT
73  PRINT "ENTER POWER VALUE IN WATTS"
74  INPUT Power
75  PRINT
76  PRINT "ENTER SHROUD SPACING IN mm"
77  INPUT Space$
78  !PRINT
79  !CREATE BDAT "THRED15:,700,1",45
80  !ASSIGN @Path3 TO "THRED15:,700,1"
81  !PRINT DATE$(TIMEDATE)
82  !PRINT Power," WATT INPUT POWER"
83  !PRINT " 45 STRIPS NO SHROUD"
84  !PRINT " BDAT FILE THRED15:,700,1"
85  !PRINT " "
86  !PRINT " "
89  !!!!!!!!!!!!!!!!!!!!!!!!!!!!!!! SURFACE #1-20
90  OUTPUT 709;"CONFMEAS DCV, 100-119,USE 0"
91  FOR I=1 TO 20
92  ENTER 709;Volts(I)
93  T(I)=.0006797+(25825.1328*Volts(I))-(607789.2467*(Volts(I)*Volts(I)))-(219
52034.3364*(Volts(I)^3))+(8370810996.1874*(Volts(I)^4))+.039
94  NEXT I
95  !!!!!!!!!!!!!!!!!!!!!!!!!!!!!!! SURFACE #21-40
96  OUTPUT 709;"CONFMEAS DCV,200-219,USE 0"
97  FOR I=21 TO 40
98  ENTER 709;Volts(I)
99  T(I)=.0006797+(25825.1328*Volts(I))-(607789.2467*(Volts(I)*Volts(I)))-(219
52034.3364*(Volts(I)^3))+(8370810996.1874*(Volts(I)^4))+.039
100 NEXT I
101 !!!!!!!!!!!!!!!!!!!!!!!!!!!!!!! SURFAC #41-45
102 OUTPUT 709;"CONFMEAS DCV,300-304,USE 0"
103 FOR I=41 TO 45
104 ENTER 709;Volts(I)
105 T(I)=.0006797+(25825.1326*Volts(I))-(607789.2467*(Volts(I)*Volts(I)))-(219
52034.3364*(Volts(I)^3))+(8370810996.1874*(Volts(I)^4))+.039
106 NEXT I

```

```

107   !!! PRINT OUTPUT TEMPERATURES
108   !PRINT " "
109   !FOR I=1 TO 45
110   !PRINT "HEATER #";I," TEMPERATURE IN DEG. C =";T(I)
111   !NEXT I
112   !OUTPUT @Path3;T(*)
115   !PRINT " "
116   !PRINT "          BATH TEMPERATURES (TOP TO BOTTOM)"
117   !PRINT " "
118   OUTPUT 709;"CONFMEAS DCV,317-319,USE 0"
119   FOR I=57 TO 59
120   ENTER 709;Volts(I)
121   T(I)=.0006797+(25825.1328*Volts(I))-(607789.2467*(Volts(I)*Volts(I)))-(219
52034.3364*(Volts(I)^3))+(8370810996.1874*(Volts(I)^4))+.036
122   !PRINT "TEMP. DEG. C ";T(I)
124   NEXT I
126   T(22)=25
127   T(29)=25
133   !PRINT "INPUT AMBIENT TEMPERATURE"
134   Tamb=(T(57)+T(58)+T(59))/3
135   PRINTER IS 701
136   PRINT " "
137   PRINT DATE$(TIMEDATE)
138   PRINT "DATA REDUCTION OUTPUT"
139   PRINT " "
140   PRINT "POWER LEVEL (WATTS)      :",Power
141   PRINT
142   PRINT "SHOUL POSITION (mm)      :",Space$
143   PRINT
144   PRINT "AMBIENT TEMPERATURE (C) :",Tamb
145   PRINT
146   PRINT
147   '
148   !ASSIGN @Path TO Filenames
149   !ENTER @Path;T(*)
150   '
151   G=9.81
152   Kpg=.1421
153   Delx=.006731
154   As=.0239*.0078
155   Per=2*.0239+2*.0078
156   Lbar=As/Per
157   AS="Qcond"
158   BS="X/L"
159   CS="NDT"
160   DS="LOG(Nux)"
161   ES="LOG(Grx*)"
162   FS="DELT"
163   GS="Hx"
164   HS="Nux"
165   IS="Grx*"
166   JS="Temp"
168   PRINTER IS CRT

```

```

169  !!!!!!!!!!!!!!!!!!!!!!!!!!!!!!!!!!!!!!!!!!!!!!!!!!!!!!!
170  !          ENTER CONDUCTION LOSSES          !
171  !!!!!!!!!!!!!!!!!!!!!!!!!!!!!!!!!!!!!!!!!!!!!!!!!!!!!!!
172  PRINT "INPUT CONDUCTION LOSSES AS COMPUTED FROM ELLPACK"
173  INPUT Qcond
174  !!!!!!!!!!!!!!!!!!!!!!!!!!!!!!!!!!!!!!!!!!!!!!!!!!!!!!!
175  CREATE BDAT Filenames$,45
176  ASSIGN @Path3 TO Filenames$
177  PRINTER IS 701
178  FOR I=1 TO 45
179  PRINT " "
180  PRINT " "
181  PRINT "                SURFACE #".I

182  PRINT " "
183  PRINT USING "2X,AAAAA,3X,AAA,3X,AAA,3X,AAAAA,2X,AAAAA,3X,AAA,4X,AA
,4X,AAA,3X,AAAA,2X,AAAA";A$,B$,C$,D$,E$,F$,G$,H$,I$,J$
184  Qconv=Power-Qcond
185  Qflux=Qconv/As
186  Delt=T(I)-Tamb
187  Tfilm=273.15+(T(I)+Tamb)/2
188  Beta=(-7.944858E-8*(Tfilm^2))+(5.7356479E-5*Tfilm)-.0097810563
189  Spvol=(4.69699E-9*(Tfilm^2))+(-2.53745E-6*Tfilm)+.001341903
190  Dynvisc=(3.2348511E-7*(Tfilm^2))+(-.00021474487*Tfilm)+.036166792
191  Kinvisc=Spvol*Dynvisc
192  Kf=(1.418181818E-3*Tfilm)+.1866
193  Pr=(4.65706E-3*(Tfilm^2))+(-2.922094*Tfilm)+463.3319
194  Theta1=Power/(.0220*Kf)
195  Ndt1(I)=Delt/Theta1
196  Nd=Ndt1(I)
197  Temp=T(I)
198  Theta=Qflux*Lbar/Kf
199  Ndt(I)=Delt/Theta
200  Hx=Qflux/Delt
201  Grm=(6*Beta*Qflux*(Lbar)^4)/(Kf*Kinvisc^2)
202  Nux=Hx*Lbar/Kf
203  Lgr(I)=LGT(Grm)
204  Lnu(I)=LGT(Nux)
205  Lg=Lgr(I)
206  Lnn=Lnu(I)
207  Xtol=(31.75-(6.985+(I-16)*1.270))/31.75
208  PRINT USING "1X,D.DDDD,2X,D.DDD,1X,D.DDD,2X,D.DDD,5X,D.DDD,4X,DD.DDD,2X,DD
DD.D,1X,DD.DDD,DDDDD.D,1X,DD.DD";Qcond,Xtol,Nd,Lnn,Lg,Delt,Hx,Nux,Grm,Temp
209  NEXT I
210  OUTPUT @Path3;T(*),Ndt1(*),Ndt(*),Lnu(*),Lgr(*)
211  PRINTER IS CRT
212  END

```

# APPENDIX G

## NONUNIFORM POWER PROGRAM

```

1      !!!!!!!!!!!!!!!!!!!!!!!!!!!!!!!!!!!!!!!!!!!!!!!!!!!!!!!!!!!!!!!!!!!!!!!!!!!!!!!
2      !!!                POWER INPUT PROGRAM                                !!!
4      !!!!!!!!!!!!!!!!!!!!!!!!!!!!!!!!!!!!!!!!!!!!!!!!!!!!!!!!!!!!!!!!!!!!!!!!!!!!!!!
5      !OUTPUT 709;"LOCAL CLR"
7      OUTPUT 709;"RST"
10     REAL Volts(51)
20     REAL Pow(51)
30     REAL Ptot,Pavg,Perdif
920    OUTPUT 709;"CONFMEAS DCV,308-315,USE 0"
930    FOR I=1 TO 8
931    J=9-I
940    ENTER 709;Volts(J)
950    PRINT " "
952    NEXT I
953    OUTPUT 709;"RST"
954    OUTPUT 709;"CONFMEAS DCV,316,USE 0"
955    ENTER 709;Volts(46)
956    OUTPUT 709;"RST"
971    OUTPUT 709;"CONFMEAS DCV,403-417,USE 0"
972    FOR I=9 TO 23
973    ENTER 709;Volts(I)
977    NEXT I
978    OUTPUT 709;"RST"
979    OUTPUT 709;"CONFMEAS DCV,400-401,USE 0"
980    FOR I=47 TO 48
981    ENTER 709;Volts(I)
982    NEXT I
983    OUTPUT 709;"RST"
985    OUTPUT 709;"CONFMEAS DCV,503-517,USE 0"
986    FOR I=24 TO 38
987    ENTER 709;Volts(I)
989    NEXT I
990    OUTPUT 709;"RST"
991    OUTPUT 709;"CONFMEAS DCV,500-501,USE 0"
992    FOR I=49 TO 50
993    ENTER 709;Volts(I)
994    NEXT I
996    OUTPUT 709;"RST"
997    OUTPUT 709;"CONFMEAS DCV,502-608,USE 0"
998    FOR I=39 TO 45
999    ENTER 709;Volts(I)
1000   NEXT I
1001   OUTPUT 709;"RST"
1002   OUTPUT 709;"CONFMEAS DCV,600,USE 0"
1003   ENTER 709;Volts(51)
1004   OUTPUT 709;"RST"
1005   PRINT " "
1006   PRINT " "
1050   PRINT "INPUT VOLTAGE D.C. VOLTS PAN 1";Volts(46)
1051   PRINT "INPUT VOLTAGE D.C. VOLTS PAN 2";Volts(47)
1052   PRINT "INPUT VOLTAGE D.C. VOLTS PAN 3";Volts(48)
1053   PRINT "INPUT VOLTAGE D.C. VOLTS PAN 4";Volts(49)

```

```

1054 PRINT "INPUT VOLTAGE D.C. VOLTS PAN 5";Volts(50)
1055 PRINT "INPUT VOLTAGE D.C. VOLTS PAN 6";Volts(51)
1060 PRINT " "
1070 PRINT " "
1080 Resist=2.0
1109 R2=Resist*Resist
1119 Pow(2)=(Volts(46)-Volts(2))*(Volts(2)*(Resist+.4)-Volts(46)*.4)/R2
1149 Pow(5)=(Volts(46)-Volts(5))*(Volts(5)*(Resist+.2)-Volts(46)*.2)/R2
1179 Pow(9)=(Volts(47)-Volts(9))*(Volts(9)*(Resist+.3)-Volts(47)*.3)/R2
1189 Pow(10)=(Volts(47)-Volts(10))*(Volts(10)*(Resist+.45)-Volts(47)*.45)/R2
1194 Pow(18)=(Volts(48)-Volts(18))*(Volts(18)*(Resist+.55)-Volts(48)*.55)/R2
1197 Pow(23)=(Volts(48)-Volts(23))*(Volts(23)*(Resist+.55)-Volts(48)*.55)/R2
1198 Pow(24)=(Volts(49)-Volts(24))*(Volts(24)*(Resist+.1)-Volts(48)*.1)/R2
1199 Pow(25)=(Volts(49)-Volts(25))*(Volts(25)*(Resist+.3)-Volts(48)*.3)/R2
1238 Pow(29)=(Volts(49)-Volts(29))*(Volts(29)*(Resist+.45)-Volts(49)*.45)/R2
1241 Pow(32)=(Volts(50)-Volts(32))*(Volts(32)*(Resist+.6)-Volts(50)*.6)/R2
1243 Pow(34)=(Volts(50)-Volts(34))*(Volts(34)*(Resist+.3)-Volts(50)*.3)/R2
1244 Pow(35)=(Volts(50)-Volts(35))*(Volts(35)*(Resist+.6)-Volts(50)*.6)/R2
1245 Pow(36)=(Volts(50)-Volts(36))*(Volts(36)*(Resist+.6)-Volts(50)*.6)/R2
1246 Pow(37)=(Volts(50)-Volts(37))*(Volts(37)*(Resist+.6)-Volts(50)*.6)/R2
1247 Pow(39)=(Volts(51)-Volts(39))*(Volts(39)*(Resist+.3)-Volts(51)*.3)/R2
1248 Pow(40)=(Volts(51)-Volts(40))*(Volts(40)*(Resist+.3)-Volts(51)*.3)/R2
1250 Pow(42)=(Volts(51)-Volts(42))*(Volts(42)*(Resist+.55)-Volts(51)*.55)/R2
1251 Pow(43)=(Volts(51)-Volts(43))*(Volts(43)*(Resist+.45)-Volts(51)*.45)/R2
1252 Pow(44)=(Volts(51)-Volts(44))*(Volts(44)*(Resist+.55)-Volts(51)*.55)/R2
1281 Pow(2)=(Volts(46)-Volts(2))*(Volts(2)*(Resist+.4)-Volts(46)*.4)/R2
1284 Pow(5)=(Volts(46)-Volts(5))*(Volts(5)*(Resist+.2)-Volts(46)*.2)/R2
1290 Pow(4)=(Volts(46)-Volts(4))*(Volts(4)*(Resist+.1)-Volts(46)*.1)/R2
1294 Pow(9)=(Volts(47)-Volts(9))*(Volts(9)*(Resist+.3)-Volts(47)*.3)/R2
1295 Pow(25)=(Volts(49)-Volts(25))*(Volts(25)*(Resist+.3)-Volts(49)*.3)/R2
1297 Pow(29)=(Volts(49)-Volts(29))*(Volts(29)*(Resist+.2)-Volts(49)*.2)/R2
1298 Resist=1.972
1299 R2=Resist*Resist
1300 Pow(15)=(Volts(47)-Volts(15))*(Volts(15)*(Resist+.2)-Volts(47)*.2)/R2
1301 Resist=1.9184
1302 R2=Resist*Resist
1303 Pow(14)=(Volts(47)-Volts(14))*(Volts(14)*(Resist+.1)-Volts(47)*.1)/R2
1304 Resist=1.886
1305 R2=Resist*Resist
1306 Pow(4)=(Volts(46)-Volts(4))*(Volts(4)*(Resist+.1)-Volts(46)*.1)/R2
1307 Pow(6)=(Volts(46)-Volts(6))*(Volts(6)*(Resist+.1)-Volts(46)*.1)/R2
1308 Pow(30)=(Volts(49)-Volts(30))*(Volts(30)*(Resist+.4)-Volts(49)*.4)/R2
1309 Resist=1.862
1310 R2=Resist*Resist
1311 Pow(27)=(Volts(49)-Volts(27))*(Volts(27)*(Resist+.5)-Volts(49)*.5)/R2
1312 Pow(28)=(Volts(49)-Volts(28))*(Volts(28)*(Resist+.0)-Volts(49)*.0)/R2
1313 Pow(31)=(Volts(50)-Volts(31))*(Volts(31)*(Resist+.65)-Volts(50)*.65)/R2
1314 Pow(38)=(Volts(50)-Volts(38))*(Volts(38)*(Resist+.3)-Volts(50)*.3)/R2
1315 Resist=1.852
1316 R2=Resist*Resist
1317 Pow(24)=(Volts(49)-Volts(24))*(Volts(24)*(Resist+.1)-Volts(49)*.1)/R2
1318 Pow(33)=(Volts(50)-Volts(33))*(Volts(33)*(Resist+.7)-Volts(50)*.7)/R2
1319 Resist=1.8333
1320 R2=Resist*Resist
1321 Pow(11)=(Volts(47)-Volts(11))*(Volts(11)*(Resist+.5)-Volts(47)*.5)/R2
1322 Pow(12)=(Volts(47)-Volts(12))*(Volts(12)*(Resist+.1)-Volts(47)*.1)/R2
1323 Pow(13)=(Volts(47)-Volts(13))*(Volts(13)*(Resist+.2)-Volts(47)*.2)/R2
1325 Pow(41)=(Volts(51)-Volts(41))*(Volts(41)*(Resist+.1)-Volts(51)*.1)/R2
1326 Pow(45)=(Volts(51)-Volts(45))*(Volts(45)*(Resist+.6)-Volts(51)*.6)/R2

```



```

1327 Resist=1.8182
1328 R2=Resist*Resist
1329 Pow(21)=(Volts(48)-Volts(21))*(Volts(21)*(Resist+.7)-Volts(48)*.7)/R2
1330 Resist=1.8
1331 R2=Resist*Resist
1332 Pow(8)=(Volts(46)-Volts(8))*(Volts(8)*(Resist+.2)-Volts(46)*.2)/R2
1333 Pow(19)=(Volts(48)-Volts(19))*(Volts(19)*(Resist+.2)-Volts(48)*.2)/R2

1334 Pow(20)=(Volts(48)-Volts(20))*(Volts(20)*(Resist+.7)-Volts(48)*.7)/R2
1335 Pow(22)=(Volts(48)-Volts(22))*(Volts(22)*(Resist+.2)-Volts(48)*.2)/R2
1336 Resist=1.6667
1337 R2=Resist*Resist
1338 Pow(1)=(Volts(46)-Volts(1))*(Volts(1)*(Resist+.3)-Volts(46)*.3)/R2
1339 Pow(3)=(Volts(46)-Volts(3))*(Volts(3)*(Resist+.7)-Volts(46)*.7)/R2
1340 Pow(7)=(Volts(46)-Volts(7))*(Volts(7)*(Resist+.2)-Volts(46)*.2)/R2
1341 Pow(16)=(Volts(48)-Volts(16))*(Volts(16)*(Resist+.4)-Volts(48)*.4)/R2
1342 Pow(17)=(Volts(48)-Volts(17))*(Volts(17)*(Resist+.4)-Volts(48)*.4)/R2
1343 Pow(26)=(Volts(49)-Volts(26))*(Volts(26)*(Resist+.2)-Volts(49)*.2)/R2
1344 FOR I=1 TO 45
1345 PRINT "BLOCK # ";I," POWER = ";Pow(I)," WATTS"
1346 WAIT .5
1347 NEXT I
1348 Ptot=0
1349 FOR I=1 TO 15
1350 Ptot=Ptot+Pow(I)
1351 NEXT I
1352 FOR I=31 TO 45
1353 Ptot=Ptot+Pow(I)
1354 NEXT I
1355 Pavgsides=Ptot/30
1356 PRINT " "
1357 PRINT "AVERAGE POWER SIDES= ";Pavgsides," WATTS"
1358 PRINT " "
1359 Ptot=0
1360 FOR I=16 TO 30
1361 Ptot=Ptot+Pow(I)
1362 NEXT I
1363 Pavgcenter=Ptot/15
1364 PRINT "AVERAGE POWER CENTER= ";Pavgcenter," WATTS"
1365 PRINT " "
1366 PRINT " "
1367 FOR I=1 TO 15
1368 Perdif=ABS((Pavgsides-Pow(I))/Pavgsides)*100
1369 PRINT "HEATER #";I," PERCENT DEVIATION ";Perdif
1370 WAIT .5
1371 NEXT I
1372 FOR I=16 TO 30
1373 Perdif=ABS((Pavgcenter-Pow(I))/Pavgcenter)*100
1374 PRINT "HEATER #";I," PERCENT DEVIATION ";Perdif
1375 WAIT .5
1376 NEXT I
1377 FOR I=31 TO 45
1378 Perdif=ABS((Pavgsides-Pow(I))/Pavgsides)*100
1379 PRINT "HEATER #";I," PERCENT DEVIATION ";Perdif
1380 WAIT .5
1381 NEXT I
1382 END

```

# APPENDIX H

## NONUNIFORM DATA REDUCTION PROGRAM

```

10  !!!!!!!!!!!!!!!!!!!!!!!!!!!!!!!!!!!!!!!!!!!!!!!!!!!!!!!!!!!!!!!!!!!!!!!
20  !!          TEMPERATURE ACQUISITION AND REDUCTION PROGRAM          !!
30  !!          (STEADY STATE)                                          !!
31  !!  PROGRAM PERFORMS THE REQUIRED FUNCTIONS NEEDED TO OBTAIN DATA  !!
32  !!  FROM THE ACQUISITION SYSTEM AND CONVERT THE THERMOCOUPLE OUT-  !!
33  !!  PUT VOLTAGES INTO TEMPERATURE VALUES.  THE TEMPERATURES ARE  !!
34  !!  PRINTED OUT AND THEN REDUCED TO COMPARE WITH THEORETICAL VALUES !!
40  !!!!!!!!!!!!!!!!!!!!!!!!!!!!!!!!!!!!!!!!!!!!!!!!!!!!!!!!!!!!!!!!!!!!!!!
50  REAL Volts(60)
60  REAL T(60)
65  REAL Ndt(45),Ndt1(45),Lnu(45),Lgr(45)
66  REAL Power1,Power2,Tamb,G,Kpg,Delt,As,Per,Ta,Qconv,Lbar
67  REAL Qflux,Delt,Tfilm,Beta,Spvol,Dynvisc,Qcond
68  REAL Kinvisc,Kf,Pr,Theta,Hx,Grm,Hux
69  PRINTER IS CRT
70  PRINT "ENTER OUTPUT DATA FILE NAME"
71  INPUT Filename$
72  PRINT
73  PRINT "ENTER TWO POWER VALUE IN WATTS"
74  INPUT Power1,Power2
75  PRINT
76  PRINT "ENTER SHROUD SPACING IN mm"
77  INPUT Space$
78  !PRINT
79  !CREATE BDAT "THRED15:,700,1",45
80  !ASSIGN @Path3 TO "THRED15:,700,1"
81  !PRINT DATE$(TIMEDATE)
83  !PRINT Power," WATT INPUT POWER"
84  !PRINT " 45 STRIPS NO SHROUD"
85  !PRINT " BDAT FILE THRED15:,700,1"
86  !PRINT " "
89  !!!!!!!!!!!!!!!!!!!!!!!!!!!!!!! SURFACE #1-20
90  OUTPUT 709;"CONFMEAS DCV, 100-119,USE 0"
91  FOR I=1 TO 20
92  ENTER 709;Volts(I)
93  T(I)=.0006797+(25825.1328*Volts(I))-(607789.2467*(Volts(I)*Volts(I)))-(219
52034.3364*(Volts(I)^3))+(8370810996.1874*(Volts(I)^4))+.039
94  NEXT I
95  !!!!!!!!!!!!!!!!!!!!!!!!!!!!!!! SURFACE #21-#40
96  OUTPUT 709;"CONFMEAS DCV,200-219,USE 0"
97  FOR I=21 TO 40
98  ENTER 709;Volts(I)
99  T(I)=.0006797+(25825.1328*Volts(I))-(607789.2467*(Volts(I)*Volts(I)))-(219
52034.3364*(Volts(I)^3))+(8370810996.1874*(Volts(I)^4))+.039
100 NEXT I
101 !!!!!!!!!!!!!!!!!!!!!!!!!!!!!!! SURFAC #41-#45
102 OUTPUT 709;"CONFMEAS DCV,300-304,USE 0"
103 FOR I=41 TO 45
104 ENTER 709;Volts(I)
105 T(I)=.0006797+(25825.1328*Volts(I))-(607789.2467*(Volts(I)*Volts(I)))-(219
52034.3364*(Volts(I)^3))+(8370810996.1874*(Volts(I)^4))+.039
106 NEXT I

```

```

107  !!! PRINT OUTPUT TEMPERATURES
108  !PRINT " "
109  !FOR I=1 TO 45
110  !PRINT "HEATER #";I," TEMPERATURE IN DEG. C =" ;T(I)
111  !NEXT I
112  !OUTPUT @Path3;T(*)
115  !PRINT " "
116  !PRINT "          BATH TEMPERATURES (TOP TO BOTTOM)"
117  !PRINT " "
118  OUTPUT 709;"CONFMEAS DCV,317-319,USE 0"
119  FOR I=57 TO 59
120  ENTER 709;Volts(I)
121  T(I)=.0006797+(25825.1328*Volts(I))-(607789.2467*(Volts(I)*Volts(I)))-(219
52034.3364*(Volts(I)^3))+(8370810996.1874*(Volts(I)^4))+.036
122  !PRINT "TEMP. DEG. C ";T(I)
124  NEXT I
125  T(22)=25
126  T(29)=25
133  !PRINT "INPUT AMBIENT TEMPERATURE"
134  Tamb=(T(57)+T(58)+T(59))/3
135  PRINTER IS 701
136  PRINT " "
137  PRINT DATE$(TIMEDATE)
138  PRINT "DATA REDUCTION OUTPUT"
139  PRINT " "
140  PRINT "POWER LEVELS (WATTS)      :",Power1,Power2
141  PRINT
142  PRINT "SHROUD POSITION (mm)      :",Space$
143  PRINT
144  PRINT "AMBIENT TEMPERATURE (C) :",Tamb
145  PRINT
146  PRINT
147  !
148  !ASSIGN @Path TO Filenames$
149  !ENTER @Path;T(*).
150  !
151  G=9.81
152  Kpg=.1421
153  Delx=.006731
154  As=.0239*.0078
155  Per=2*.0239+2*.0078
156  Lbar=As/Per
157  A$="Qcond"
158  B$="X/L"
159  C$="NDT"
160  D$="LOG(Nux)"
161  E$="LOG(Grx*)"
162  F$="DELT"
163  G$="Hx"
164  H$="Nux"
165  I$="Grx*"
166  J$="Temp"
168  PRINTER IS CRT
169  !!!!!!!!!!!!!!!!!!!!!!!!!!!!!!!!!!!!!!!!!!!!!!!!!!!!!!!!!!!!!!!!!!!!!!!!!!!!!!!
170  !          ENTER CONDUCTION LOSSES          !
171  !!!!!!!!!!!!!!!!!!!!!!!!!!!!!!!!!!!!!!!!!!!!!!!!!!!!!!!!!!!!!!!!!!!!!!!!!!!!!!!
172  PRINT "INPUT SIDE COLUMN CONDUCTION LOSSES AS COMPUTED FROM ELLPACK"
173  INPUT Qcond
174  !!!!!!!!!!!!!!!!!!!!!!!!!!!!!!!!!!!!!!!!!!!!!!!!!!!!!!!!!!!!!!!!!!!!!!!!!!!!!!!
175  CREATE B0AT Filenames$,45
176  ASSIGN @Path3 TO Filenames$
177  PRINTER IS 701

```

```

178 FOR I=1 TO 15
179 PRINT " "
180 PRINT " "
181 PRINT " SURFACE #",I
182 PRINT " "
183 PRINT USING "2X,AAAA,3X,AAA,3X,AAA,3X,AAAAAAA,2X,AAAAAAA,3X,AAA,4X,AA
,4X,AAA,3X,AAAA,2X,AAAA";AS,BS,CS,DS,ES,FS,GS,HS,IS,JS
184 Qconv=Power1-Qcond
185 Qflux=Qconv/As
186 Delt=T(I)-Tamb
187 Tfilm=273.15+(T(I)+Tamb)/2
188 Beta=(-7.944858E-8*(Tfilm^2))+(5.7356479E-5*Tfilm)-.0097810563
189 Spvol=(4.69699E-9*(Tfilm^2))+(-2.53745E-6*Tfilm)+.001341903
190 Dynvisc=(3.2348511E-7*(Tfilm^2))+(-.00021474487*Tfilm)+.036166792
191 Kinvisc=Spvol*Dynvisc
192 Kf=(1.418181818E-3*Tfilm)+.1866
193 Pr=(4.65706E-3*(Tfilm^2))+(-2.922094*Tfilm)+463.3319
194 Theta1=Power1/(.0220*Kf)
195 Ndt1(I)=Delt/Theta1
196 Nd=Ndt1(I)
197 Temp=T(I)
198 Theta=Qflux*Lbar/Kf
199 Ndt(I)=Delt/Theta
200 Hx=Qflux/Delt
201 Grm=(6*Beta*Qflux*(Lbar)^4)/(Kf*Kinvisc^2)
202 Nux=Hx*Lbar/Kf
203 Lgr(I)=LGT(Grm)
204 Lnu(I)=LGT(Nux)
205 Lnn=Lnu(I)
206 Lg=Lgr(I)
208 Xtol=(31.75-(6.985+(I-16)*1.270))/31.75
209 PRINT USING "1X,D.DDDD,2X,D.DDD,1X,D.DDD,2X,D.DDD,5X,D.DDD,4X,DD.DDD,2X,DD
DD.D,1X,DD.DDD,DDDDD.D,1X,DD.DD";Qcond,Xtol,Nd,Lnn,Lg,Delt,Hx,Nux,Grm,Temp
210 NEXT I
211 PRINTER IS CRT
217 !!!!!!!!!!!!!!!!!!!!!!!!!!!!!!!!!!!!!!!!!!!!!!!!!!!!!!!!!!!!!!!
218 ! ENTER CONDUCTION LOSSES !
219 !!!!!!!!!!!!!!!!!!!!!!!!!!!!!!!!!!!!!!!!!!!!!!!!!!!!!!!!!!!!!!!
220 PRINT "INPUT CENTER COLUMN CONDUCTION LOSSES AS COMPUTED FROM ELLPACK"
221 INPUT Qcond
222 !!!!!!!!!!!!!!!!!!!!!!!!!!!!!!!!!!!!!!!!!!!!!!!!!!!!!!!!!!!!!!!
225 PRINTER IS 701
226 FOR I=16 TO 30
227 PRINT " "
228 PRINT " "
229 PRINT " SURFACE #",I
230 PRINT " "
231 PRINT USING "2X,AAAA,3X,AAA,3X,AAA,3X,AAAAAAA,2X,AAAAAAA,3X,AAA,4X,AA
,4X,AAA,3X,AAAA,2X,AAAA";AS,BS,CS,DS,ES,FS,GS,HS,IS,JS
232 Qconv=Power2-Qcond
233 Qflux=Qconv/As
234 Delt=T(I)-Tamb
235 Tfilm=273.15+(T(I)+Tamb)/2
236 Beta=(-7.944858E-8*(Tfilm^2))+(5.7356479E-5*Tfilm)-.0097810563
237 Spvol=(4.69699E-9*(Tfilm^2))+(-2.53745E-6*Tfilm)+.001341903
238 Dynvisc=(3.2348511E-7*(Tfilm^2))+(-.00021474487*Tfilm)+.036166792
239 Kinvisc=Spvol*Dynvisc
240 Kf=(1.418181818E-3*Tfilm)+.1866
241 Pr=(4.65706E-3*(Tfilm^2))+(-2.922094*Tfilm)+463.3319
242 Theta1=Power2/(.0220*Kf)

```

```

243 Ndt1(I)=Delt/Theta1
244 Nd=Ndt1(I)
245 Temp=T(I)
246 Theta=Qflux*Lbar/Kf
247 Ndt(I)=Delt/Theta
248 Hx=Qflux/Delt
249 Grm=(G*Beta*Qflux*(Lbar)^4)/(Kf*Kinvisc^2)
250 Nux=Hx*Lbar/Kf
252 Lgr(I)=LGT(Grm)
253 Lnu(I)=LGT(Nux)

254 Lnn=Lnu(I)
255 Lg=Lgr(I)
256 Xtol=(31.75-(6.985+(I-16)*1.270))/31.75
257 PRINT USING "1X,D.DDDD,2X,D.DDD,1X,D.DDD,2X,D.DDD,5X,D.DDD,4X,DD.DDD,2X,DD
DD.D,1X,DD.DDD,DDDDD.D,1X,DD.DD":Qcond,Xtol,Nd,Lnn,Lg,Delt,Hx,Nux,Grm,Temp
258 NEXT I
259 PRINTER IS CRT
260 !!!!!!!!!!!!!!!!!!!!!!!!!!!!!!!!!!!!!!!!!!!!!!!!!!!!!!!
261 !          ENTER CONDUCTION LOSSES          !
262 !!!!!!!!!!!!!!!!!!!!!!!!!!!!!!!!!!!!!!!!!!!!!!!!!!!!!!!
263 PRINT "INPUT SIDE COLUMN CONDUCTION LOSSES AS COMPUTED FROM ELLPACK"
264 INPUT Qcond
265 !!!!!!!!!!!!!!!!!!!!!!!!!!!!!!!!!!!!!!!!!!!!!!!!!!!!!!!
266 PRINTER IS 701
267 FOR I=31 TO 45
268 PRINT " "
269 PRINT " "
270 PRINT "                SURFACE #",I
271 PRINT " "
272 PRINT USING "2X,AAAAA,3X,AAA,3X,AAA,3X,AAAAA,2X,AAAAA,3X,AAAA,4X,AA
,4X,AAA,3X,AAAA,2X,AAAA":As,Bs,Cs,Ds,Es,Fs,Gs,Hs,Is,J$
273 Qconv=Power1-Qcond
274 Qflux=Qconv/As
275 Delt=T(I)-Tamb
276 Tfilm=273.15+(T(I)+Tamb)/2
277 Beta=(-7.944858E-8*(Tfilm^2))+(5.7356479E-5*Tfilm)-.0097810563
278 Spvol=(4.69699E-9*(Tfilm^2))+(-2.53745E-6*Tfilm)+.001341903
279 Dynvisc=(3.2348511E-7*(Tfilm^2))+(-.00021474487*Tfilm)+.036166792
280 Kinvisc=Spvol*Dynvisc
281 Kf=(1.418181818E-3*Tfilm)+.1866
282 Pr=(4.65706E-3*(Tfilm^2))+(-2.922094*Tfilm)+463.3319
283 Theta1=Power1/(.0220*Kf)
284 Ndt1(I)=Delt/Theta1
285 Nd=Ndt1(I)
286 Temp=T(I)
287 Theta=Qflux*Lbar/Kf
288 Ndt(I)=Delt/Theta
289 Hx=Qflux/Delt
290 Grm=(G*Beta*Qflux*(Lbar)^4)/(Kf*Kinvisc^2)
291 Nux=Hx*Lbar/Kf
292 Lgr(I)=LGT(Grm)
293 Lnu(I)=LGT(Nux)
294 Lnn=Lnu(I)
295 Lg=Lgr(I)
296 Xtol=(31.75-(6.985+(I-16)*1.270))/31.75
297 PRINT USING "1X,D.DDDD,2X,D.DDD,1X,D.DDD,2X,D.DDD,5X,D.DDD,4X,DD.DDD,2X,DD
DD.D,1X,DD.DDD,DDDDD.D,1X,DD.DD":Qcond,Xtol,Nd,Lnn,Lg,Delt,Hx,Nux,Grm,Temp
298 NEXT I
299 OUTPUT @Path3;T(*),Ndt1(*),Ndt(*),Lnu(*),Lgr(*)
300 PRINTER IS CRT
301 END

```

## LIST OF REFERENCES

1. Bergles, A. E., and Bar-Cohen, A., Direct Liquid Cooling of Microelectronic Components, *Advances in Thermal Modeling of Electronic Components and Systems*, Vol. 2, Bar-Cohen, A. and Kraus, A. D., Eds., ASME Press, 1990.
2. Nakayama, A., Thermal Management of Electronic Equipment: A Review of Technology and Research Topics, *Advances in Thermal Modeling of Electronic Components and Systems*, Vol. 1, Hemisphere, 1988.
3. Incropera, F. P., "Convection Heat Transfer in Electronic Equipment Cooling", *ASME J. Heat Transfer* 110, 1097, 1988.
4. Incropera, F. P., and Dewitt, D. P., *Introduction to Heat Transfer*, Wiley, New York, 1985.
5. Sathe, S. B., and Joshi, Y., "Natural Convection Arising from a Heat Generating Substrate-Mounted Protrusion in a Liquid-Filled Two-Dimensional Enclosure", submitted for publication.
6. Gaiser, A. O., *Natural Convection Liquid Immersion Cooling of High Density Columns of Discrete Heat Sources in a Vertical Channel*, M.E. Thesis, Naval Postgraduate School, Monterey, CA, June 1989.
7. Joshi, Y., Willson T., and Hazard, S. J., III, "An Experimental Study of Natural Convection Cooling of an Array of Heated Protrusions in a Vertical Channel in Water", *Journal of Electronic Packaging*, March 1989.
8. Park, K. A., and Bergles, A. E., "Natural Convection Heat Transfer Characteristics of Simulated Microelectronic Chips", *Transactions of the ASME* 90, 109, February 1987.
9. Bar-Cohen A., and Schweitzer, H., "Convective Immersion Cooling of Parallel Vertical Plates", *IEEE Transactions on Components, Hybrids, and Manufacturing Technology*, Vol. 8, 3, September 1985.
10. Milanez, L. F., and Bergles, A. E., "Studies on Natural Convection Heat Transfer from Thermal Sources on a Vertical Surface", *Proceedings of the Eighth International Heat Transfer Conference*, Vol. 3, 1347, 1986.

11. Jaluria, Y., "Interaction of Natural Convection Wakes Arising From Thermal Sources on a Vertical Surface", *Journal of Heat Transfer* 107, 883 November 1985.
12. Patankar, S. V., *Numerical Heat Transfer and Fluid Flow*, Hemisphere/McGraw-Hill 1980.
13. Halcrest Company, *An Introduction to Thermochromic Liquid Crystal Products*, 1989.
14. Paje, Rufino A., *Experiments on Liquid Immersion Natural Convection cooling of Leadless Chip Carriers Mounted on Ceramic Substrate*, M.E. Thesis, Naval Postgraduate School, Monterey, CA, September 1989.

## INITIAL DISTRIBUTION LIST

- |   |   |
|---|---|
| 1. Defense Technical Information Center<br>Cameron Station<br>Alexandria, VA 22304-6145   | 2 |
| 2. Library, Code 0142<br>Naval Postgraduate School<br>Monterey, CA 93943-5002   | 2 |
| 3. Mr. Howard Stevens<br>Head, Electrical Research Center<br>David Taylor Research Center<br>Annapolis, MD 21402  | 1 |
| 4. Superintendent<br>Naval Postgraduate School<br>Attn: Professor A. J. Healey, Code ME/Hy<br>Department of Mechanical Engineering<br>Monterey, CA 93943-5004   | 1 |
| 5. Superintendent<br>Naval Postgraduate School<br>Attn: Professor Y. Joshi, Code ME/Ji<br>Department of Mechanical Engineering<br>Monterey, CA 93943-5004       | 3 |
| 6. Superintendent<br>Naval Postgraduate School<br>Attn: Professor M. D. Kelleher, Code ME/Kk<br>Department of Mechanical Engineering<br>Monterey, CA 93943-5004 | 1 |
| 7. Superintendent<br>Naval Postgraduate School<br>Attn: Professor A. D. Kraus, Code EE/Ks<br>Department of Electrical Engineering<br>Monterey, CA 93943-5004    | 1 |



- |     |  |   |
|-----|--|---|
| 8.  | Superintendent<br>Naval Postgraduate School<br>Attn: Professor S. Sathe ME/St<br>Department of Mechanical Engineering<br>Monterey, CA 93943-5004 | 1 |
| 9.  | Mr. Duane Embree<br>Naval Weapons Support Center<br>Code 6042<br>Crane, IN 47522   | 1 |
| 10. | Mr. Alan Bosler<br>Naval Weapons Support Center<br>Code 6051<br>Crane, IN 47522  | 1 |
| 11. | Superintendent<br>Naval Postgraduate School<br>Attn: Curricular Officer, Code 34<br>Monterey, CA 93943-5004                                      | 1 |
| 12. | Mr. Joseph Cipriano<br>Executive Director<br>Weapons and Combat Systems Directorate<br>Naval Sea Systems Command<br>Washington, D.C. 200362-5101 | 1 |
| 13. | Lt. Larry O. Haukenes<br>Route 1, Box 14<br>Roberts, WI 54023  | 2 |